THE USE OF UNDETERMINED MULTIPLIERS IN THE ANALYSIS AND OPTIMUM DESIGN OF ELASTIC STRUCTURES

BY

TZU-YANG CHEN

A DISSERTATION PRESENTED TO THE GRADUATE SCHOOL
OF THE UNIVERSITY OF FLORIDA IN PARTIAL FULFILLMENT
OF THE REQUIREMENTS FOR THE DEGREE OF
DOCTOR OF PHILOSOPHY

UNIVERSITY OF FLORIDA

1989

ACKNOWLEDGEMENTS

The author sincerely wishes to thank the chairman of his supervisory committee, Dr. Ali A. Seireg, for his guidance and advice throughout the research.

The author wishes to express his appreciation to the other members of his supervisory committee, Dr. Joseph Duffy, Dr. George N. Sandor, Dr. Gary K. Matthew and Dr. Ulrich H. Kurzweg for their assistance in this work.

The author would like to thank Wei Lin and Chun-Yin Wu for their help in preparing the drawings and assistance in using computers, and Lindsay Wells for his help in getting this dissertation in proper form. Without their help, this work could not be done.

The author also wants to thank his friends for helping him to get accustomed to life in the United States of America.

Finally, the author would like to express his deepest appreciation to his parents and his brother and sister for their financial support, encouragement and enduring patience throughout this study.

TABLE OF CONTENTS

ACKNOWLEDGEMENTS ii

ABSTRACT v

CHAPTER

1 INTRODUCTION 1

The Energy Principle 1
Rayleigh-Ritz Method Using Undetermined Multipliers in Structural Mechanics 4

2 THEORETICAL BACKGROUND. 8

Principle of Virtual Work 8
Principle of Minimum Potential Energy 10
Application of Variational Calculus in Structural Mechanics 12
Rayleigh-Ritz Method 13
Lagrangian Multiplier Method 18
Rayleigh-Ritz Method Using Lagrangian Multipliers 21

3 APPLICATIONS TO BEAM PROBLEMS 23

Introduction 23
Simply-Supported Beams 25
Clamped-Supported Beams 27
Clamped-Clamped Beams 29
Cantilever Beams 32
Cantilever Beams with the Free End Flexibly Supported 36
Beams Supported on Elastic Foundations. 41
Multi-Span Beams 42

4 APPLICATIONS TO PLATE PROBLEMS 47

Introduction 47
Plates with All Edges Simply Supported 50
Plates with One Edge Clamped and Three Edges Simply Supported 55
Plates with All Edges Clamped 62
Nonrectangular Plates 66

Plates with Mixed Boundary Conditions 70
Stiffened Plates 74
Honeycomb Sandwich Plates 80

5 APPLICATIONS TO PLATES WITH HOLES 90

Introduction 90
Square Plates with Clamped Square Holes 92
Simulation of a Cantilever Beam From a Clamped Beam 93
Square Plates with Free Square Holes 101

6 APPLICATIONS TO SHELL PROBLEMS 107

Introduction 107
Cylindrical Shells of Infinite Length Supported by a Rigid Ring 109
Cylindrical Shells of Infinite Length Reinforced by a Narrow Ring 115
Cylindrical Shells of Finite Length with Both Ends Clamped 121
Clamped Cylindrical Shells with Circumferential Ring Reinforcements 125
Shells Reinforced by Rings and Longitudinal Stiffeners 127

7 APPLICATIONS TO STRUCTURAL DESIGN 136

Beam Design 137
Plate Design 148

8 CONCLUSIONS AND RECOMMENDATIONS 165

Conclusions 165
Selection of the Coordinate Functions 167
Limitations of the Method 168
Recommendations 169

APPENDIX 170

REFERENCES 192

BIOGRAPHICAL SKETCH 196

Abstract of Dissertation Presented to the Graduate School of the University of Florida in Partial Fulfillment of the Requirements for the Degree of Doctor of Philosophy

THE USE OF UNDETERMINED MULTIPLIERS IN THE ANALYSIS AND OPTIMUM DESIGN OF ELASTIC STRUCTURES

By

Tzu-Yang Chen

August 1989

Chairman: Dr. Ali A. Seireg
Major Department: Mechanical Engineering

The study reported in this dissertation investigates the use of undetermined multipliers with the Rayleigh-Ritz method for the solution of general elasticity problems with complex geometries and boundary conditions. Beam, plate and shell problems are considered for illustrations. A procedure incorporating the undetermined multiplier method is given for the optimum design of beams and stiffened plates.

Several cases of beams on multiple supports, plates with holes, plates with reinforcements and reinforced shells are investigated through the use of the Raleigh-Ritz method incorporating the undetermined multipliers. The result shows that this approach provides an excellent tool for the analysis and optimum design of complex structures.

Although the method requires some manual integration, the result of the integration can be applied to similar problems

with different boundary conditions without any major change in formulation. The formulation of this method has a unified character for similar problems. The simplicity and elegance of this method is particularly evident when dealing with a class of problems with different boundary conditions.

This method gives a positive definite matrix for solving the generated system of linear equations. Choleski's decomposition scheme is incorporated to further increase the overall efficiency of the solution. The Newton-Raphson method is also incorporated with the undetermined multiplier approach to give an excellent and efficient design procedure. This method shows considerable advantages over the finite element method for the class of problems considered in this study.

CHAPTER 1
INTRODUCTION

The Energy Principle

Structural mechanics has long been a well-developed branch of science. Many principles have been formulated to describe the stresses and deformations in elastic bodies. In applying these principles to the analysis and design of mechanical system components, an essential step is to mathematically model the real situation, and obtain either an analytical or numerical solution from the model.

From the point of view of formulating theoretical models for the analysis of elastic structures, and the determination of numerical solutions, the energy principle holds a position of vital importance[1][2]. The essence of the energy principle for mechanical structures is that when the behavior of an elastic element follows the rule of "minimum energy," the application of variational calculus will result in a differential equation governing the behavior of the element.

There are many methods which have been developed on the basis of the energy principle. Most of these methods are based on the "principle of minimum potential energy." The energy principle can be applied by using the formal procedure

of the calculus of variations to determine the stationary condition for a functional (the potential energy in the case of elastic systems) so as to yield the differential equations and appropriate boundary conditions[3][4][5][6]. Instead of using the formal procedure, however, there are alternatives. These are the direct methods[1], which substitute an assumed solution involving adjustable parameters for the functional. The stationary condition is determined with respect to these parameters. Among these methods, the most widely used are the Rayleigh-Ritz method[1][7], the Galerkin method[1], and the finite element method[8][9], which is the most popular approach. All of these methods have inherent advantages and disadvantages, depending upon the particular application.

The finite element method is very flexible[10]. It can be applied to general elasticity problems, even in nonlinear domains[11][12]. It can even be applied to plasticity problems[13]. This method, however, has disadvantages, the most severe being the extensive preprocessing and postprocessing effort that is required. Another disadvantage is that it is necessary to choose a very fine mesh in regions with steep stress gradients[7]. This leads to the construction and solution of a large number of equations with a large number of unknowns. In other words, if there is no efficient computing machine, the finite element method cannot be practically used. There are also certain difficulties when

the finite element method is applied to problems including curved boundaries[7].

Basically, with all boundary conditions satisfied in an elasticity problem, the Galerkin method directly provides a solution to the differential equations, and is applicable whether the transformation into a variational problem is possible or not. In other words, the Galerkin method can supply an approximate solution without the construction of the functional (the potential energy). This advantage, however, is not important in view of the fact that in elasticity, an expression for the total potential energy can always be formulated. Also, its limitations, which have been widely discussed by Kanagasundaram and Harimhallo[14], make it more difficult to apply than the Rayleigh-Ritz method.

In contrast to the Galerkin method, the construction of the functional is essential to the Rayleigh-Ritz method. This, however, presents no difficulty in applying the method, because the potential energy can be formed directly by differentiation under the integral sign. Furthermore, while the Galerkin method requires the satisfaction of any traction boundary condition together with the geometric boundary conditions, the Rayleigh-Ritz method requires only the satisfaction of the geometrical boundary conditions[3]. It has been pointed out[1] that the Rayleigh-Ritz method is very effective in obtaining approximate solutions to boundary value problems. Further, this method is more efficient than the

finite element method, since it does not require the solution of as many equations. Actually, the Rayleigh-Ritz method is regarded as the basis of the direct methods[7]. The finite element method can be considered a special case of the Rayleigh-Ritz method.

Rayleigh-Ritz Method Using Undetermined Multipliers in Structural Mechanics

The application of the Rayleigh-Ritz method in simple structural analysis can be found in many books, for example references[3][4][5][15][16]. These applications are generally limited to the simplest problems, such as a simply-supported beam, or a simply-supported plate, and only occasionally to more complex problems[17]. This is because the Rayleigh-Ritz method requires that the assumed solution satisfies the boundary conditions, and it may not be always possible to find a solution which meets the boundary condition requirement and minimizes the functional at the same time.

In this study, an alternative way to apply the Rayleigh-Ritz method will be developed. The alternative, which will be called the modified Rayleigh-Ritz method, incorporates the Lagrangian rule[18][19][20] in a way such that the satisfaction of the boundary conditions by the assumed solution is no longer necessary. Through the use of Lagrangian multipliers (also known as undetermined multipliers), the boundary conditions can be forced to be

satisfied. The result will still minimize the potential energy, only this time the minimization is done under the restriction that the boundary conditions be satisfied. In this way, it is not necessary to find an assumed solution which satisfies the boundary conditions and the minimization requirement of the potential energy at the same time.

By applying the modified Rayleigh-Ritz method, many difficult problems in classic elasticity theory can be solved. Several authors[3][21][22] have applied the concept of the Lagrangian rule to handle constraints inside the domains of plates. These applications, however, still require that the assumed solution satisfies both the boundary conditions and the minimization of the potential energy simultaneously. It is proposed that boundary conditions, as well as other constraints, can be satisfied by modifying the Rayleigh-Ritz method with Lagrangian multipliers, and it would not be necessary to explicitly find an assumed solution which satisfies both the boundary conditions and the minimization of the potential energy.

Although classical theories have been very successful in the analysis of many structural elements, including beams, plates and shells, there are still many problems in these categories that are difficult to solve by classical methods. An example is the problem of a plate with mixed boundaries. There are generally no closed-form solutions for these problems, and their analysis is left to sophisticated and

expensive numerical schemes such as the finite element method. However, the Rayleigh-Ritz method incorporating the undetermined multipliers can be applied to solve this type of problem. It has been found that this modified Rayleigh-Ritz method has good potential for dealing with such problems more efficiently than the finite element method.

Another problem that the classical method cannot handle easily is the problem of a stiffened plate. There are two common ways to deal with this type of problem. One is to divide the plate into smaller elements bounded by the stiffeners, which generally requires the solution of a large system of simultaneous equations[3]. The other approach is to transfer the stiffened plate into an equivalent orthotropic plate. This approach has been favored by many researchers[23][24][25][26] for its simplicity. However, there is no guarantee that the stresses obtained will match at each point of the stiffened plate. Although this difficulty can be overcome by choosing the spacing of the stiffeners to be much smaller than the dimensions of the plate[27], it does not provide a practical way to handle more general problems of this type. On the other hand, by establishing suitable constraints between the plate and the stiffeners, this type of problem becomes well suited for efficient and effective solution by the modified Rayleigh-Ritz method.

The modified Rayleigh-Ritz method can also provide an excellent tool for optimizing elastic structures. In structural optimization, numerous techniques are used[28], such as design sensitivity, integer programming, and sequential linear programming. Usually, the basic method used for the optimization of structures of complex shapes is the finite element method[29]. As mentioned before, the finite element method requires considerable preprocessing and postprocessing effort in analyzing structures and, thus, is an expensive method. For example, for the aircraft wing structures discussed by Seong[29], it may take the finite element method many hours to complete a design on a super computer. Furthermore, it may be difficult to ensure the accuracy of the finite element method in some cases[30].

Since the optimal design process is iterative in nature and requires many evaluations of the objective function, the overall efficiency of the proposed method, when used in conjunction with efficient schemes for solving nonlinear equations, makes it a valuable tool to use in a wide variety of structural design tasks.

CHAPTER 2
THEORETICAL BACKGROUND

Principle of Virtual Work

As mentioned in the previous chapter, the energy principle is very important in solving problems of elastic structures. It originates from the principle of virtual work, which states that for a body in static equilibrium, the virtual work done by the loads acting upon it is zero[1][15][31].

Virtual work is defined as the work done by the loads when the body undergoes a fictitious displacement called virtual displacement. The virtual displacement may consist of a translation in any direction, a rotation about any axis, or a combination of both, provided that the translation and the rotation are admissible. In mathematic form, the principle of virtual work is

$$\delta W = 0 \tag{2.1}$$

The symbol W denotes work, and δW is the virtual work.

For a deformable body as shown in figure 2.1, where the bold line represents the undeformed configuration and the thin line represents the deformed configuration, equation (2.1) can be written as[15]

$$\delta W = \delta W_{ext} + \delta W_{int} = 0 \tag{2.2}$$

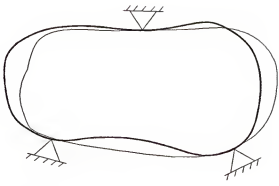

Figure 2.1 A deformable body

In equation (2.2), δW_{ext} represents the work done by the external loads during the process of an admissible virtual deformation of the body. An admissible deformation is one that satisfies the boundary conditions. If the body shown in figure 2.1 is regarded as a combination of an infinite number of small elements, δW_{int} is the work done by the internal forces between small elements of the body. If Hooke's law or another load-deformation law is applicable to the deformable body, the internal forces will have a potential energy U which is equal to the internal work W_{int}, with opposite sign[1]:

$$U = -W_{int} \tag{2.3}$$

Substituting equation (2.3) in equation (2.2) yields

$$\delta W_{ext} = \delta U \tag{2.4}$$

This means that the work done by external loads is transferred to the strain energy stored in the deformed body.

Principle of Minimum Potential Energy

If the external loading is conservative, it has a potential Ψ[1]:

$$\Psi = -W_{ext} \tag{2.5}$$

Substituting equations (2.3) and (2.5) in equation (2.2) yields

$$\delta W = (-\delta U) + (-\delta \Psi) = 0 \tag{2.6}$$

or equivalently,

$$\delta U + \delta \Psi = \delta (U + \Psi) = 0 \tag{2.7}$$

The sum of the potential of both external and internal forces is defined as the total potential of the system and denoted by Π, i.e.,

$$\Pi = U + \Psi \tag{2.8}$$

Then, from equation (2.7),

$$\delta \Pi = \delta (U + \Psi) = 0 \tag{2.9}$$

This equation states that for any admissible virtual deformation the deformable body can take, the change in total potential energy is zero[16].

If the virtual deformation is regarded as an infinitesimal variation of the body's configuration from its current equilibrium state, then $\delta\Pi$ represents the variation of total potential energy due to the change in configuration. Because of equation (2.9), it is clear that the variation in potential energy should be zero. In other words, Π has a stationary value when the body is in equilibrium[15].

Equation (2.9) can then be interpreted to mean that of all admissible configurations a deformable body can take, those satisfying the equilibrium condition result in a stationary value of the total potential energy[16]. This constitutes the principle of stationary potential energy, and an admissible configuration means a configuration satisfying the boundary conditions.

By combining equation (2.5) with equations (2.6) and (2.9), the principle of stationary potential energy can be written as

$$\delta\Pi = \delta U - \delta W_{ext} = \delta(U - W_{ext}) = 0 \qquad (2.10)$$

If the unloaded configuration of the deformable body (the bold line in figure 2.1) is taken as the reference datum, the potential energy contributed by external loads is the work done by these loads when the body undergoes deformation from its unloaded state to the final equilibrium configuration (the thin line in figure 2.1)[15].

A stationary value, by definition, may be a minimum, a maximum or a neutral value. However, since the potential energy function can be shown to be positive definite[16], it can be concluded that Π is a minimum when the body is in static equilibrium. It can then be stated that of all admissible configurations, those satisfying the condition of equilibrium result in a minimum value of the total potential energy of the system[16].

Application of Variational Calculus in Structural Mechanics

Variational calculus is mainly concerned with the stationary value of a definite integral called a functional. The integral involves some functions which are not known, and the purpose is to determine the unknown functions so as to make the functional stationary. In view of the fact that the configuration of an elastic body in static equilibrium results in a minimum total potential energy of the body, it can be understood that this type of problem is well suited to variational calculus. As a matter of fact, this is a major application of variational calculus.

Consider the following functional:

$$\Pi = \int_{x0}^{x1} F(x,v,v',v'')\ dx \tag{2.11}$$

where F is an explicit function of x, v, v', and v", and x_0 and x_1 are fixed numbers. A function v=v(x) is sought to make Π stationary. If Π is an extremum, then $\delta\Pi=0$. The optimum function v which makes the functional an extremum satisfies Euler's equation, which, in this case, is[4][5]

$$\frac{\partial F}{\partial v} - \frac{d}{dx}\left(\frac{\partial F}{\partial v'}\right) + \frac{d^2}{dx^2}\left(\frac{\partial F}{\partial v''}\right) = 0 \tag{2.12}$$

provided that v and v' are prescribed at $x=x_0$ and $x=x_1$.

If v and v' are not specified, the following conditions, in addition to equation (2.12), should also be satisfied to make $\delta\Pi$ vanish:

$$\frac{\partial F}{\partial v'} - \frac{d}{dx}\left(\frac{\partial F}{\partial v''}\right) = 0 \tag{2.13}$$

and

$$\frac{\partial F}{\partial v''} = 0 \tag{2.14}$$

Equations (2.13) and (2.14) are customarily referred to as natural boundary conditions[4][5].

Consider the problem of a beam subjected to a lateral load p(x). If the origin of a coordinate system is located at one end of the beam, and the positive x axis of the coordinate system is running toward the other end, then the potential energy is[15]

$$\Pi = \int_0^{\ell} \left[\frac{EI}{2}(v'')^2 - p(x)v\right] dx \tag{2.15}$$

where ℓ is the length of the beam, EI is the bending rigidity. In equation (2.15), v denotes the deflection function (the equilibrium configuration) of the beam. Substituting $(1/2)EI(v'')^2$-pv as F in equation (2.12) yields

$$\frac{d^2}{dx^2}\left(EI\frac{d^2v}{dx^2}\right) - p(x) = 0 \tag{2.16}$$

which is the well-known governing equation for a beam subjected to a lateral load function p(x).

Rayleigh-Ritz Method

In the previous sections, as an application of variational calculus to beam problems, the equivalence between

the differential equation which governs the deflection of a beam and the energy formulation was demonstrated. This equivalence can be utilized in many ways to numerically handle problems of elastic systems. One of these methods is the Rayleigh-Ritz method[1][5].

A deformable body with its properties (mass, stiffness, etc.) distributed in a continuous manner is referred to as a continuum. A continuum usually has an infinite number of degrees of freedom and, thus, can assume an infinite number of deformed configurations. It is customary to describe the response of such a system with a differential equation, or several equations, together with boundary conditions. Sometimes, it is hard to solve the differential equation(s) with the prescribed boundary conditions. It is, however, possible to approximate the real system with a system possessing only a finite number of degrees of freedom by assuming certain characteristics of the deformation.

To do so, a reasonable deformed configuration involving some undetermined parameters is assumed. Taking a one-dimensional problem as an example, if $v(x)$ is the function which makes the potential energy Π minimum, then it is approximated in the Rayleigh-Ritz method by another function $v_N(x)$. This function is a linear combination of a set of prescribed coordinate functions $\Phi_n(x)$ in the following form:

$$v(x) \approx v_N(x) = \sum_{n=1}^{N} a_n \Phi_n(x) \tag{2.17}$$

where a_n are unknown parameters, called displacement parameters, and are to be determined by minimizing the potential energy Π. Usually, the coordinate functions Φ_n are chosen in such a way that no matter how the parameters a_n are determined, expression (2.17) always satisfies the boundary conditions.

With equation (2.17), the potential energy Π can be calculated on the basis of the knowledge of the coordinate functions Φ_n. The potential energy becomes a function of the displacement parameters a_n only. Instead of dealing with a functional as described in the previous sections, we are now handling a function and, thus, we have an ordinary extremum problem. The potential energy is put in the form of a function of the parameters a_n, i.e.,

$$\Pi = \Pi(a_1, a_2, \ldots, a_n, \ldots, a_N) \tag{2.18}$$

where the domain of the function Π may be regarded as the whole N-dimensional Euclidean space with the parameters a_n as the set of coordinates. The potential energy function Π is, at least, of the class C^1 in the N-dimensional Euclidean space[2]. This means that the function itself, as well as its first derivative, is continuous.

In accordance with differential calculus, the necessary and sufficient condition for a stationary point is

$$\frac{\partial \Pi}{\partial a_n} = 0 \qquad n=1,2,\ldots,N \tag{2.19}$$

The solution of the simultaneous algebraic equations (2.19)

corresponds to the stationary point of the function Π. It has already been shown that this stationary point is a minimum point.

In linear elasticity problems, Π is quadratic in a_n so the differentiation indicated (2.19) produces a set of linear simultaneous equations[1]. This considerably reduces the work to solve the problem. However, it must be understood that the variational problem has been replaced by an ordinary extremum problem through the use of the set of prescribed coordinate functions Φ_n and, in general, these two are not equivalent. Therefore, the solution obtained from the ordinary extremum problem will only be an approximation to that of the variational problem.

The efficiency of the Rayleigh-Ritz method is clearly dependent upon the choice of the coordinate functions $\Phi_n(x)$. In the sense of efficiency, it is advantageous to satisfy all the boundary conditions in applying this procedure. This is, however, not necessary in the sense of the applicability of the method to more complicated problems. This will be explained later.

The Rayleigh-Ritz method requires that the number of the coordinate functions, N, be determined. This is accomplished by applying a convergence criterion to the sequence of approximating functions $v_1(x)$, $v_2(x)$, ..., $v_N(x)$, where $v_n(x)$ $(n=1,2,\ldots,N)$ is a linear combination of coordinate functions as indicated in equation (2.17). It will be shown in the

following chapters that whenever the difference between the Nth and (N+1)st approximation is sufficiently small, the solution may be considered convergent.

It should be clearly understood that, in contrast to the coefficients of a Fourier expansion, the parameters a_n are different for each different approximation and must be re-determined each time a new approximation is chosen[5]. However, a significant characteristic that this method displays should also be noted. If

$$v_N(x) = \sum_{n=1}^{N} a_n \Phi_n(x) \tag{2.20}$$

is the Nth approximation to the true function v(x) and

$$v_{N+1}(x) = \sum_{n=1}^{N+1} a_n^* \Phi_n(x) \tag{2.21}$$

is the (N+1)st approximation, then the latter will be better, or at least no worse, than the former. By taking a large enough number of the coordinate functions, a convergent result can be obtained.

The sequence of approximations of the Rayleigh-Ritz method will converge in a mean square sense throughout the region of interest (x_0,x_1)[5], i.e.,

$$\int_{x0}^{x1} [v(x) - \sum_{n=1}^{N} a_n \Phi_n(x)]^2 \, dx < \epsilon \tag{2.22}$$

where ϵ is a positive real number, and

$$\lim_{n\to\infty} \int_{x0}^{x1} [v(x) - \sum_{n=1}^{N} a_n \Phi_n(x)]^2 \, dx = 0 \qquad (2.23)$$

provided that the set of coordinate functions Φ_n is complete. An example of a set of complete functions is the complete Fourier series, including both sine and cosine functions. This series will be used as the coordinate functions in the following investigation. However, other functions can also be chosen to serve as coordinate functions.

The Rayleigh-Ritz method can also be applied to problems with two or more independent variables, such as problems of plates and shells. For the case of two independent variables, the approximation can be written as

$$v(x,y) \approx v_N(x,y) = \sum_{n=1}^{N} a_n \Phi_n(x,y) \qquad (2.24)$$

or

$$v(x,y) \approx v_N(x,y) = \sum_{m=1}^{Nm} \sum_{n=1}^{Nn} a_{mn} \Phi_m(x) \Theta_n(y) \qquad (2.25)$$

where a_n or a_{mn} are parameters to be determined such that $\Pi(a_n)$ or $\Pi(a_{mn})$ is stationary.

Lagrangian Multiplier Method

Consider the problem of extremizing a function of N variables $a_1, a_2, \ldots, a_N$:

$$\Pi = \Pi(a_1, a_2, \ldots, a_N) \qquad (2.26)$$

subject to the constraints:

$$G_i(a_1, a_2, \ldots, a_N) = 0 \qquad i=1,2,\ldots,I_c \qquad (2.27)$$

where $I_c < N$ must hold. Since Π is made an extremum,

$$d\Pi = \sum_{n=1}^{N} \frac{\partial \Pi}{\partial a_n} da_n = 0 \tag{2.28}$$

Because of the constraint equations (2.27), not all a_n are independent. Only $(N-I_c)$ of the variables a_n are independent. Therefore, the differentials da_n are not arbitrary and are subject to the constraints:

$$dG_i = \sum_{n=1}^{N} \frac{\partial G_i}{\partial a_n} da_n = 0 \qquad i=1,2,\ldots,I_c \tag{2.29}$$

Multiplying equations (2.29) with the Lagrangian multipliers λ_i $(i=1,2,\ldots,I_c)$ and adding them to equation (2.28) yields

$$d\Pi + \sum_{i=1}^{I_c} \lambda_i dG_i$$

$$= \sum_{n=1}^{N} \left(\frac{\partial \Pi}{\partial a_n} + \sum_{i=1}^{I_c} \lambda_i \frac{\partial G_i}{\partial a_n} \right) da_n \tag{2.30}$$

Since λ_i are arbitrary, it is always possible to choose them in such a way that I_c of the N parenthesized terms will vanish, and only $(N-I_c)$ sets of terms are left. Furthermore, since the remaining $(N-I_c)$ differentials, da_n, can be considered independent, the terms inside the remaining parentheses must be zero. Therefore, the stationary point can be found directly from

$$\frac{\partial \Pi}{\partial a_n} + \sum_{i=1}^{I_c} \lambda_i \frac{\partial G_i}{\partial a_n} = 0 \qquad n=1,2,\ldots,N \tag{2.31}$$

together with equations (2.27). Equations (2.27) and (2.31)

consist of $(N+I_c)$ equations with $(N+I_c)$ unknowns $(a_1, a_2, \ldots, a_N, \lambda_1, \lambda_2, \ldots, \lambda_{Ic})$.

The Lagrangian function, L, is formed as follows:

$$L(a_1, a_2, \ldots, a_N, \lambda_1, \lambda_2, \ldots, \lambda_{Ic}) =$$

$$\Pi(a_1, a_2, \ldots, a_N) + \sum_{i=1}^{Ic} \lambda_i G_i(a_1, a_2, \ldots, a_N) \qquad (2.32)$$

The stationary point of the function L can be obtained by taking the partial derivatives of L with respect to the $(N+I_c)$ variables $a_1, a_2, \ldots, a_N, \lambda_1, \lambda_2, \ldots, \lambda_{Ic}$ and equating them to zero:

$$\begin{aligned} \partial L / \partial a_n &= 0 \qquad n=1,2,\ldots,N \\ \partial L / \partial \lambda_i &= 0 \qquad i=1,2,\ldots,I_c \end{aligned} \qquad (2.33)$$

Performing the differentiations of the above equations also results in equations (2.27) and (2.31). This is the Lagrangian rule[4][32], and it provides a concise way to simultaneously obtain the optimization equation (2.31) and the constraint equation (2.27).

By using the Lagrangian rule in the Rayleigh-Ritz method, the satisfaction of the boundary conditions required by the Rayleigh-Ritz method is no longer necessary. The applicability of the Rayleigh-Ritz method can, thus, be extended to more complicated problems with a wide variety of boundary conditions. This will be explained in the next section.

Rayleigh-Ritz Method Using Lagrangian Multipliers

Conventionally, the coordinate functions $\Phi_n(x)$ of the Rayleigh-Ritz method must be so chosen that the boundary conditions are all satisfied. The Lagrangian multiplier method provides a measure to overcome this limitation. By applying the Lagrangian multiplier method, it is not necessary to limit the choice of coordinate functions by requiring that the boundary conditions be satisfied. The unsatisfied boundary conditions may be treated as constraint equations (2.27)[18][19][20].

Since the configuration of a deformed body can be approximated by a linear combination of the coordinate functions with the unknown parameters a_n, the boundary conditions can also be expressed as a combination of these coordinate functions and, thus, as a function of the unknown parameters. If the unsatisfied boundary conditions are regarded as the constraint equations, then the problem of extremizing the potential function Π becomes a constrained optimization problem. The number of constraints is dependent upon how many boundary conditions are not satisfied. By applying the Lagrangian method, the same equation as equation (2.32) can be obtained with Π denoting the total potential energy of a given elastic system and G_i denoting the unsatisfied boundary conditions. The unknown parameters a_n,

as well as the Lagrangian multipliers λ_i, can then be easily obtained.

It is also possible to use the same approach to transfer any geometrical limitation on the deformation of the body to a constraint equation, such as in the case of a multi-span beam where the interior supports restrict the deformation of the beam. The restrictions caused by the interior supports may be regarded as constraints, and transferred into equations that can be expressed in terms of the parameters a_n. These constraints can be included in the process of extremizing the potential energy, and the solution so obtained will satisfy all boundary conditions together with those geometrical constraints imposed on the interior of the deformable body.

The use of Lagrangian multipliers to modify the Rayleigh-Ritz method is the approach that is proposed in this study to handle the analysis and optimum design of elastic structures. In order to maintain focus on the essence of this new approach, only simple structural elements such as beams, plates, and shells with linearly elastic deformations will be considered. The principle of superposition will therefore hold for all the cases studied. The illustrated examples, although simple, exhibit all the basic features of more complex problems. The next chapter will be devoted exclusively to beam problems where the application of the method can be illustrated with minimum complexity.

CHAPTER 3
APPLICATIONS TO BEAM PROBLEMS

Introduction

The governing equations of an elastostatic problem can be grouped into three sets[33]:

1. Equilibrium equations in terms of stress components
2. Compatibility equations in terms of strain components
3. Constitutive equations relating the stresses and the strains

Boundary conditions corresponding to set 1 are named force boundary conditions and those corresponding to set 2 are called geometry boundary conditions. All boundary conditions fall into these two categories.

For a beam subjected to a lateral load p(x), the equilibrium equation is[15]

$$\frac{d^2M(x)}{dx^2} = -p(x) \tag{3.1}$$

where M(x) denotes the bending moment of the beam and x is the coordinate along the beam. The compatibility equation is[15]

$$\frac{d^2v(x)}{dx^2} = -\rho(x) \tag{3.2}$$

where v(x) is the deflection function of the beam and $\rho(x)$ is the curvature. The constitutive equation requires that[15]

$$M(x) = -EI\rho(x) \tag{3.3}$$

By combining these equations, the governing differential equation of a beam subjected to a lateral load is obtained. This was shown in equation (2.16). Since the differential equation is of the fourth order, four boundary conditions are necessary to complete the solution. Usually, the boundary conditions at each end of the beam are a combination of any two of the following:

i. v(x)
ii. dv(x)/dx
iii. M(x)
iv. V(x) = dM(x)/dx

where V(x) denotes the shear force. Equations (i) and (ii) are geometry boundary conditions which relate to generalized displacements of the deflection of the beam, and the remaining two are force boundary conditions which relate, as the name suggests, to generalized forces. Using equation (3.2), equations (iii) and (iv) can be rewritten as

$$M(x) = -EI\frac{d^2v(x)}{dx^2} \tag{3.4.1}$$

and

$$V(x) = -EI\frac{d^3v(x)}{dx^3} \tag{3.4.2}$$

It is therefore possible to express any boundary conditions in terms of the deflection function v(x). Since only linearly ealstic deformations are considered in this study, the above expressions will be applied only to beams deflecting in the linearly elastic range.

In analyzing beam problems with the Rayleigh-Ritz method, the deflection of the beam is assumed to be a combination of some suitably chosen coordinate functions. For all the examples discussed below, Fourier series are chosen as the coordinate functions because they satisfy a wide range of boundary conditions. If the coordinate system is taken the same as that shown in figure 3.1, then the deflection function can be assumed as

$$v(x) = \sum_{n=1}^{\infty} a_n \sin\left(\frac{n\pi x}{\ell}\right) \tag{3.5}$$

where ℓ is the length of the beam. If the bending rigidity EI is constant, the strain energy of the beam is[15]

$$U = \int_0^{\ell} \frac{EI}{2} \left(\frac{d^2v}{dx^2}\right)^2 dx = \frac{EI\pi^4}{4\ell^3} \sum_{n=1}^{\infty} a_n^2 n^4 \tag{3.6}$$

The work done by the external load p(x) acting on the beam takes the following form:

$$W = \int_0^{\ell} p(x)v(x)dx = \sum_{n=1}^{\infty} a_n \int_0^{\ell} p(x)\sin\left(\frac{n\pi x}{\ell}\right)dx \tag{3.7}$$

Accordingly, the total potential energy of the beam is

$$\begin{aligned} \Pi &= U - W \\ &= \frac{EI\pi^4}{4\ell^3} \sum_{n=1}^{\infty} a_n^2 n^4 - \sum_{n=1}^{\infty} a_n \int_0^{\ell} p(x)\sin\left(\frac{n\pi x}{\ell}\right)dx \end{aligned} \tag{3.8}$$

Simply-Supported Beams

For the simply-supported beam shown in figure 3.1, the boundary conditions for both ends are v=0 and M=0 (or v"=0,

if divided by the bending rigidity EI). Since sine functions already satisfy these boundary conditions at both x=0 and x=ℓ, no constraint is necessary for this case.

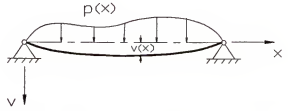

Figure 3.1 A simply-supported beam

If p(x) is a uniform load, i.e., $p(x)=p_0$, then

$$W = \sum_{n=1}^{\infty} a_n \frac{p_0 \ell}{n\pi} (1-\cos(n\pi)) \tag{3.9}$$

and

$$\Pi = \frac{EI\pi^4}{4\ell^3} \sum_{n=1}^{\infty} a_n^2 n^4 - \frac{p_0 \ell}{\pi} \sum_{n=1}^{\infty} a_n \frac{1 - \cos(n\pi)}{n} \tag{3.10}$$

Taking partial derivatives of equation (3.10) with respect to the parameters a_n and setting them equal to zero gives

$$\frac{\partial \Pi}{\partial a_n} = \frac{EI\pi^4 n^4}{2\ell^3} a_n - \frac{p_0 \ell (1 - \cos(n\pi))}{n\pi} = 0 \tag{3.11}$$

Thus the parameters a_n can be obtained as

$$a_n = \frac{2p_0 \ell^4 (1 - \cos(n\pi))}{EIn^5\pi^5} \tag{3.12}$$

It should be noted that in this case these parameters are also the coefficients of the Fourier expansion of the theoretical deflection of a simply-supported beam subjected to a uniformly distributed load[15][34]. The Nth approximation

$$v_N(x) = \sum_{n=1}^{N} a_n \sin\left(\frac{n\pi x}{\ell}\right) \tag{3.13}$$

is simply a truncated Fourier series, and it gets closer to v(x) as N becomes larger. Although it happens that the parameters a_n are equal to the Fourier coefficients for this case, in general they are different. When the boundary conditions are not identically satisfied, the parameters a_n deviate from the Fourier coefficients. This can be illustrated by the following case.

Clamped-Supported Beams

Consider a clamped-supported beam acted upon by a uniformly distributed load $p(x)=p_0$ as shown in figure 3.2.

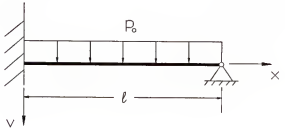

Figure 3.2 A clamped-supported beam

By choosing the same coordinate functions, the formulation of the total potential energy is the same as that of the simply-supported beam case. The boundary conditions, however, are not all satisfied by the coordinate functions. The unsatisfied boundary condition is v'=0 at x=0, which can be written as

$$G_1(a_n) = \sum_{n=1}^{\infty} a_n n = 0 \tag{3.14}$$

Applying the proposed modification to the Rayleigh-Ritz method, the Lagrangian function takes the form

$$L = \Pi + \lambda G_1(a_n)$$

$$= \frac{EI\pi^4}{4\ell^3} \sum_{n=1}^{\infty} a_n{}^2 n^4 - \frac{p_0 \ell}{\pi} \sum_{n=1}^{\infty} a_n \frac{1 - \cos(n\pi)}{n} + \lambda \sum_{n=1}^{\infty} a_n n \tag{3.15}$$

By taking partial derivatives of the Lagrangian with respect to a_n as before, it is found that

$$a_n = \frac{2\ell^3}{EI\pi^4 n^4} \left(\frac{p_0 \ell (1 - \cos(n\pi))}{n\pi} - \lambda n \right) \tag{3.16}$$

Substituting a_n into equation (3.14), the undetermined multiplier λ can be found by the following equation:

$$\lambda \sum_{n=1}^{\infty} \frac{1}{n^2} = \sum_{n=1}^{\infty} \frac{p_0 \ell (1 - \cos(n\pi))}{n^4 \pi} \tag{3.17}$$

The calculation of the undetermined multiplier λ is generally not possible if the upper limit of the summation is infinity. To make it feasible to calculate λ, the first N terms of the series (3.5) are taken as an approximation (the Nth approximation as described in Chapter 2). In this case, equation (3.17) becomes

$$\lambda \sum_{n=1}^{N} \frac{1}{n^2} = \sum_{n=1}^{N} \frac{p_0 \ell (1 - \cos(n\pi))}{n^4 \pi} \tag{3.18}$$

The undetermined multiplier λ can now be obtained easily. By substituting λ in equation (3.16), the parameters a_n can be calculated and thus the deflection of the beam can be found.

Table 3.1 gives a comparison of the Fourier coefficients of the theoretical deflection function with the parameters a_n from the modified Rayleigh-Ritz method. As can be seen from the table, the parameters of the new method get closer to the Fourier coefficient as N gets larger.

Table 3.1 Comparison of the Fourier series with three approximations

n	F. S.	5th App.	10th App.	20th App.
1	5.00817	4.01582	4.51443	4.76198
2	-1.00786	-1.13190	-1.06958	-1.03863
3	-0.24484	-0.28159	-0.26312	-0.25395
4	-0.12598	-0.14149	-0.13370	-0.12983
5	-0.06032	-0.06826	-0.06427	-0.06229

Figure 3.3 shows the deflection curves of the three different approximations indicated in table 3.1, together with the theoretical deflection curve[15]. The deflections shown in the figure have been normalized by the expression $p_0\ell^4/EI$. It can be seen from figure 3.3 that as N increases, the approximations approach the theoretical result. The error at $x=\ell/2$ is about 4.6% for the 20th approximation.

Clamped-Clamped Beams

One of the advantages of the proposed method is that it is easy to modify the boundary conditions without any major change in the formulation. Taking the previous case as an example, it is easy to obtain the deflection curve of a clamped-clamped beam (figure 3.4) from the previous

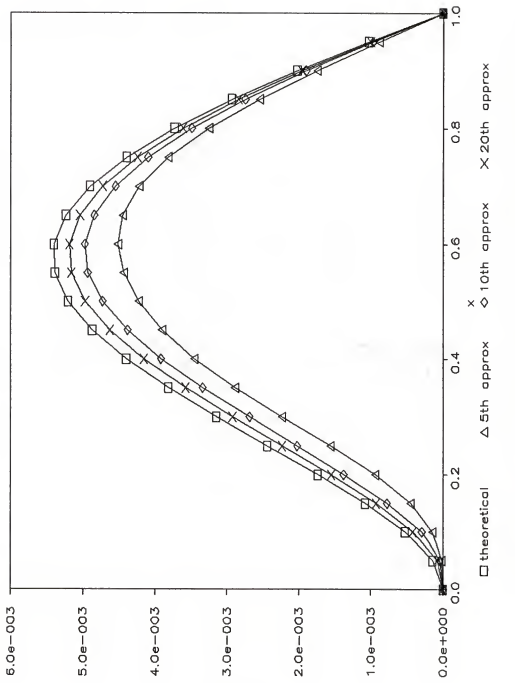

Figure 3.3 Deflection curves of a clamped-supported beam

formulation by simply adding one more constraint to the supported end of the clamped-supported beam. This forces the slope of the deflection curve to be zero at the supported end. If the Nth approximation is taken, then this constraint is

$$G_2(a_n) = \sum_{n=1}^{N} a_n n \cos(n\pi) = 0 \tag{3.19}$$

Since the approximate function of (3.13) has already satisfied the requirement of zero deflection at both ends of the beam, equation (3.19) and equation (3.14) constitute the only constraints needed for the present case.

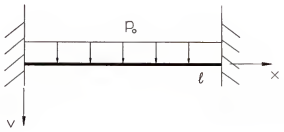

Figure 3.4 A clamped-clamped beam

The Lagrangian function takes the form

$$L = \Pi + \sum_{i=1}^{I_c} \lambda_i G_i \tag{3.20}$$

where I_c denotes the number of constraints to be imposed on the beam, and is two in this case (the approximate deflection function $v_N(x)$ of equation (3.13) has already satisfied the boundary conditions of zero deflection at both ends of the beam). Following the same procedure used in the previous section, it is found that

$$a_n = \frac{2\ell^3}{EI\pi^4 n^4}\left[\frac{p_0\ell(\ 1 - \cos(n\pi)\ )}{n\pi} - \lambda_1 n - \lambda_2 n\cos(n\pi)\right] \tag{3.21}$$

By substituting a_n into G_1 and G_2, two algebraic equations with two unknowns λ_1 and λ_2 are obtained. By solving these equations and substituting the result in equation (3.21), the displacement parameters a_n can be obtained. The results for the 10th, the 30th, and the 50th approximations are plotted in figure 3.5. The deflections shown in the figure have been normalized by the expression $p_0\ell^4/EI$. The theoretical deflection[15] is also plotted in the same figure for comparison. The error of the 30th approximation at the center of the beam is about 5.5% and that for the 50th approximation is 3.3%.

Cantilever Beams

Under certain conditions, for example a cantilever beam, it is necessary to use more complicated series, such as ones including both sine and cosine functions, as the coordinate functions. The nature of the sine functions alone makes it impossible to provide a deflection at the free end and, similarly, it is not possible to obtain a slope other than zero at the free end from the cosine functions alone. Consider the cantilever beam shown in figure 3.6. A uniform load p_0 is distributed over the left half of the beam.

Assume that the defection curve is a linear combination of both sine and cosine functions as follows:

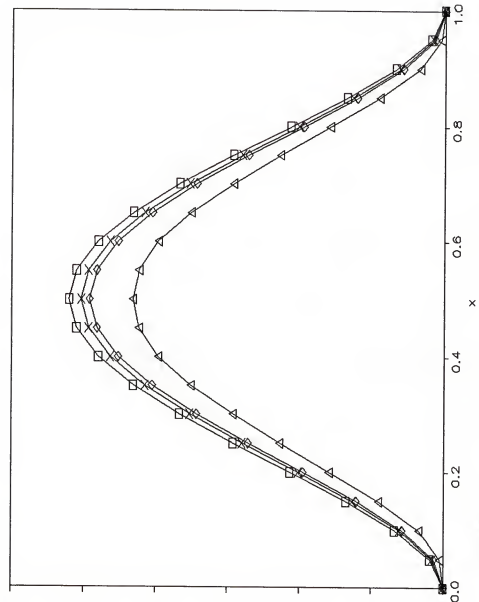

Figure 3.5 Deflection curves of a clamped-clamped beam

$$v_N(x) = a_0 + \sum_{n=1}^{N} a_n \cos(n\pi x/\ell) + \sum_{n=1}^{N} b_n \sin(n\pi x/\ell) \quad (3.22)$$

The strain energy stored in the beam for this assumed deflection is

$$U = \frac{EI\pi^4}{4\ell^3}\left[\sum_{n=1}^{N} (a_n^2+b_n^2)n^4 + \right.$$

$$\left. \sum_{n=1}^{N} \sum_{\substack{m=1 \\ m\neq n}}^{N} \left(a_n b_m \frac{4n^2m^3}{\pi(n^2-m^2)} \left(\cos(n\pi)\cos(m\pi) - 1 \right) \right) \right] \quad (3.23)$$

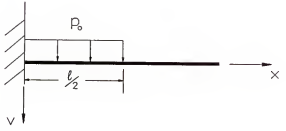

Figure 3.6 A cantilever beam

The work done by the external load is

$$W = \frac{p_0 a_0 \ell}{2} + \sum_{n=1}^{N} \frac{p_0 a_n \ell}{n\pi} \sin\left(\frac{n\pi}{2}\right) + \sum_{n=1}^{N} \frac{p_0 b_n \ell}{n\pi} \left(1-\cos\left(\frac{n\pi}{2}\right)\right) \quad (3.24)$$

The boundary conditions are v=0 and v'=0 at x=0, and v"=0 and v"'=0 at x=ℓ, none of which are satisfied by the approximation (3.22). The constraints are thus

$$G_1 = a_0 + \sum_{n=1}^{N} a_n = 0 \quad (3.25.1)$$

$$G_2 = \sum_{n=1}^{N} b_n n = 0 \quad (3.25.2)$$

$$G_3 = \sum_{n=1}^{N} a_n n^2 \cos(n\pi) = 0 \qquad (3.25.3)$$

$$G_4 = \sum_{n=1}^{N} b_n n^3 \cos(n\pi) = 0 \qquad (3.25.4)$$

The Lagrangian function takes the same form as equation (3.20) with $I_c=4$. By taking partial derivatives of the Lagrangian with respect to parameters a_0, a_n, and b_n (n=1,2,...,N), a set of (2N+1) linear algebraic equations with a_0, a_n, b_n (n=1,2,...,N), and λ_i (i=1,2,...,I_c) as unknowns is obtained. These equations take the following form:

$$\frac{EI\pi^4}{4\ell^3}\left[\, 2a_n n^4 + \sum_{\substack{m=1 \\ m\neq n}}^{N} b_m \frac{4n^2m^3}{\pi(n^2-m^2)}(\cos(n\pi)\cos(m\pi)-1)\,\right]$$

$$+ \lambda_1 + \lambda_3 n^2 \cos(n\pi) = \frac{p_0\ell}{n\pi}\sin\left(\frac{n\pi}{2}\right)$$

$$n=1,2,\ldots,N \qquad (3.26.1)$$

$$\frac{EI\pi^4}{4\ell^3}\left[\, 2b_n n^4 + \sum_{\substack{m=1 \\ m\neq n}}^{N} a_m \frac{4m^2n^3}{\pi(m^2-n^2)}(\cos(n\pi)\cos(m\pi)-1)\,\right]$$

$$+ \lambda_2 n + \lambda_4 n^3 \cos(n\pi) = \frac{p_0\ell}{n\pi}\left[1-\cos\left(\frac{n\pi}{2}\right)\right]$$

$$n=1,2,\ldots,N \qquad (3.26.2)$$

$$\lambda_1 = p_0\ell/2 \qquad (3.26.3)$$

The parameters a_0, a_n, and b_n (n=1,2,...,N), and the Lagrangian multipliers, λ_i (i=1,2,...,I_c), can be obtained by solving the above equations, together with the constraint equations (3.25). Figure 3.7 shows the comparison of the fifth and the tenth approximations with the theoretical solution[15]. The

deflections shown in the figure have been normalized by the expression $p_0\ell^4/EI$.

As can be seen from figure 3.7, the 10th approximation almost coincides with the theoretical curve. A very good approximation can be obtained by using only ten cosine and sine functions. Again, it should be noted that using only sine functions or only cosine functions would not result in an acceptable solution.

It is also possible to obtain a good approximation by replacing the cosine functions with a linear term, i.e., $v_0(x)=a_0x$. To do so, $v_0(x)$ should be added to equation (3.13), and then the same procedure followed. Since the second derivative of $v_0(x)$ vanishes, the formulation for strain energy is not affected. Only the formulation for work would need to be modified.

Cantilever Beams with the Free End Flexibly Supported

As shown in the previous case, the method presented in this investigation makes it very easy to change the boundary conditions of a beam problem without any major modification of the formulation. To further extend this method, let us consider a cantilever beam with the free end supported by a spring with stiffness K as shown in figure 3.8. Although in the classical method, this type of problem is treated differently from the previous case, the proposed method produces a formulation that is quite similar.

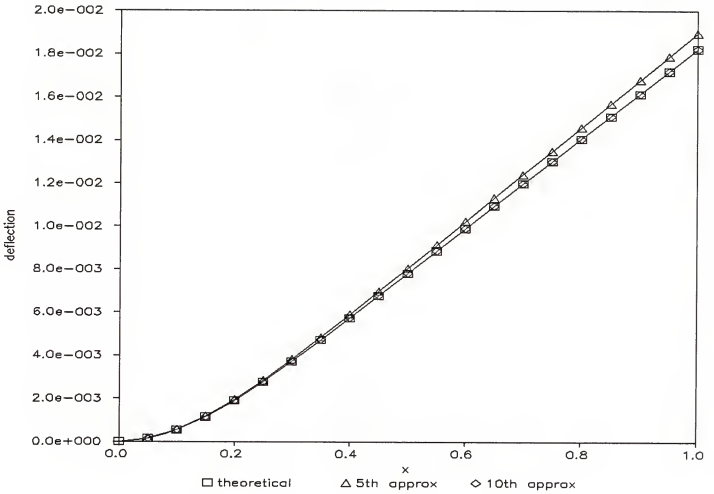

Figure 3.7 Deflection curves of a cantilever beam

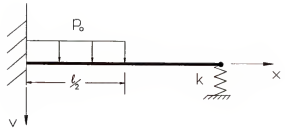

Figure 3.8 A cantilever beam with the free end flexibly supported

The spring stores energy when it is deflected. The amount of potential energy stored in the spring should be added to the total potential energy. Assuming the spring is not preloaded and the deflection of the spring is η, the potential energy of the spring can be written as

$$\Pi_s = K\eta^2/2 \tag{3.27}$$

Compatibility between the compression of the spring and the deflection of the beam requires that

$$G_5 = \left(a_0 + \sum_{n=1}^{N} a_n \cos(n\pi) \right) - \eta = 0 \tag{3.28}$$

This equation is also an equality constraint equation.

Following the same procedure as in the previous section, similar equations can be obtained, along with one additional equation obtained by taking the partial derivative of L with respect to η, which is

$$K\eta - \lambda_5 = 0 \tag{3.29}$$

where λ_5 is the undetermined multiplier associated with the constraint equation G_5. It can be seen from equation (3.29) that the Lagrangian multiplier associated with the constraint

of the deflection of the beam and the compression of the spring is the reaction force between them. In this situation, the Lagrangian multiplier associated with the compression of the spring has the dimension of force. The product of the multiplier and the deflection constraint, which has the dimension of deflection, has the dimension of work. This makes the dimension of the Lagrangian function consistent. It may be deduced from these observations that multipliers associated with generalized displacement constraints (deflections or slopes of the deflection curve) have the dimensions of generalized forces. Furthermore, it can also be deduced that the multipliers are the generalized forces required to insure compliance with the desired boundary conditions. In other words, forces are superimposed on the elastic body through the use of the undetermined multipliers to modify the boundary conditions as required.

Solving equations (3.25), (3.26), (3.28), and (3.29) simultaneously can give the deflection of the beam. Taking $K=18EI/\ell^3$, figure 3.9 shows the result obtained from the classical method and the result of the fifth approximation. The deflections shown in the figure have been normalized by the expression $p_0\ell^4/EI$. It can be seen that the error is negligible in the plot. The compression of the spring obtained from the proposed method is $2.60682\text{x}10^{-3}(p_0\ell^4/EI)$ and that obtained from the classical method is $(1/384)(p_0\ell^4/EI)$; the error is approximately 1%. The reaction force obtained

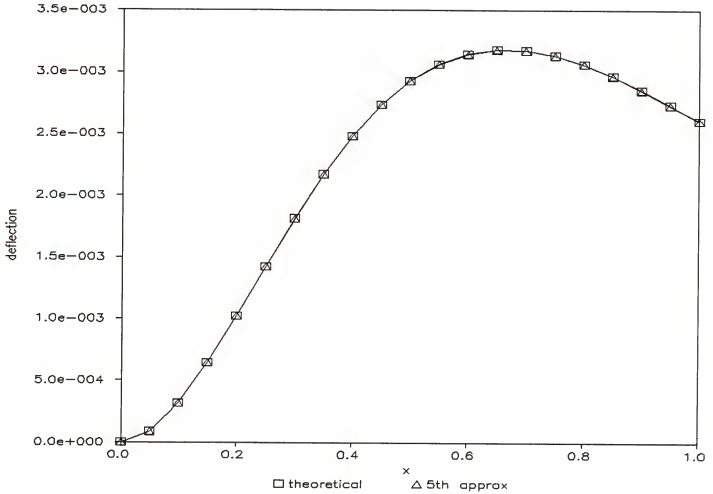

Figure 3.9 Deflection curves of a cantilever beam with the free end flexibly supported

from the proposed method is $4.69228 \times 10^{-2} p_0 \ell$, which is about 0.1% more than the value calculated from the classical method.

Beams Supported on Elastic Foundations

By extending the previous case, a beam placed on an elastic foundation can be treated in a similar way. The elastic foundation can be regarded as a combination of a number of springs. Consider the following situation (figure 3.10), a simply-supported beam, resting on an elastic foundation with modulus K_f, is bent by a moment M_0, acting at one end of the beam.

Figure 3.10 A beam supported on an elastic foundation

By using the approximation series (3.13), the formulation of the strain energy of the beam is the same as equation (3.6) except that the upper limit of the summation is replaced by N. The energy stored in the foundation is

$$U_f = \frac{K_f}{2} \int_0^{\ell} v^2 \, dx = \frac{K_f \ell}{4} \sum_{n=1}^{N} a_n^2 \tag{3.30}$$

The work done by M_0 is

$$W = \frac{M_0 \pi}{\ell} \sum_{n=1}^{N} a_n n \tag{3.31}$$

The Lagrangian function takes the following form:

$$L = \frac{EI\pi^4}{4\ell^3} \sum_{n=1}^{N} a_n^2 n^4 + \frac{K_f \ell}{4} \sum_{n=1}^{N} a_n^2 - \frac{M_0 \pi}{\ell} \sum_{n=1}^{N} a_n n \qquad (3.32)$$

By taking partial derivatives of L with respect to a_n and solving for a_n, it is found that

$$a_n = \frac{M_0 \pi n}{\ell} \Big/ \left(\frac{EI\pi^4 n^4}{2l^3} + \frac{K_f \ell}{2} \right) \qquad (3.33)$$

Figure 3.11 shows the comparison between the theoretical solution[35] and the results of the third and the fifth approximations, in which K_f is taken as 64EI. The deflections shown in the figure have been normalized by the expression $M_0\ell^2/EI$. The figure shows that only five sine functions give an excellent fit to the theoretic curve.

Multi-Span Beams

It has been mentioned previously that the proposed method can be applied to solve the problem of multi-span beams. In this case, a two-span beam (figure 3.12) is taken as an example to demonstrate the applicability of the method. By taking the same approximation series as equation (3.22), the formulation for strain energy of the beam takes the same form as equation (3.23). The work done by the concentrated load P is

$$W = P\, v_N(x_p)$$

$$= P \left[a_0 + \sum_{n=1}^{N} a_n \cos(n\pi x_p/\ell) + \sum_{n=1}^{N} b_n \sin(n\pi x_p/\ell) \right] \qquad (3.34)$$

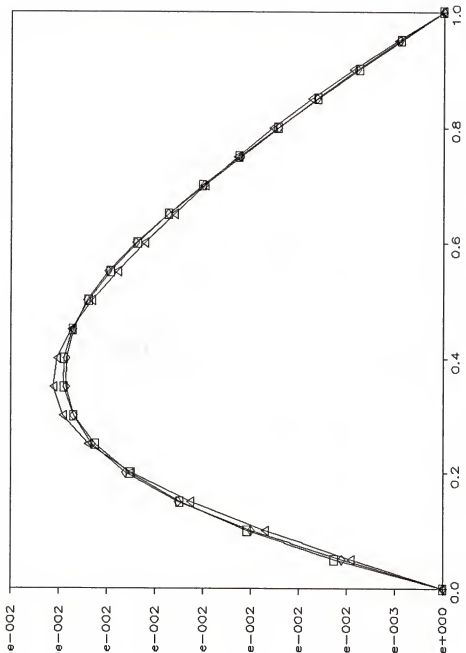

Figure 3.11 Deflection curves of a beam supported on an elastic foundation

The constraint equations due to the unsatisfied boundary conditions are given as

$$G_1 = a_0 + \sum_{n=1}^{N} a_n = 0 \tag{3.35.1}$$

$$G_2 = \sum_{n=1}^{N} a_n n^2 = 0 \tag{3.35.2}$$

$$G_3 = a_0 + \sum_{n=1}^{N} a_n \cos(n\pi) = 0 \tag{3.35.3}$$

$$G_4 = \sum_{n=1}^{N} a_n n^2 \cos(n\pi) = 0 \tag{3.35.4}$$

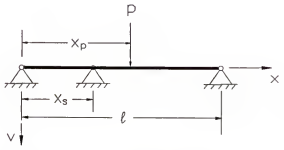

Figure 3.12 A multi-span beam

The interior support will prevent the beam from bending under the effect of the force P and, thus, will constrain the deflection of the beam at $x=x_s$. This gives an additional constraint equation which must be satisfied as well as the boundary conditions in the process of extremizing the potential energy. This constraint can be put in the following form:

$$G_5 = a_0 + \sum_{n=1}^{N} a_n \cos(n\pi x_s/\ell) + \sum_{n=1}^{N} b_n \sin(n\pi x_s/\ell) = 0 \qquad (3.35.5)$$

Using the same procedure of solving for the parameters a_0, a_n, and b_n (n=1,2,...,N) as in the previous cases, the result shown in figure 3.13 is obtained. Taking N=5 gives an approximation having almost no difference from the theoretical result obtained with classical techniques. The classical method usually takes two steps: first solving the deflection due to the external force P and determining the reaction of the interior support, and then superimposing the deflections due to both force P and the reaction. If there is more than one interior support, the classical method becomes tedious. However, for the proposed method, the only difference is the number of constraints. This does not change the basic formulation and does not introduce any additional complexity to the solution process.

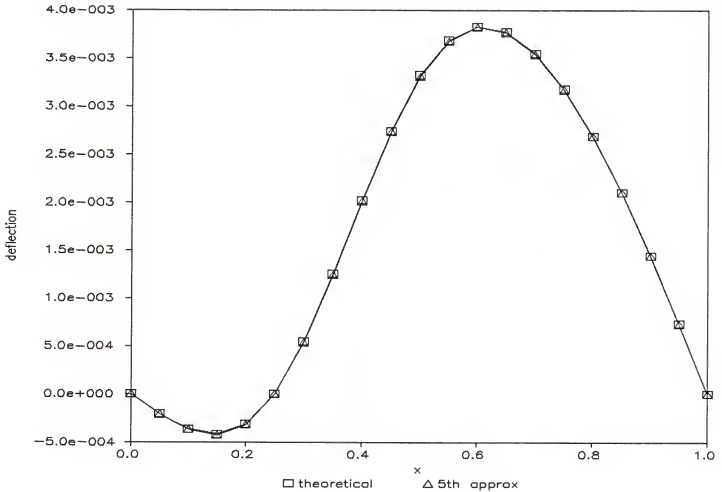

Figure 3.13 Deflection curves of a multi-span beam

CHAPTER 4
APPLICATIONS TO PLATE PROBLEMS

Introduction

In this investigation, a plate is defined as an elastic body bounded by two flat surfaces. The distance between the surfaces is the thickness of the plate. The plane parallel to the surfaces and bisecting the thickness is called the middle plane. The bending property of the plate depends upon its dimensions, especially the thickness. Based on the amount of deflection and the thickness of the plate, plate problems can be grouped into three categories[3]:

1. thin plate with small deflection
2. thin plate with large deflection
3. thick plate

Usually, thick plate problems are treated as three-dimensional problems. The problem of a thin plate with large deflections is a nonlinear elasticity problem. Both of these categories are not considered in this investigation. The first category, which is the only one to be dealt with in this study, is considered linearly elastic in classical plate theory.

The development of the theory of bending of a thin plate is based on the following assumptions attributed to Kirchhoff[3][16][36]:

1. The linear filament of the plate which is initially normal to the middle plane remains straight and normal to the middle plane after bending.
2. There is no deformation in the middle plane, i.e., this plane remains neutral and unstretched.
3. Normal stress in the direction transverse to the middle plane is small compared to the other normal stresses, and the normal strain in that direction is small enough to be disregarded.

These assumptions are good if the deflection is small in comparison with the thickness. They enable us to express the potential energy of the bent plate in terms of the curvatures of the bent plate. Furthermore, they also make it possible to express all the stresses in terms of the deflection of the plate.

In the following discussion, the middle plane is supposed to be coincident with the xy plane and the deflection is in the z direction. Thus, the deflection is a function of both x and y. With this in mind, the compatibility equation requires that

$$\rho_x = 1/r_x = -\partial^2 v/\partial x^2 \tag{4.1}$$

and similarly,

$$\rho_y = 1/r_y = -\partial^2 v/\partial y^2 \tag{4.2}$$

where ρ denotes the curvatures, r denotes the corresponding radii and v is the deflection function of the plate. The subscript x denotes the x-direction and y denotes the y-direction. The equilibrium of forces requires that[3]

$$\partial^2 M_x/\partial x^2 + \partial^2 M_y/\partial y^2 - \partial^2 M_{xy}/\partial x \partial y = -p(x,y) \tag{4.3}$$

where M_x and M_y denote, respectively, the bending moment in the x and y directions. The symbol M_{xy} denotes the twisting moment

and p(x,y) is the transverse load acting upon a surface of the plate.

The constitutive equation requires that[3]

$$M_x = D(\rho_x+\nu\rho_y) = -D(\partial^2 v/\partial x^2+\nu\partial^2 v/\partial y^2) \tag{4.4}$$

$$M_x = D(\rho_x+\nu\rho_y) = -D(\partial^2 v/\partial x^2+\nu\partial^2 v/\partial y^2) \tag{4.5}$$

$$M_{xy} = D(1-\nu)\partial^2 v/\partial x\partial y \tag{4.6}$$

where ν is Poisson's ratio. The symbol D is the flexural rigidity of the plate and is defined as

$$D = Eh^3/[12(1-\nu)] \tag{4.7}$$

In equation (4.7), E is Young's modulus and h is the thickness of the plate.

By combining these equations, the governing equation of the plate is obtained as follows[3]:

$$\frac{\partial^4 v}{\partial x^4} + 2\frac{\partial^4 v}{\partial x^2\partial y^2} + \frac{\partial^4 v}{\partial y^4} = \frac{p}{D} \tag{4.8}$$

Equation (4.8) is the Lagrange equation which relates the transverse deflection v(x,y) to the applied load p(x,y).

The boundary conditions at the edges of the plate can be categorized as follows[3][16][36]:

1. clamped edge along which v and $\partial v/\partial n$ vanish
2. simply-supported edge along which v and M_n vanish
3. free edge along which M_n and V_n vanish

In the above statements, the derivative with respect to n means a derivative with respect to the normal to the edge, and M_n and V_n denote, respectively, the moment and the shear force in the normal direction to the edges.

Equation (4.8), as well as the above boundary conditions, can also be obtained by the energy principle[3][16][36]. The process of variation was worked out by Lord Rayleigh in his book "Theory of Sound"[37]. It has also been shown by other researchers[6][17] that the solution to equation (4.8) minimizes the potential energy of the plate. The potential energy takes the following form:

$$\Pi = U - W \tag{4.9}$$

where U is the strain energy of the plate, and is obtained by performing the integration of the strain energy density of the plate over the whole plate. The strain energy U for a plate is formulated as[3]

$$U = \frac{D}{2}\int_A \{(\frac{\partial^2 v}{\partial x^2}+\frac{\partial^2 v}{\partial y^2})^2 - 2(1-\nu)[\frac{\partial^2 v}{\partial x^2}\frac{\partial^2 v}{\partial y^2}-(\frac{\partial^2 v}{\partial x \partial y})^2]\}dA \tag{4.10}$$

The symbol A denotes the surface area of the plate. If a load p(x,y) acts upon one surface of the plate, the work done by the load is

$$W = \int_A p(x,y)v(x,y)\ dA \tag{4.11}$$

Plates with All Edges Simply Supported

The problem of a plate with all edges simply supported has been cited by many authors, for example Richards[1], Timoshenko[3], Saada[16], and Love[36], to demonstrate the usage of the Rayleigh-Ritz method in plate problems. Taking a rectangular

plate with dimensions ℓ_x and ℓ_y (shown in figure 4.1) as an example, the coordinate functions are chosen to be sine functions for both the x and y directions, i.e.,

$$v(x,y) \approx \sum_{m=1}^{Nm} \sum_{n=1}^{Nn} a_{mn} \sin(m\pi x/\ell_x) \sin(n\pi y/\ell_y) \qquad (4.12)$$

To simplify the problem, N_m and N_n will be taken the same throughout this study. With the deflection surface approximated by the series of equation (4.12), the strain energy is expressed as

$$U = \frac{D\ell_x\ell_y}{8} \sum_{m=1}^{Nm} \sum_{n=1}^{Nn} a_{mn}^2 \left[\left(\frac{m\pi}{\ell_x}\right)^2 + \left(\frac{n\pi}{\ell_y}\right)^2 \right]^2 \qquad (4.13)$$

which is obtained by performing the integration of equation (4.10).

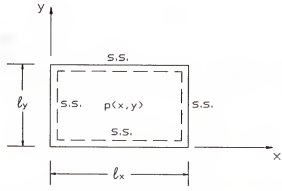

Figure 4.1 A plate with all edges simply supported

Similarly, by performing the integration of equation (4.11), the formula for the work done by the applied load p(x,y) can be obtained. This formula is expressed as a function of the parameters a_{mn}. If the external load p(x,y) is a uniformly distributed load, i.e., $p(x,y)=p_0$, then the work done by p_0 can be formulated as

$$W = \frac{p_0 \ell_x \ell_y}{\pi^2} \sum_{m=1}^{Nm} \sum_{n=1}^{Nn} a_{mn} \left(\frac{1-\cos(m\pi)}{m}\right)\left(\frac{1-\cos(n\pi)}{n}\right) \qquad (4.14)$$

Since the second derivative of a sine coordinate function vanishes at the edges of the rectangular plate, i.e., $\partial^2 v/\partial x^2=0$ at $x=0$ and $x=\ell_x$ and $\partial^2 v/\partial y^2=0$ at $y=0$ and $y=\ell_y$, all boundary conditions for the rectangular simply-supported plate are satisfied by the approximation series (4.12) and no constraint is necessary. In this case, the Lagrangian function is the potential energy of the plate, i.e.,

$$L = \Pi = U - W \qquad (4.15)$$

Using the same approach as in the beam problems, the partial derivatives of L with respect to each a_{mn} are taken, and set equal to zero. The displacement parameters a_{mn} are obtained as

$$a_{mn} = S_{mn} / (2E_{mn}) \qquad (4.16)$$

where

$$E_{mn} = \frac{D\ell_x\ell_y}{8}\left[\left(\frac{m\pi}{\ell_x}\right)^2 + \left(\frac{n\pi}{\ell_y}\right)^2\right]^2 \qquad (4.17)$$

and

$$S_{mn} = \frac{p_0 \ell_x \ell_y}{\pi^2} \left(\frac{1-\cos(m\pi)}{m}\right)\left(\frac{1-\cos(n\pi)}{n}\right) \qquad (4.18)$$

In view of the above equations, it can be seen that the numerical value of a_{mn} diminishes very quickly as m and n increase.

The result for a square plate is shown in figures 4.2 and 4.3. Figure 4.2 shows deflection curves taken along the section $y=\ell_y/2$. The deflections have been normalized by the expression $p_0\ell_x^4/D$. It can be seen from figure 4.2 that for this case it

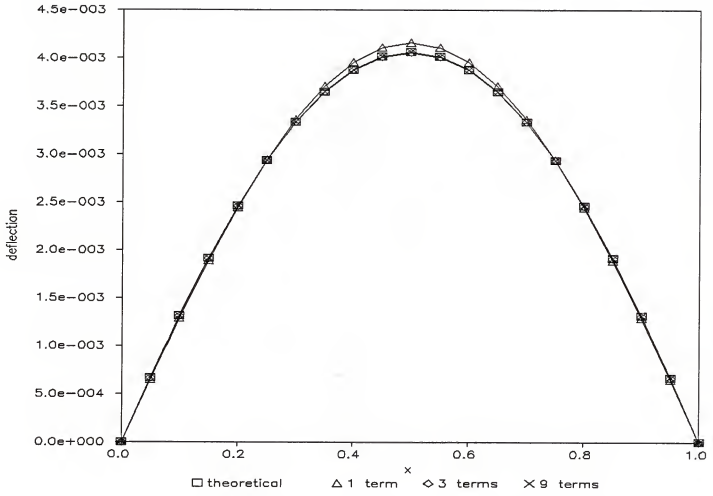

Figure 4.2 Deflection curves of a simply-supported plate taken along the section $y=\ell_y/2$

is difficult to distinguish the three-term approximation curve from the nine-term approximation curve. The difference between the one-term approximation and the nine-term approximation is about 2.4% at the point $x=\ell_x/2$ and $y=\ell_y/2$ and that between the three-term approximation and nine-term approximation is only 0.17%. From this, the sequence of approximations can be considered convergent when N_m and N_n are greater than three. Since the difference between the nine-term approximation and the theoretical deflection[3] is almost negligible, it can be seen that taking only one term of the series (4.12), i.e., $N_m=N_n=1$, will give an accurate enough result (with an error of about 2.4%) for engineering applications.

Figure 4.3 shows the deflection surface of the square plate obtained by the nine-term approximation. The deflection in figure 4.3 has been normalized in the same manner as above, and magnified 25 times with respect to the dimensions of the plate.

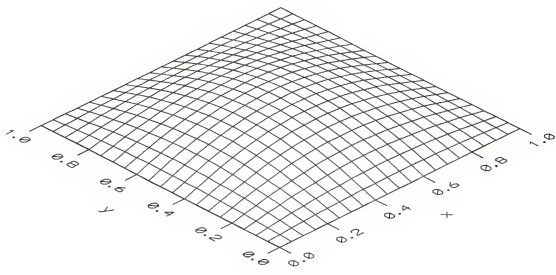

Figure 4.3 The deflection surface of a simply-supported plate

Plates with One Edge Clamped and Three Edges Simply Supported

As illustrated in the previous chapter, the Rayleigh-Ritz method using undetermined multipliers makes it very convenient to convert one beam problem to another with different boundary conditions. It will also be easy to change the boundary conditions of a plate problem without any major change in the formulation by using the modified Rayleigh-Ritz method. Consider a rectangular plate with three edges simply supported and the fourth edge clamped as shown in figure 4.4.

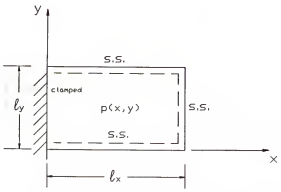

Figure 4.4 A plate with one edge clamped and three edges simply supported

With the same assumed deflection function as equation (4.12), the formulations of strain energy and work will be the same as equations (4.13) and (4.14). The boundary conditions, however, are not all satisfied by the approximate deflection function. What is not satisfied is the slope at the fixed boundary, i.e.,

$$\partial v / \partial x = 0 \qquad \text{for } x=0 \tag{4.19}$$

Since it is extremely difficult, if not impossible, to find a continuous function to serve as a "Lagrangian multiplier" to force the slope to be zero along the whole edge x=0, an alternative way of applying the concept of Lagrangian multipliers must be taken.

In this alternative approach, the boundary conditions are only satisfied using undetermined multipliers at a finite number of points chosen from the edge x=0, and the segments in between are disregarded. It can be understood that as the number of points at which the boundary conditions are satisfied approaches infinity, the actual boundary condition will be exactly satisfied. It is, however, possible to obtain a good approximation by choosing only a finite number of points along the edge x=0 to impose the constraints[18][19][20]. As will be demonstrated at the end of this section, five points are usually good enough for a single edge.

Assume that, in this case, I_1 points have been chosen from the edge x=0 to impose the slope constraint, the following constraint equations are obtained:

$$G_i(a_{mn}) = \sum_{m=1}^{Nm} \sum_{n=1}^{Nn} a_{mn} (m\pi/\ell_x) \sin(n\pi y_i/\ell_y)$$

$$= \sum_{m=1}^{Nm} \sum_{n=1}^{Nn} a_{mn} Q_{mni} = 0 \qquad i=1,2,\ldots,I_1 \qquad (4.20)$$

where y_i are the coordinates of the constraint points. The definition of Q_{mni} can be obtained directly from the above equations. By

following the same procedure demonstrated in the previous chapter, the Lagrangian function is formed as follows:

$$L = \Pi + \sum_{i=1}^{I1} \lambda_i G_i$$

$$= \sum_{m=1}^{Nm} \sum_{n=1}^{Nn} [\, E_{mn} a_{mn}^{\,2} - S_{mn} a_{mn} + \sum_{i=1}^{I1} (\lambda_i Q_{mni} a_{mn}) \,] \qquad (4.21)$$

Taking partial derivatives of L with respect to each a_{mn} and equating the resulting equations to zero, we obtain the following equations:

$$2E_{mn} a_{mn} = S_{mn} - \sum_{i=1}^{I1} \lambda Q_{mni}$$

$$m=1,2,\ldots,N_m, \qquad n=1,2,\ldots,N_n \qquad (4.22)$$

and it follows that

$$a_{mn} = (S_{mn} - \sum_{i=1}^{I1} \lambda Q_{mni}) \;/\; (2E_{mn}) \qquad (4.23)$$

Substituting equation (4.23) into the constraint equations (4.20), the following set of simultaneous equations in the Lagrangian multipliers λ_i is obtained:

$$\sum_{i=1}^{I1} \lambda_i \; (\sum_{m=1}^{Nm} \sum_{n=1}^{Nn} \frac{Q_{mni} Q_{mni'}}{2E_{mn}}) = \sum_{m=1}^{Nm} \sum_{n=1}^{Nn} \frac{S_{mn} Q_{mni'}}{2E_{mn}}$$

$$i'=1,2,\ldots,I_1 \qquad (4.24)$$

It should be noted that the number of unknowns are reduced from $N_m N_n + I_1$ to I_1. This considerably simplifies the solution of the simultaneous linear equations. There are many ways to solve the equations, such as the Gaussian elimination method or Choleski's decomposition scheme. The latter is much more efficient than the former, if the system of equations to be solved is positive

definite[38]. Besides the efficiency, Choleski's decomposition scheme also needs less computer memory than other methods in solving these kinds of problems. It can be easily proven that the system of equations (4.24) is positive definite. Thus, Choleski's scheme is well suited for their solution.

Figure 4.5 shows a comparison between the theoretical deflection and three approximate deflections for a square plate with a edge clamped. The curves taken along the section $y=\ell_y/2$ have been normalized by the expression $p_0\ell_x^4/D$. The number of terms for the three approximations are 11, 15 and 21, respectively. The number of constraint points along the clamped edge is taken to be five, i.e., $I_1=5$. As can be seen from figure 4.5, the approximation curves approach the theoretical curve as the number of terms increases. The deflection at the centroid of the plate is $2.65573\times10^{-3}(p_0\ell_x^4/D)$ for the 11-term approximation, $2.73920\times10^{-3}(p_0\ell_x^4/D)$ for the 15-term approximation, and $2.79734\times10^{-3}(p_0\ell_x^4/D)$ for the 21-term approximation. The difference between the 11-term approximation and the 21-term approximation is approximately 5% and that between the 15-term approximation and the 21-term approximation is 2%. It can be seen that the 11-term approximation is good enough in the sense of convergence. The theoretical deflection at the centroid is $0.0028(p_0\ell_x^4/D)$[3] which is almost the same as that obtained from the 21-term approximation. This shows that the 11-term approximation is good enough for practical application, since the error is only 2%.

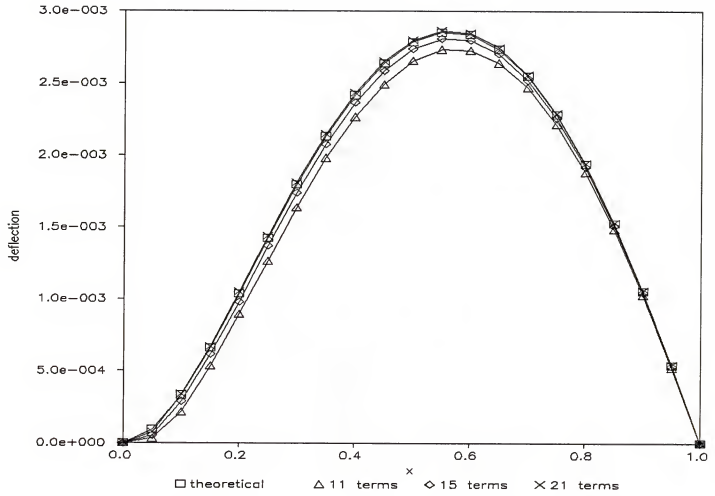

Figure 4.5 Deflection curves of a plate with one edge clamped and three edges simply supported taken along the section $y=\ell_y/2$

Figure 4.6 shows the deflection surface obtained from the 21-term approximation. The deflection in this figure has been normalized in the same way as above and magnified 35 times relative to the dimensions of the plate.

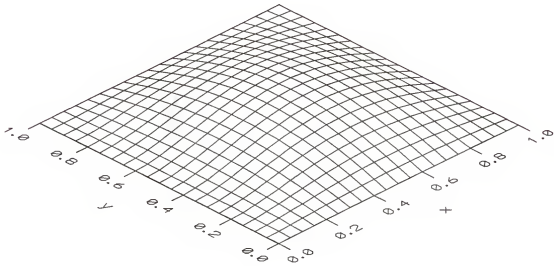

Figure 4.6 The deflection surface of a plate with one edge clamped and three edges simply supported

Since only discrete points along the edge x=0 are constrained to have zero slope, a variation of the slope along this edge between any two successive constraint points can be expected. This, however, is only a local phenomena. From figure 4.7, a diagram plotted with the deflection at the centroid of the plate versus the number of constraint points, it can seen that as the number of constraint points becomes greater than five, the deflection of the centroid becomes nearly a constant. As was stated earlier, there will be an exact clamped edge along x=0 as the number of constraint points approaches infinity.

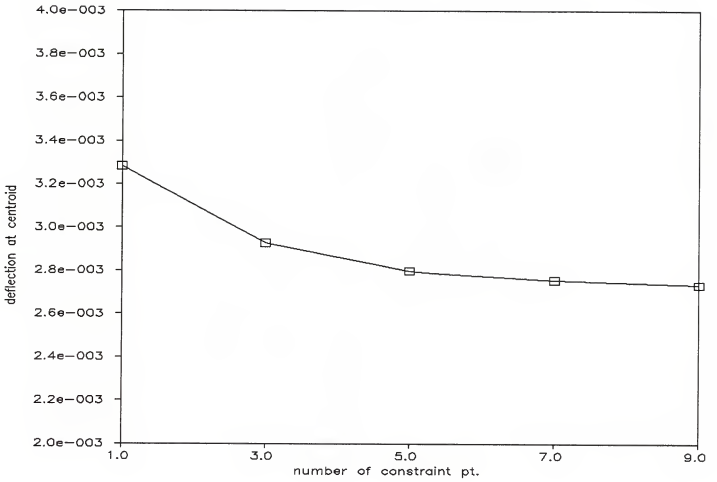

Figure 4.7 Deflection at the centroid versus number of constraint points

However, the deflection will be approximately the same as the case where only five constraint points were taken. Obviously, the local variation will not effect the deflection of the plate when a large enough number of constraint points is taken.

Plates with All Edges Clamped

Using the same strategy, it is also possible to change the previous case to one with all edges clamped (figure 4.8). The theoretical solution for this problem is very tedious and it is not possible to have a general theoretical expression for the deflection[3]. However, the method presented in this study makes the formulation the same as the previous case, with the exception of increasing the number of constraint equations.

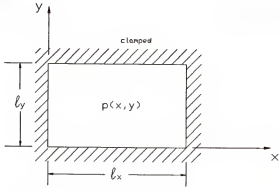

Figure 4.8 A clamped plate

In order to make every edge clamped, in addition to equation (4.20), the following constraint equations must be added:

$$G_i(a_{mn}) = \sum_{m=1}^{Nm} \sum_{n=1}^{Nn} a_{mn}(m\pi/\ell_x)\cos(m\pi)\sin(n\pi y_i/\ell_y) = 0$$
$$i=I_1+1, I_1+2, \ldots, I_2 \qquad (4.25.1)$$

$$G_i(a_{mn}) = \sum_{m=1}^{Nm} \sum_{n=1}^{Nn} a_{mn}(n\pi/\ell_y)\sin(m\pi x_i/\ell_x) = 0$$
$$i=I_2+1, I_2+2, \ldots, I_3 \qquad (4.25.2)$$

$$G_i(a_{mn}) = \sum_{m=1}^{Nm} \sum_{n=1}^{Nn} a_{mn}(n\pi/\ell_y)\sin(m\pi x_i/\ell_x)\cos(n\pi) = 0$$
$$i=I_3+1, I_3+2, \ldots, I_4 \qquad (4.25.3)$$

The constraint equation (4.20) corresponds to the slope boundary condition along edge x=0 where I_1 points are taken. Equation (4.25.1) corresponds to the edge $x=\ell_x$ where (I_2-I_1) points are taken, equation (4.25.2) corresponds to the edge y=0 where (I_3-I_2) points are taken, and equation (4.25.4) corresponds to the edge $y=\ell_y$ where (I_4-I_3) points are taken. If Q_{mni} is defined as follows:

$$Q_{mni} = \begin{cases} (m\pi/\ell_x)\sin(n\pi y_i/\ell_y) & \text{if } i \le I_1 \\ (m\pi/\ell_x)\cos(m\pi)\sin(n\pi y_i/\ell_y) & \text{if } I_1 < i \le I_2 \\ (n\pi/\ell_y)\sin(m\pi x_i/\ell_x) & \text{if } I_2 < i \le I_3 \\ (n\pi/\ell_y)\sin(m\pi x_i/\ell_x)\cos(n\pi) & \text{if } I_3 < i \le I_4 \end{cases} \qquad (4.26)$$

then all formulations will be the same as the previous case, except that the number of constraint equations is I_4.

Since it is almost impossible to obtain a general theoretical deflection formulation for this problem, the result obtained from the finite element method will be taken as a reference for comparison. The finite element method is commonly considered an accurate numerical scheme and is often used as a comparison reference[17][39]. For a clamped square plate, the theoretical maximum deflection, which occurs at the centroid, can be computed

to be $0.00126(p_0\ell_x^4/D)$ and that for the finite element method is $0.00127(p_0\ell_x^4/D)$. The difference is less than 1%, and shows the accuracy of the finite element method in this type of problem. It should be noted that both the finite element method and the modified Rayleigh-Ritz method provide only approximate solutions. In general, these approximations are not the same but will be close to one another.

Taking a square plate as an example, figure 4.9 shows a comparison between the deflections obtained from the finite element method with 400 square elements and three approximations using 11, 15, and 21 terms respectively. The deflection curves shown in the figure are taken along the section $y=\ell_y/2$ and have been normalized by the expression $p_0\ell_x^4/D$. As can be seen from the plot, convergence occurs when the number of terms reaches 21. The difference between the 15- and 21-term approximations is about 3.6%, and the difference between the 21-term approximation and the result obtained from the finite element method is about 0.5%. The 21-term approximation can be regarded as a very good approximation for engineering applications.

Figure 4.10 shows the deflection surface obtained from the 21-term approximation. The deflection in the figure has also been normalized in the same way as above and magnified 80 times with respect to the dimensions of the pate.

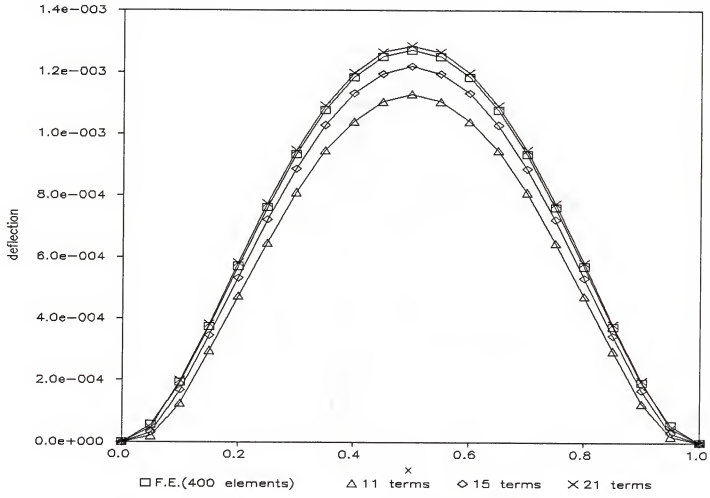

Figure 4.9 Deflection curves of a clamped plate taken along the section $y=\ell_y/2$

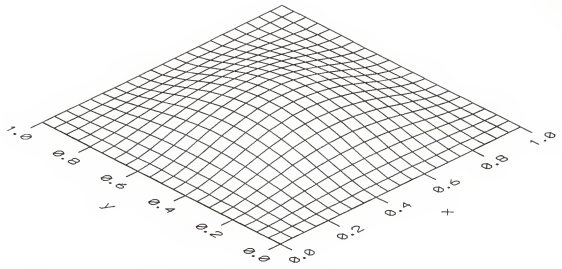

Figure 4.10 The deflection surface of a clamped plate

Nonrectangular Plates

One of the advantages of the proposed method is that it is possible to obtain the deflection surface of a nonrectangular plate from the formulation of a rectangular plate. The concept of approximating a nonrectangular plate from a rectangular plate requires imposing suitable constraints to the interior of the rectangular plate so as to make the geometrical situation at the constrained points the same as what is to be expected along the boundary of the nonrectangular plate.

Taking a circular plate as an example (shown in figure 4.11), a circle is "drawn" inside the rectangular plate (a square in this case) and constraint points are taken along the circle. The two constraints which need to be imposed on the chosen points are that the deflection at these points should be zero, and that the slope in the normal direction to the circle should be zero.

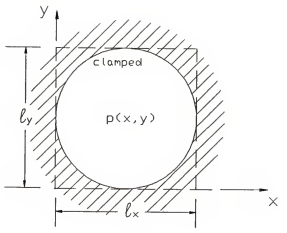

Figure 4.11 A clamped circular plate

If the same series as equation (4.12) is used, and the applied load is uniform, the above-mentioned constraints, in mathematical form, are

$$G_j = v(x_i,y_i) = \sum_{m=1}^{Nm}\sum_{n=1}^{Nn} a_{mn}\sin(m\pi x_i/\ell_x)\sin(n\pi y_i/\ell_y)$$

$$i=1,2,\ldots,I_1, \quad j=i \tag{4.27}$$

and

$$G_j = \partial v/\partial n = \cos(\theta)\partial v/\partial x + \sin(\theta)\partial v/\partial y$$

$$= \sum_{m=1}^{Nm}\sum_{n=1}^{Nn} a_{mn}\left[\frac{\cos(\theta)m\pi}{\ell_x}\cos\left(\frac{m\pi x_i}{\ell_x}\right)\sin\left(\frac{n\pi y_i}{\ell_y}\right)\right.$$

$$\left. + \frac{\sin(\theta)n\pi}{\ell_y}\sin\left(\frac{m\pi x_i}{\ell_x}\right)\cos\left(\frac{n\pi y_i}{\ell_y}\right)\right]$$

$$i=1,2,\ldots,I_1, \quad j=i+I_1 \tag{4.28}$$

where θ is the angle between the outward normal to the circle and the x axis. In equations (4.27) and (4.28), x_i and y_i are the coordinates of the constraint points and I_1 is the number

of constraint points. Since two constraints are imposed on each constraint point, the total number of constraint equations is $2I_1$.

If Q_{mni} is defined as follows:

$$Q_{mni} = \sin(m\pi x_i/\ell_x)\sin(n\pi y_i/\ell_y) \qquad \text{if } i \le I_1$$

$$= \frac{\cos(\theta)\,m\pi}{\ell_x}\cos\left(\frac{m\pi x_i}{\ell_x}\right)\sin\left(\frac{n\pi y_i}{\ell_y}\right)$$

$$+ \frac{\sin(\theta)\,n\pi}{\ell_y}\sin\left(\frac{m\pi x_i}{\ell_x}\right)\cos\left(\frac{n\pi y_i}{\ell_y}\right) \qquad \text{if } i > I_1 \tag{4.29}$$

then the formulation will take the same form as in the previous cases and the deflection surface can be obtained in the same manner.

Taking a square plate as the original plate and imposing constraints on a circle whose center is the centroid of the square and whose radius is equal to half of the length of the plate (figure 4.11), the result shown in figure 4.12 can be obtained. The deflection curves shown in figure 4.12 have been normalized by the expression $p_0\ell_x^4/D$. These curves, along with the theoretical curve[3], are taken along a diameter of the circle. The numbers of terms for the three approximations are 15, 17, and 21, respectively. The difference of the maximum deflection between the 15 and 21 term approximations is 7.3% but that between the 17 and 21 term approximations is only 1.5%. The convergence can be considered to occur when the number of terms is 21. As compared to the theoretical value, the error of the maximum deflection of the 21-term approximation is less than 3%.

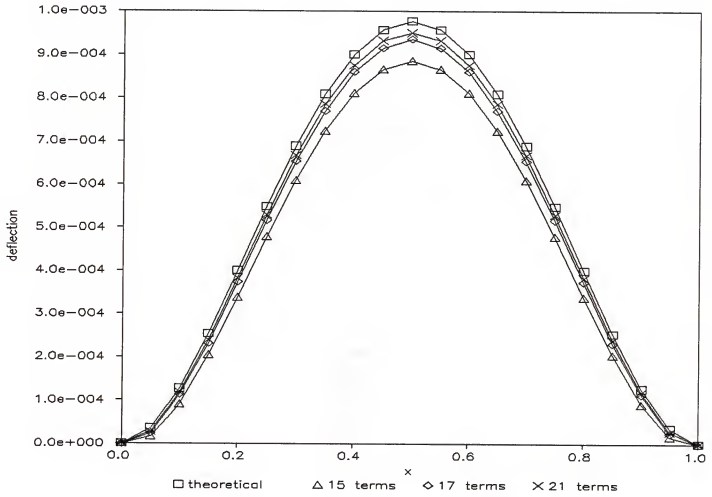

Figure 4.12 Deflection curves of a clamped circular plate taken along a diameter

In figure 4.13, the deflection surface obtained with the 21-term approximation is shown. The deflection in the figure has been normalized in the same way as above and magnified 100 times with respect to the dimensions of the plate.

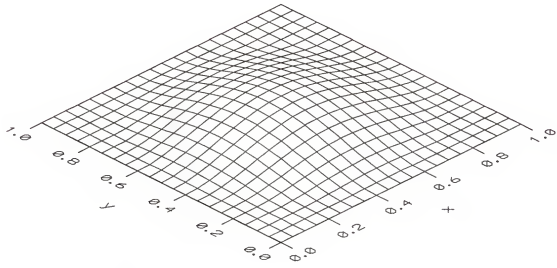

Figure 4.13 The deflection surface of a circular plate

Plates with Mixed Boundary Conditions

The problem of plates with mixed boundary conditions is a very difficult one in the classical theory of plates. Generally, the finite element method and the finite difference method are applied to solve this type of problem. Since the proposed method allows the boundary conditions to be satisfied through the use of Lagrangian multipliers on a finite number of discrete points along the boundary, it is possible to handle a mixed boundary condition problem without any major modification of the established formulations.

The strategy of applying the proposed method to a mixed boundary condition problem is to impose suitable constraints according to the desired boundary conditions at every constraint point where the boundary conditions are not completely satisfied by the approximation series, and to disregard those points where boundary conditions are satisfied. The situation shown in figure 4.14 is taken as an example for illustration.

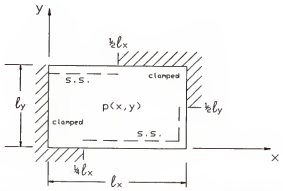

Figure 4.14 A plate with mixed boundary conditions

The constraint points are chosen inside the following regions along the edges of the plate:

region 1: $x=0$ and $0 \le y \le \ell_y$

region 2: $x=\ell_x$ and $\ell_y/2 \le y \le \ell_y$

region 3: $y=0$ and $0 \le x \le \ell_x/4$

region 4: $y=\ell_y$ and $\ell_x/2 \le x \le \ell_x$

With the same approximation series as equation (4.12), the constraint imposed on regions 1 and 2 is $\partial v/\partial x=0$, and that on regions 3 and 4 is $\partial v/\partial y=0$. With a similar definition of Q_{mni} as equation

(4.26), the formulations will be the same as in the previous cases. The general procedure is also the same.

Figure 4.15 shows a comparison between the result obtained from the finite element method with 400 elements and two approximations with the number of terms equal to 21 and 23. Since it is impossible to obtain a theoretical solution for this case, the result of the finite element method is taken as a reference with the same reason as that stated previously. In this example, the length of the plate ℓ_x is taken to be twice the width ℓ_y, The deflection curves, which are taken along the section $x=\ell_x/2$, have been normalized by the expression $p_0\ell_x^4/D$. The difference between the 21- and 23-term approximations is about 2.2% and that between the 23-term approximation and the finite element method is 4.7%. It can be seen from the figure that the left side is simply supported and the right side is clamped, as required by figure 4.14. This can also be seen from figure 4.16, which shows the entire deflection surface obtained with the 23-term approximation. Figure 4.16 has also been normalized in the same way as figure 4.15 has.

In figure 4.16, the trace of the simple support along the edges parallel to the x axis can be easily identified, but is not readily seen on the edge $y=\ell_y$. Since ℓ_y is only half of ℓ_x, the edges parallel to the y axis resist deflection more than the edges parallel to the x axis.

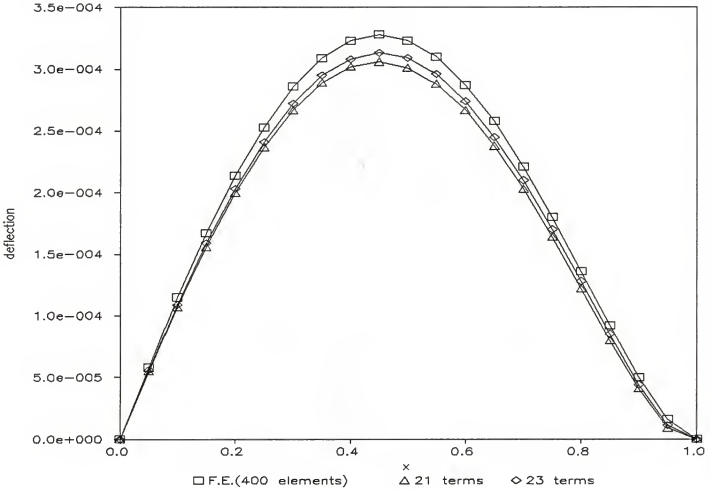

Figure 4.15 Deflection curves of a plate with mixed boundary conditions taken along the section $x=\ell_x/2$

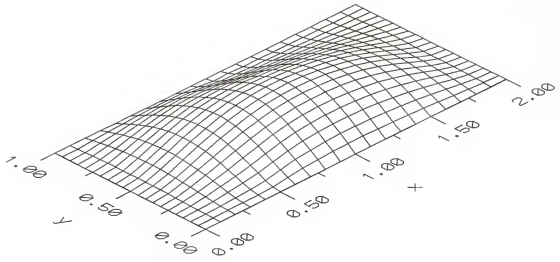

Figure 4.16 The deflection surface of a mixed boundary plate

Stiffened Plates

The problem of a stiffened plate can also be conveniently handled by the modified Rayleigh-Ritz method. The stiffeners, which are in the form of beams in this investigation, store energy when they are bent. The bending of the stiffeners is the same as the beam bending which has been discussed in the previous chapter. The deflections of the stiffeners should be compatible with the deflection of the plate. This constitutes the constraints between the plate and the stiffeners.

As a demonstration of how to apply the proposed method to a stiffened plate, a simply-supported square plate reinforced by only one stiffener is considered, as shown in figure 4.17.

If the deflection function of the stiffener is taken as the equation

$$u(\xi) = \sum_{k=1}^{Nk} d_k \sin\left(\frac{k\pi\xi}{\ell_\xi}\right) \tag{4.30}$$

where ℓ_ξ is the length of the stiffener and ξ is the local coordinate describing the stiffener, then the strain energy stored in the stiffener is

$$U_s = \frac{EI\pi^4}{4\ell_\xi^3} \sum_{k=1}^{Nk} d_k^2 k^4 \tag{4.31}$$

which is similar to equation (3.6). The strain energy of the stiffener U_s should be added to the Lagrangian.

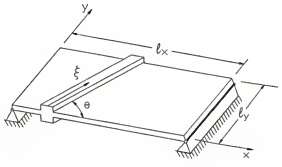

Figure 4.17 A stiffened plate

The relationships between the coordinate ξ and x and y are

$$\xi\cos(\theta) = x - x_0 \tag{4.32.1}$$

$$\xi\sin(\theta) = y - y_0 \tag{4.32.2}$$

where x_0 and y_0 are the coordinates of the origin of the local coordinate ξ in terms of the coordinate system x and y. The deflection compatibility requires that $v(x,y) = u(\xi)$ along the stiffener. If the deflection surface of the plate is approximated by the same sine series as equation (4.12), then choosing a finite

number (I_1) of discrete points along the stiffener will result in the following constraint equations:

$$G_i(a_{mn},d_k) = v(x_i,y_i) - u(\xi_i) = 0 \qquad i=1,2,..,I_1 \qquad (4.33)$$

where x_i, y_i and ξ_i follow the relationships of (4.32). These equations can be rewritten as

$$\sum_{m=1}^{Nm}\sum_{n=1}^{Nn} a_{mn}Q_{mni} - \sum_{k=1}^{Nk} d_k T_{ki} = 0 \qquad i=1,2,...,I_1 \qquad (4.34)$$

where

$$T_{ki} = \sin(k\pi\xi_i/\ell_\xi) \qquad (4.35.1)$$

and

$$Q_{mni} = \sin(m\pi x_i/\ell_x)\sin(n\pi y_i/\ell_y) \qquad (4.35.2)$$

The Lagrangian L is

$$L = \Pi + \sum_{i=1}^{I1} \lambda_i G_i$$

$$= \sum_{m=1}^{Nm}\sum_{n=1}^{Nn} [E_{mn}a_{mn}^2 - S_{mn}a_{mn} + \sum_{i=1}^{I1}(\lambda_i Q_{mni}a_{mn})] - \sum_{k=1}^{Nk} d_k \left(\sum_{i=1}^{I1} \lambda_i T_{ki}\right) \qquad (4.36)$$

Following the same procedure as the previous cases, and taking partial derivatives of the Lagrangian function L with respect to all parameters a_{mn} and d_k, the following relationships between the parameters and the Lagrangian multipliers are obtained:

$$a_{mn} = \frac{S_{mn}}{2E_{mn}} - \sum_{i=1}^{I1} \lambda_i \frac{Q_{mni}}{2E_{mn}} \qquad (4.37)$$

and

$$d_k = \sum_{k=1}^{I1} \lambda_i \; [\; T_{ki} \; / \; (2F_k) \;] \tag{4.38}$$

where

$$F_k = \frac{EI_s \ell_\xi}{4} \left(\frac{k\pi\xi}{\ell_\xi} \right)^4 \tag{4.39}$$

Substituting equations (4.37) and (4.38) into equation (4.34), the following equations in λ_i are obtained:

$$\sum_{i=1}^{I1} \lambda_i \left(\sum_{m=1}^{Nm} \sum_{n=1}^{Nn} \frac{Q_{mni} Q_{mni'}}{2E_{mn}} + \sum_{k=1}^{Nk} \frac{T_{ki} T_{ki'}}{2F_k} \right)$$

$$= \sum_{m=1}^{Nm} \sum_{n=1}^{Nn} \frac{S_{mn} Q_{mni'}}{2E_{mn}} \qquad i'=1,2,\ldots,I_1 \tag{4.40}$$

Solving for the undetermined multipliers in the above equations and substituting them into equations (4.37) and (4.38), the parameters a_{mn} and d_k are found. With these parameters, the deflection of the plate can be readily calculated.

Since it takes more terms for the proposed method to meet the requirement of unsatisfied boundary conditions (by the assumed deflection function) than to satisfy the compatibility requirement between the stiffener and the plate, less terms are necessary to give a convergent solution for the present case (where the boundary conditions are all simply supported and are automatically satisfied by the assumed deflection function) than for some of the previous cases with boundary conditions not all satisfied by the assumed deflection function, for example, the plate with mixed boundary conditions. Therefore, it takes only nine terms to obtain a convergent result for the case of a square plate

reinforced by a stiffener with $x_0=\ell_x/2$ and $y_0=0$, and θ equal to 90 degrees. Figure 4.18 shows the deflection surface of the stiffened square plate. The relative rigidity, which is defined as the product of the flexural rigidity of the plate times the thickness of the plate divided by the bending rigidity of the stiffener (Dh/EI_s) is computed to be 6.156×10^{-4}. In figure 4.18, the trace of the stiffener can be easily identified. The deflection surface has been normalized in the same manner as the previous cases.

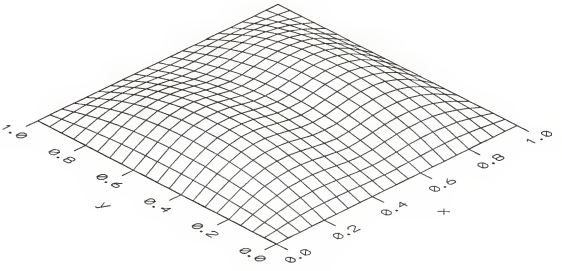

Figure 4.18 The deflection surface of a plate reinforced by a stiffener parallel to the y axis

If there is more than one stiffener, the strain energy of each stiffener should be added to the total potential energy. Each stiffener should be assumed to have a different deflection function with a different set of unknown displacement parameters, and the compatibility between the plate and each stiffener

should be regarded as constraints. The number of sets of parameters will be equal to the number of stiffeners, plus one set of parameters for the plate itself. Relationships between each set of parameters and the undetermined multipliers are obtained by differentiating the Lagrangian with respect to each parameter of each set. Combining these relationships with the constraints of deflection compatibility, a set of simultaneous equations similar to equation (4.40) is obtained. Thus the deflection of the plate can be obtained.

Figure 4.19 shows the deflection surface of a square plate diagonally reinforced by two stiffeners. For this case, a convergent result can be obtained with a nine-term approximation. The relative rigidity is 1.0×10^{-4} for both stiffeners. The traces of the stiffeners are easy to identify from the figure. The deflection surface has been normalized as before.

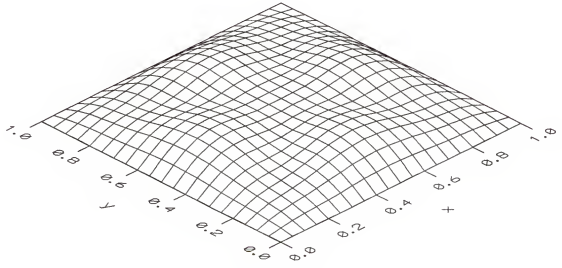

Figure 4.19 The deflection surface of a diagonally stiffened plate

Although the stiffened plate examples shown above are simple, the application of the proposed method to this type of problem can clearly be extended to more complex geometries. In the following section, a demonstration of how to handle a stiffened double plate, called a honeycomb sandwich plate, will be considered to illustrate the versatility of the proposed method.

Honeycomb Sandwich Plates

It is extremely difficult for conventional methods, even for the finite element method, to handle the problem of honeycomb sandwich plates. Neither the theoretical solution nor a finite element method solution is therefore available for the case shown in figure 4.20. However, by extending the procedure used to analyze the stiffened plates discussed in the previous section, it is possible to conveniently deal with this type of problem with the proposed method. This is one of the advantages of the proposed method over conventional methods.

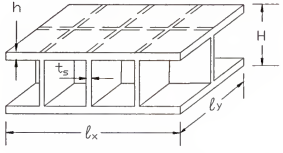

Figure 4.20 A honeycomb sandwich plate

A sandwich plate can be regarded as a combination of three parts, two of them are the top and bottom plates and the third represents the stiffeners. Since it was pointed out at the outset of this chapter that the plate problems dealt with in this study are considered linearly elastic, the principle of superposition is applicable. The deflection of the top or bottom plate of the sandwich structure can then be viewed as a superposition of two parts. One is the overall deflection of the whole structure and the other is the deflection of the top or bottom plate when the stiffeners are assumed rigid.

The deflection of either plate can then be obtained by superimposing their "local" deflection on the "global" deflection. The terminologies "local" and "global" are used as an indication of the deflection of the plates when the stiffeners are assumed rigid, and the overall deflection of the whole structure. Kirchhoff's assumptions for the analysis of plates will be taken to be valid. The strain energy stored in both the top plate and the bottom plate thus consists of three parts. The first is due to the local deflection when the global deflection is zero, the second is due to the global deflection when the local deflection does not exist, and the third is the interaction between the local and global deflections. Although we are dealing with a linear system, it is not possible to apply the principle of superposition to energy. It is for this reason that the third part of the strain energy is necessary. The third part can be regarded as

a gain in strain energy when the stress produced by the local deflection undergoes the global deflection.

To treat the honeycomb structure as three parts, the deflection functions for the top plate, the bottom plate, and the whole structure are independently assumed. The overall deflection function of the whole structure can be regarded as the deflection of a pseudo plate which is located on the middle plane of the whole structure, and which is parallel to both the top and bottom plates. The deflection functions for the top and bottom plates cover only their local deflections. Therefore the deflection function of the top plate on its intersection with the stiffeners has a zero value, and the same is true for the bottom plate. This is the constraint for the local deflection functions of both the top and the bottom plate. The real deflection of the top or bottom plate is the sum of its local deflection and the deflection of the pseudo plate.

To follow the same rule of calculating the potential energy and forming the constraint equations as was used in the previous cases, the local deflection functions for the top and bottom plates are taken respectively to be

$$v_t(x,y) = \sum_{m=1}^{Nm} \sum_{n=1}^{Nn} b_{mn} \sin(m\pi x/\ell_x) \sin(n\pi y/\ell_y) \qquad (4.41)$$

and

$$v_b(x,y) = \sum_{m=1}^{Nm} \sum_{n=1}^{Nn} c_{mn} \sin(m\pi x/\ell_x) \sin(n\pi y/\ell_y) \qquad (4.42)$$

The subscripts t and b denote, respectively, the top plate and the bottom plate. The global deflection function is taken to be the same as equation (4.12). The deflection functions of the stiffeners are taken as

$$u_i(\xi_i) = \sum_{n=1}^{N} d_n \sin\left(\frac{n\pi\xi_i}{\ell_i}\right) \qquad i=1,2,\ldots,I_r \tag{4.43}$$

where I_r is the number of stiffeners, ξ_i is the local coordinate describing the ith stiffener, and ℓ_i is the length of the ith stiffener.

The strain energy due to the local deflection of the top plate is

$$U_{t1} = \frac{D\ell_x\ell_y}{8} \sum_{m=1}^{Nm} \sum_{n=1}^{Nn} b_{mn}^2 \left[\left(\frac{m\pi}{\ell_x}\right)^2 + \left(\frac{n\pi}{\ell_y}\right)^2\right]^2 \tag{4.44}$$

and that of the bottom plate is

$$U_{b1} = \frac{D\ell_x\ell_y}{8} \sum_{m=1}^{Nm} \sum_{n=1}^{Nn} c_{mn}^2 \left[\left(\frac{m\pi}{\ell_x}\right)^2 + \left(\frac{n\pi}{\ell_y}\right)^2\right]^2 \tag{4.45}$$

The strain energy due to the global deflection of the top plate is

$$U_2 = \frac{D_c\ell_x\ell_y}{8} \sum_{m=1}^{Nm} \sum_{n=1}^{Nn} a_{mn}^2 \left[\left(\frac{m\pi}{\ell_x}\right)^2 + \left(\frac{n\pi}{\ell_y}\right)^2\right]^2 \tag{4.46}$$

where D_c is defined as

$$D_c = D + \frac{Eh}{(1-\nu^2)} \frac{(H-h)^2}{4} \tag{4.47}$$

The symbol H denotes the overall height of the honeycomb structure. Because of the symmetry about the middle plane of the whole structure, the strain energy due to the global deflection of the bottom

plate is the same as equation (4.46). The third part of the strain energy for the top plate is

$$U_{t3} = \frac{D\ell_x\ell_y}{4}\sum_{m=1}^{Nm}\sum_{n=1}^{Nn} a_{mn}b_{mn}\left[\left(\frac{m\pi}{\ell_x}\right)^2 + \left(\frac{n\pi}{\ell_y}\right)^2\right]^2 \qquad (4.48)$$

and that for the bottom plate is

$$U_{b3} = \frac{D\ell_x\ell_y}{4}\sum_{m=1}^{Nm}\sum_{n=1}^{Nn} a_{mn}c_{mn}\left[\left(\frac{m\pi}{\ell_x}\right)^2 + \left(\frac{n\pi}{\ell_y}\right)^2\right]^2 \qquad (4.49)$$

The strain energy of each stiffener is

$$U_{si} = \frac{EI\pi^4}{4\ell_i^3}\sum_{k=1}^{Nk} d_{ik}^2 k^4 \qquad i=1,2,\ldots,I_r \qquad (4.50)$$

If the external load applied on the top surface of the structure is uniformly distributed with intensity p_t, then the work done by this load is

$$W_t = \frac{p_t\ell_x\ell_y}{\pi^2}\sum_{m=1}^{Nm}\sum_{n=1}^{Nn}(a_{mn}+b_{mn})\left(\frac{1-\cos(m\pi)}{m}\right)\left(\frac{1-\cos(n\pi)}{n}\right) \qquad (4.51)$$

Similarly, the work done by a uniform load with intensity p_b distributed over the bottom surface of the structure is

$$W_b = \frac{p_b\ell_x\ell_y}{\pi^2}\sum_{m=1}^{Nm}\sum_{n=1}^{Nn}(a_{mn}+c_{mn})\left(\frac{1-\cos(m\pi)}{m}\right)\left(\frac{1-\cos(n\pi)}{n}\right) \qquad (4.52)$$

Therefore, the total potential energy is

$$\Pi = U_{t1} + U_{b1} + 2U_2 + U_{t3} + U_{b3} + \sum_{i=1}^{Ir} U_{si} - W_t - W_b \qquad (4.53)$$

The constraints between the global deflection and the deflections of the stiffeners are

$$G_{1ij} = \sum_{m=1}^{Nm} \sum_{n=1}^{Nn} a_{mn} Q_{mnij} - \sum_{k=1}^{Nk} d_{ik} T_{kij} = 0$$

$$i=1,2,\ldots,I_r,\ j=1,2,\ldots,J_i \quad (4.54.1)$$

The constraints for the deflection function of the top plate are

$$G_{2ij} = \sum_{m=1}^{Nm} \sum_{n=1}^{Nn} b_{mn} Q_{mnij} = 0$$

$$i=1,2,\ldots,I_r,\ j=1,2,\ldots,J_i \quad (4.54.2)$$

and for the bottom plate are

$$G_{3ij} = \sum_{m=1}^{Nm} \sum_{n=1}^{Nn} c_{mn} Q_{mnij} = 0$$

$$i=1,2,\ldots,I_r,\ j=1,2,\ldots,J_i \quad (4.54.3)$$

where

$$Q_{mnij} = \sin(m\pi x_{ij}/\ell_x)\sin(n\pi y_{ij}/\ell_y) \quad (4.55)$$

and

$$T_{kij} = \sin(k\pi \xi_j/\ell_i) \quad (4.56)$$

The symbol J_i denotes the number of constraint points taken on the ith stiffener.

The Lagrangian function takes the form:

$$L = \Pi + \sum_{i=1}^{Ir} \sum_{j=1}^{Ji} (\lambda_{ij} G_{1ij} + \mu_{ij} G_{2ij} + \zeta_{ij} G_{3ij}) \quad (4.57)$$

By taking partial derivatives of L with respect to all displacement parameters a_{mn}, b_{mn}, c_{mn}, and d_{ik} (i=1,2,...,I_r), and substituting the results into the constraint equations (4.54), the following equations are obtained:

$$\frac{2}{(D_c-D)\ell_x\ell_y}\left\{\sum_{i=1}^{Ir}\sum_{j=1}^{Ji}\left[(\lambda_{ij}-\mu_{ij}-\zeta_{ij})\left(\sum_{n=1}^{Nm}\sum_{m=1}^{Nn}\frac{Q_{mnij}Q_{mni'j'}}{E_{mn}}\right)\right]\right\}$$

$$-\frac{2\ell_{i'}^{3}}{EI\pi^4}\sum_{j=1}^{Ji'}\left[\lambda_{i'j}\left(\sum_{k=1}^{Nk}\frac{T_{ki'j}T_{ki'j'}}{K^4}\right)\right]=0$$

$$i'=1,2,\ldots,I_r,\ j'=1,2,\ldots,J_{i'} \qquad (4.58.1)$$

$$\frac{-2}{(D_c-D)\ell_x\ell_y}\sum_{i=1}^{Ir}\sum_{j=1}^{Ji}\left(\lambda_{ij}\sum_{n=1}^{Nm}\sum_{m=1}^{Nn}\frac{Q_{mnij}Q_{mni'j'}}{E_{mn}}\right)$$

$$+\left[\frac{2}{(D_c-D)\ell_x\ell_y}+\frac{4}{D\ell_x\ell_y}\right]\sum_{i=1}^{Ir}\sum_{j=1}^{Ji}\left(\mu_{ij}\sum_{n=1}^{Nm}\sum_{m=1}^{Nn}\frac{Q_{mnij}Q_{mni'j'}}{E_{mn}}\right)$$

$$+\frac{2}{(D_c-D)\ell_x\ell_y}\sum_{i=1}^{Ir}\sum_{j=1}^{Ji}\left(\zeta_{ij}\sum_{n=1}^{Nm}\sum_{m=1}^{Nn}\frac{Q_{mnij}Q_{mni'j'}}{E_{mn}}\right)$$

$$=\frac{4p_t}{D\pi^2}\frac{(1-\cos(m\pi))(1-\cos(n\pi))}{m\ n}\frac{Q_{mni'j'}}{E_{mn}}$$

$$i'=1,2,\ldots,I_r,\ j'=1,2,\ldots,J_{i'} \qquad (4.58.2)$$

$$\frac{-2}{(D_c-D)\ell_x\ell_y}\sum_{i=1}^{Ir}\sum_{j=1}^{Ji}\left(\lambda_{ij}\sum_{n=1}^{Nm}\sum_{m=1}^{Nn}\frac{Q_{mnij}Q_{mni'j'}}{E_{mn}}\right)$$

$$+\frac{2}{(D_c-D)\ell_x\ell_y}\sum_{i=1}^{Ir}\sum_{j=1}^{Ji}\left(\mu_{ij}\sum_{n=1}^{Nm}\sum_{m=1}^{Nn}\frac{Q_{mnij}Q_{mni'j'}}{E_{mn}}\right)$$

$$+\left[\frac{2}{(D_c-D)\ell_x\ell_y}+\frac{4}{D\ell_x\ell_y}\right]\sum_{i=1}^{Ir}\sum_{j=1}^{Ji}\left(\zeta_{ij}\sum_{n=1}^{Nm}\sum_{m=1}^{Nn}\frac{Q_{mnij}Q_{mni'j'}}{E_{mn}}\right)$$

$$=\frac{4p_b}{D\pi^2}\frac{(1-\cos(m\pi))(1-\cos(n\pi))}{m\ n}\frac{Q_{mni'j'}}{E_{mn}}$$

$$i'=1,2,\ldots,I_r,\ j'=1,2,\ldots,J_{i'} \qquad (4.58.3)$$

Solving equation (4.58) gives the undetermined multipliers λ_{ij}, μ_{ij}, and ζ_{ij}. With these multipliers, the displacement parameters can be calculated by taking partial derivatives of equation (4.57) with respect to each parameter. The computer program used to

solve the system of equations in λ_{ij}, μ_{ij}, and ζ_{ij} and to generate the deflection surface is listed in the appendix for reference.

Figures 4.21 and 4.22 show the deflection surfaces of a sandwich plate with a length of 3 units, a width of 1 unit, and an overall height of 0.1 units. The thickness of the plates is 0.01 units and that of the stiffeners is 0.01 units. Figure 4.21 shows the deflection surface of the top plate. The deflection in this figure is magnified 3,000 times with respect to the dimensions of the structure. Figure 4.22 shows the deflection surface of the bottom plate. The deflection of this figure is magnified 30,000 times with respect to the dimensions of the structure. It can be seen that the overall deflection (figure 4.22) is much smaller than the local deflection of the top plate (figure 4.21).

In figure 4.23, the maximum deflections of the top plate and the pseudo plate are shown. As expected, the difference between these two curves decreases as the thickness of the plate increases and approaches half of the overall height of the honeycomb. The load in this case is 1 force unit. Poisson's ratio is taken to be 0.3, and Young's modulus is 30×10^6 force unit over length unit square.

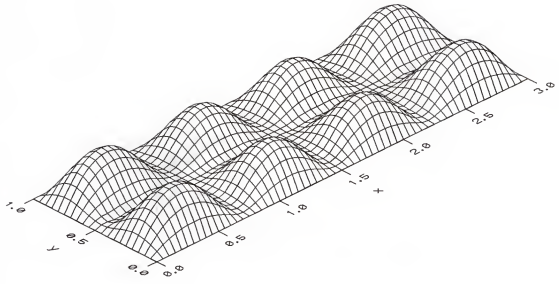

Figure 4.21 The deflection surface of the top plate

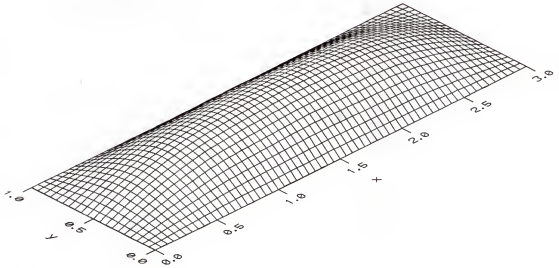

Figure 4.22 The deflection surface of the bottom plate

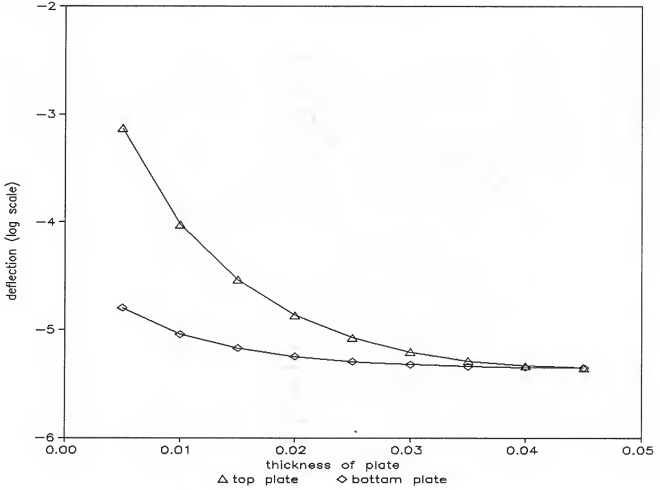

Figure 4.23 Maximum deflections of the top plate and the pseudo plate (in log scale)

CHAPTER 5
APPLICATIONS TO PLATES WITH HOLES

Introduction

A plate with arbitrarily shaped holes is a common structural element, but is extremely difficult to handle by the classical theory of plates. The finite element method, so far, is the approach that analysts prefer to use. However, as pointed out previously, the disadvantages of the preprocessing and postprocessing effort makes the finite element method an expensive way to deal with simple structural elements.

The Rayleigh-Ritz method using undetermined multipliers can be effectively applied to this type of plate problem. In the example of nonrectangular plates discussed in Chapter 4, the clamped boundary is moved inward from a rectangular plate to match the boundary curve of the nonrectangular plate, which is artificially drawn inside the rectangular plate. This concept can be further extended to the problem of plates with holes.

Taking a hole with a clamped boundary as an example, a pseudo plate of the same size as the hole can be fitted into the hole, with its boundary clamped. This pseudo plate can

then be integrated with the original plate, inside which the hole is located, and analyzed as a whole with the same procedure shown in the previous chapter. The pseudo plate inside the hole can then be disregarded. Under certain situations, such as a hole with free edges, it is necessary to superimpose additional forces (generalized forces) along the boundary so as to comply with the force boundary conditions. It has been shown[40] that load sources can be applied externally to the plate boundary to satisfy the boundary conditions at a finite number of points along the boundary. This concept is incorporated to solve the type of problem to be discussed in the following sections. With this concept, forces are artificially superimposed inside the hole but very close to its boundary, so as to make the boundary act as desired. As stated in Chapter 4, a variation between any two successive constraint points is inevitable but this variation is only a local phenomena. The following investigation is also based on Kirchhoff's three assumptions as outlined in Chapter 4.

An illustration of how to handle the problem of a square plate with a square clamped hole will be given first. This is a simple problem because the clamped edges have already provided the necessary forces to satisfy the boundary conditions and no additional forces are necessary.

Square Plates with Clamped Square Holes

The problem is described in figure 5.1. The edges of the hole are clamped and the boundary of the plate is simply supported.

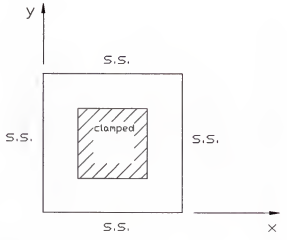

Figure 5.1 A plate with a clamped hole

As stated in the previous section, a pseudo plate is fitted into the hole and integrated with the original plate. The plates are then analyzed as a whole with the same procedure as that discussed in Chapter 4. By taking the same approximation series as equation (4.12), the formulation of the strain energy of the plate, including the pseudo plate inside the hole, is the same as equation (4.13). If the load acting upon the plate is uniform over the whole surface, including the pseudo plate, with the intensity p_0, then the formulation of the work done by the external load is the same as equation (4.14). The constraints are zero deflection and

zero normal slope, i.e., v=0 and $\partial v/\partial n=0$, along the edges of the hole. The formulation will be the same as that used in the case of nonrectangular plates provided that Q_{mni} is defined as equation (4.29).

For the proposed method, a 20-term approximation gives a convergent result. Figures 5.2 and 5.3 show comparisons of the result obtained from the 20-term approximation with that provided by the finite element method with 300 elements. Both figures have been normalized by the expression $p_0\ell_x^4/D$. Figure 5.2 is taken along the section $y=\ell_y/2$. Figure 5.3 is taken along the section $y=0.15\ell_y$. The maximum deflection occurs near $x=0.15\ell_x$ and $y=0.15\ell_y$. The maximum deflection obtained from the finite element method is $3.10725\text{x}10^{-5}(p_0\ell_x^4/D)$, and that obtained from the proposed method is $2.96271\text{x}10^{-5}(p_0\ell_x^4/D)$. The difference is less than 5%.

Figure 5.4 shows the deflection surface. The clamped edges of the hole can be identified from the plot. The deflection in figure 5.4 has been normalized in the same manner as figures 5.2 and 5.3 and magnified 1200 times with respect to the dimensions of the plate.

Simulation of a Cantilever Beam From a Clamped Beam

Although it takes no extra effort to handle a clamped hole, a more sophisticated technique is necessary to handle a hole with free edges. Before solving a plate with a free edge hole, an analogous beam problem will be considered,

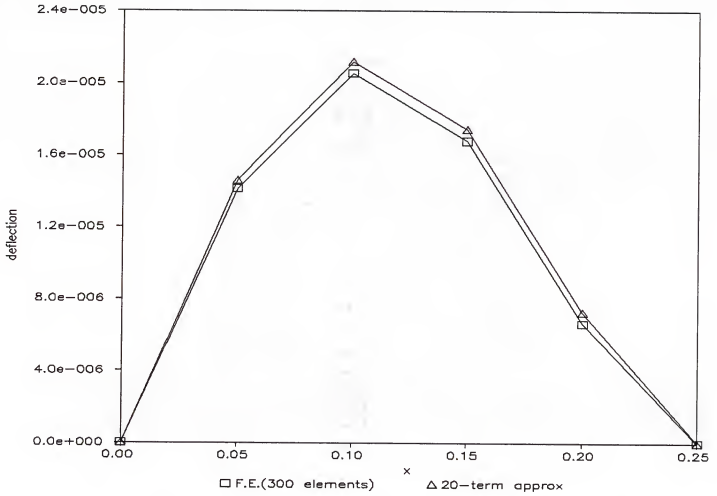

Figure 5.2 Deflection curves of a plate with a clamped hole taken along the section $y=\ell_y/2$

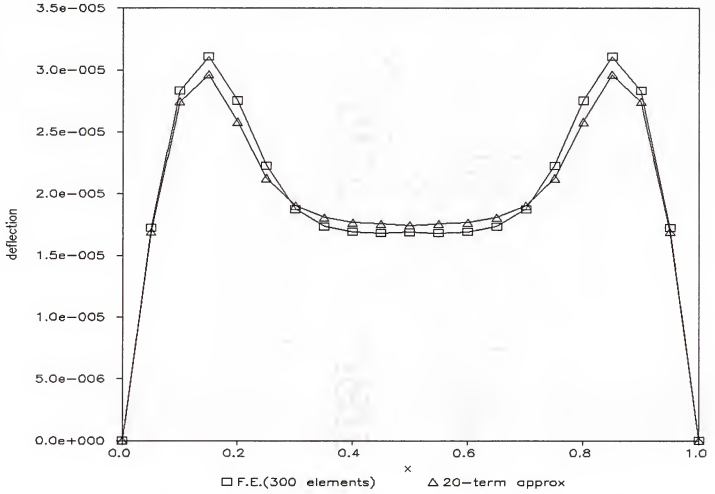

Figure 5.3 Deflection curves of a plate with a clamped hole taken along the section $y=\ell_y/4$

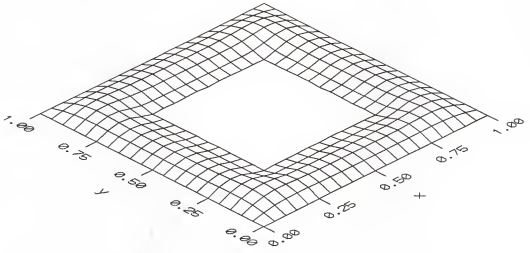

Figure 5.4 The deflection surface of a plate with a clamped hole

consisting of the simulation of a cantilever beam from a clamped-clamped beam. Consider the following condition (figure 5.5) where the middle portion of the beam is not loaded, and the other portions of the beam are uniformly loaded with load intensity p_0.

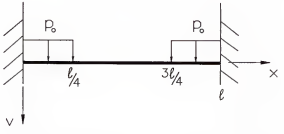

Figure 5.5 A clamped-clamped beam partially loaded

By taking the same series as equation (3.13) to be the approximate deflection function, the strain energy will take

the same form as equation (3.10) with the upper limit of the summation replaced by N. The work done by the applied load is

$$W = \sum_{n=1}^{N} a_n \frac{p_0 \ell}{n\pi} (1-\cos(n\pi/4)+\cos(3n\pi/4)-\cos(n\pi/4)) \tag{5.1}$$

Following the same procedure as illustrated in Chapter 3, the deflection curve, which is labeled iteration 1 in figure 5.6, can be obtained. The bending moment of the beam is shown in figure 5.7, also labeled iteration 1. In the same plots, another curve labeled "double cantilever" is drawn corresponding to the beam shown in figure 5.5, except that it is cut off at the center to simulate two cantilever beams. This configuration will be referred to as the "double cantilever beam." Note that when the clamped-clamped beam is cut off at the center, both halves can be treated as a uniformly loaded cantilever beam of length $\ell/4$ with an extra unloaded portion of length $\ell/4$. The unloaded portion can then be disregarded.

From the theory of beams, it is known that by applying external moments on a beam, the distribution of the bending moment of the beam can be changed. It is therefore suggested that external moments be applied at certain locations of the clamped-clamped beam to simulate a double cantilever beam. However, since adding external moments will introduce

reactions at the clamped ends, an iterative scheme will be needed to adjust the distribution of the bending moment.

In this case, in order to make both of the loaded portions of the clamped-clamped beam act like cantilever beams, external moments of the same amount as the bending moments at $x=\ell/4$ and $x=3\ell/4$ (calculated when no external moment was added, i.e., the bending moment labeled "iteration 1" in figure 5.7) are superimposed on the clamped-clamped beam at locations just inside the unloaded portion but very close to $x=\ell/4$ and $x=3\ell/4$. When these moments are applied, the resulting bending moments at $x=\ell/4$ and $x=3\ell/4$ will be smaller than before. Now this smaller amount can be superimposed at the same locations again. This will further reduce the resulting bending moments at $x=\ell/4$ and $x=3\ell/4$. By repeating this procedure, the bending moment will finally vanish at $x=\ell/4$ and $x=3\ell/4$ and the same bending moment distribution as that of a cantilever beam acted upon by uniform load can be obtained.

The process of iteration is shown in figures 5.6 and 5.7. It can be seen from figure 5.7 that the moment distribution in the loaded region is gradually reduced, and that inside the unloaded region is gradually increasing. Since the unloaded region represents a "hole," the increase in the bending moment inside the unloaded portion has no meaning. Due to the applied moment, the moment diagram has a discontinuity at $x=\ell/4$ and $x=3\ell/4$.

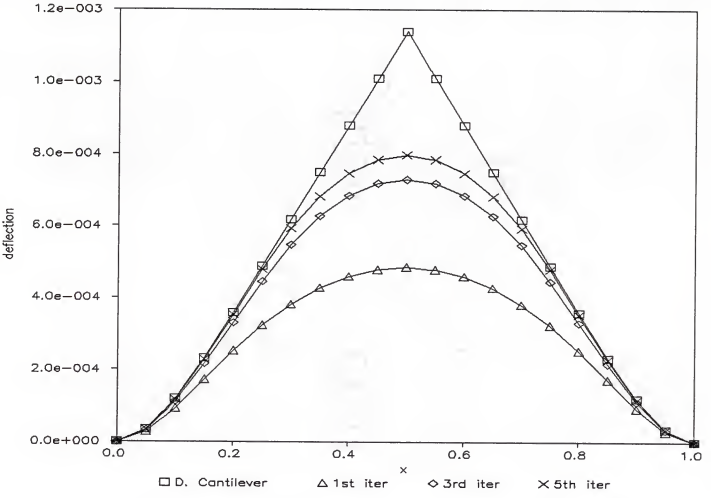

Figure 5.6 Deflection curves of the double cantilever beam

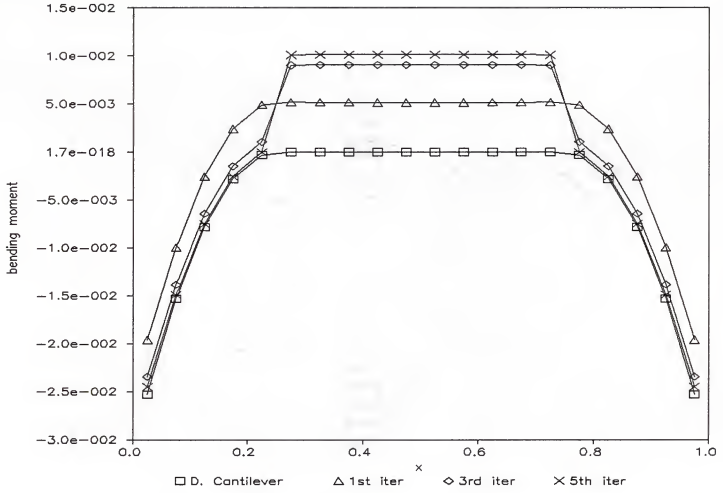

Figure 5.7 Bending moment curves of the double cantilever beam

The final result in both figures is labeled iteration 5. After five iterations, the increase in deflection at $x=\ell/4$ is less than 2% between two successive iterations. From figure 5.6, it can be seen that the deflection at $x=\ell/4$ converges to the deflection of a uniformly loaded cantilever beam with length equal to $\ell/4$ (the curve labeled double cantilever beam). From figure 5.7, it can be further understood that the moment distribution converges to that of a cantilever beam.

The same approach can now be applied to the case of plates with free holes. This is illustrated in the following section by the case of a square plate with a central square hole.

Square Plates with Free Square Holes

Consider a simply-supported plate which has a centered square hole as shown in figure 5.8. The plate is uniformly loaded with the load intensity p_0. To begin, a simply-supported plate without a hole is considered. The plate is uniformly loaded except for the portion where the hole will be placed. By choosing the same deflection function as equation (4.12), the same formulation for the strain energy as equation (4.13) will be used.

The work done by the external load is

$$W = W_p - W_h \tag{5.2}$$

where W_p is the work done by the external load when a plate without a hole is uniformly loaded, and W_h is the work done by

the external load distributed over the region where the hole is supposed to be located. In equation (5.2),

$$W_p = \frac{p_0 \ell_x \ell_y}{\pi^2} \sum_{m=1}^{Nm} \sum_{n=1}^{Nn} a_{mn} \left(\frac{1-\cos(m\pi)}{m}\right)\left(\frac{1-\cos(n\pi)}{n}\right) \quad (5.3)$$

and

$$W_h = \frac{p_0 \ell_x \ell_y}{\pi^2} \sum_{m=1}^{Nm} \sum_{n=1}^{Nn} a_{mn} \left[\left(\frac{\cos(m\pi/4)-\cos(3m\pi/4)}{m}\right) \cdot \left(\frac{\cos(n\pi/4)-\cos(3n\pi/4)}{n}\right)\right] \quad (5.4)$$

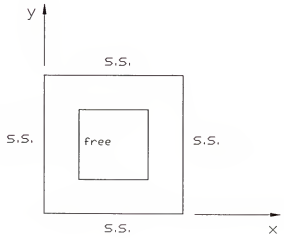

Figure 5.8 A plate with a free hole

By using the work formula (5.2) and following the same procedure as that shown in Chapter 4, the deflection surface of a simply-supported plate acted upon by a uniform load will be obtained with the hole region not loaded. The moments along the hole edges can be calculated. Since the moment of a plate at a free edge is zero, the moments along the edges

of the hole should be reduced to zero. To simulate the effect of a hole, external moments are superimposed at constraint points chosen from the edges of the hole so as to reduce the moment at each constraint point. The amount of external moment applied at each constraint point is the amount calculated from the original plate (when no external moment was added). As illustrated in the previous section, by iteratively superimposing moments at the constraint points, the bending moment along the hole edges will be gradually reduced. Since the bending moment in a plate is continuously distributed along a section, it is necessary to multiply this moment value by the distance between two successive constraint points of each section in order to transfer a distributed moment into several discrete concentrated moments.

For the case shown in figure 5.8, the maximum deflection occurs approximately at the point $x=\ell_x/4$ and $y=\ell_y/2$ or its image points distributed about the centroid of the plate. The maximum deflection, obtained with a 20-term approximation, is $3.1213\times10^{-3}(p_0\ell_x^4/D)$ for the sixth iteration and $3.24080\times10^{-3}(p_0\ell_x^4/D)$ for the seventh iteration. For every iteration, the 20-term approximation gives a convergent deflection surface with the loading of that iteration. The difference between the sixth and the seventh iteration is less than 4%. The iteration can be considered convergent.

Figures 5.9 and 5.10 show comparisons between the finite element method with 300 elements and the proposed method with

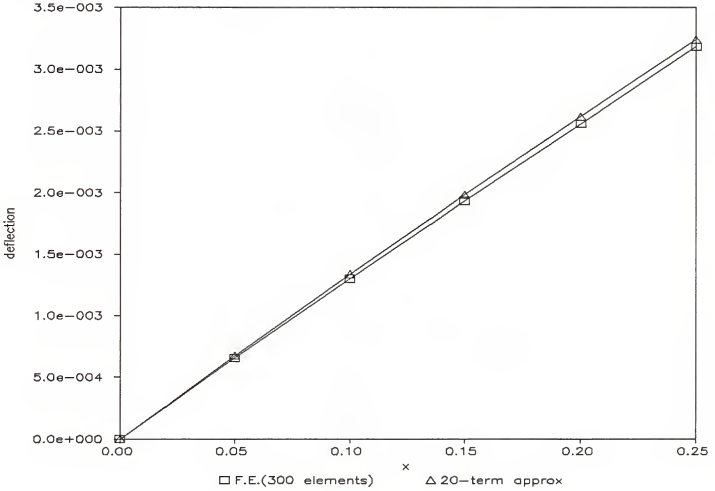

Figure 5.9 Deflection curves of a plate with a free hole taken along the section $y=\ell_y/2$

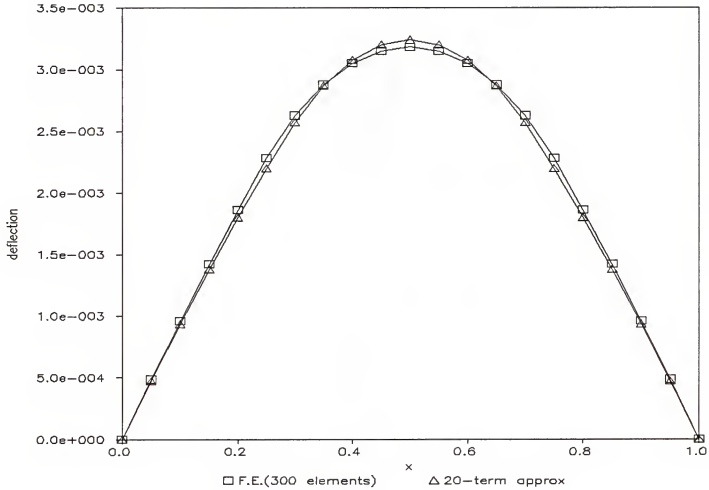

Figure 5.10 Deflection curves of a plate with a free hole taken along the section $y=\ell_y/4$

the 20-term series and seven iterations. The numerical value of the maximum deflection calculated from the finite element method with 300 elements is $3.183626 \times 10^{-3}(p_0 \ell_x^4/D)$. The difference between the finite element method and the proposed method is less than 2% for the seventh iteration. The deflections in both figures have been normalized by the expression $p_0 \ell_x^4/D$. The curve shown in figure 5.9 is taken along the section $y=\ell_y/2$, up to the edge of the hole. In figure 5.10, the curve is taken along the whole section $y=\ell_y/4$. From these figures, it can be seen that the approximation is very good.

Figure 5.11 shows the deflection surface of the case shown in figure 5.8. The deflection surface has been normalized in the same manner as before, and has been magnified 800 times with respect to the plate dimensions.

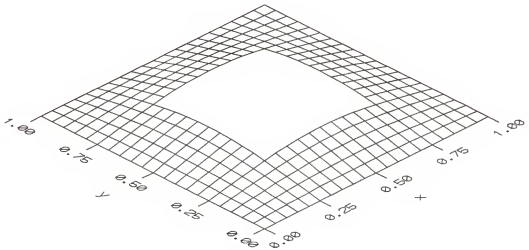

Figure 5.11 The deflection surface of a plate with a free hole

CHAPTER 6
APPLICATIONS TO SHELL PROBLEMS

Introduction

The behavior of a plate element under a transverse load is usually decided by the action of moments, including both bending moments and twisting moments, while a thin shell generally transmits the external load by a membrane stress which is uniformly distributed over the cross section of the shell and normal to it. This stress is basically determined by the static equilibrium of the shell and is independent of the bending effect[3]. Bending only has effect on areas close to boundaries and reinforcements. Although the bending has only a localized character, it is important in obtaining actual deformations near the boundaries and the reinforcements, especially when the shell is reinforced with stiffeners that are close to each other. In view of the fact that the membrane stress is generally independent of the bending effect, the stresses due to bending can be superimposed on the membrane stress to obtain a more accurate stress distribution in the region close to a boundary or a reinforced area.

The bending of a shell is more or less similar to that of a plate, and the theory of plates may be applied to shell problems in dealing with bending. Thus, it is possible to extend the approach of the proposed method presented in the previous chapters to shell problems. However, it should be noted that the proposed method can only be used to determine the bending effect, and does not supply any information about the membrane stress. In the following study, the focus shall be confined to the linear bending phenomena of axisymmetrical cylindrical shell problems.

For axisymmetrical cylindrical shells, it is possible to treat the problem as a beam supported on an elastic foundation[35]. In this case, the modulus of the "foundation" is given by

$$K_h = Eh / r^2 \tag{6.1}$$

where E is Young's modulus of the shell, r is the radius of the cylindrical shell, and h is the thickness. If the cylinder is regarded as a combination of many axial strips, then the effect of the "elastic foundation" arises from the fact that if any strip is deflected or moved radially, the adjacent strips will constrain its deflection or movement. Each strip will store an additional portion of strain energy which is the energy absorbed by the "elastic foundation." In other words, the cylindrical shell can store more strain energy by being deflected less.

Cylindrical Shells of Infinite Length Supported by a Rigid Ring

As mentioned above, bending has only a localized character for shells. The effect of bending on the deflections of shells reduces rapidly as the distance from boundaries or reinforcements increases. This phenomena will be illustrated in the following example. Consider the situation shown in figure 6.1 where a cylindrical shell is reinforced or supported by a rigid circumferential ring (in order to have a perfect rigid ring, the ring is considered very thick in the radial direction).

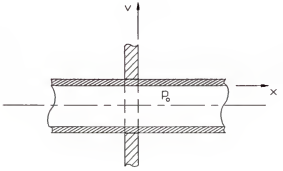

Figure 6.1 A rigidly supported cylindrical sell

The coordinate system is defined as follows (figure 6.2): The axial direction is the x axis, the radial deflection is the v axis, and the origin is located at a point on the inside surface of the shell. With the coordinates defined as above, the deflection v of the shell is a function of the x coordinate and the circumferential distance from the origin,

which will be defined as the circumferential coordinate and denoted by y.

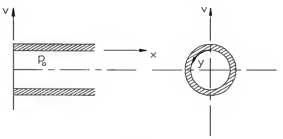

Figure 6.2 Coordinate system for the shell problems

Under a special circumstance, when both the geometrical shape and the deflection of the shell are axisymmetrical, the deflection itself is independent of the circumferential coordinate y and, thus, can be considered one-dimensional. Figure 6.1 represents one such case. If the origin is chosen on the rigid support, then clearly v=0 at x=0 for the situation shown in figure 6.1.

As in the previous chapters, a deflection function is assumed first. Since the radial deflection of any point in a circumferential element of the shell is the same, the deflection function is chosen as follows:

$$v(x) = a_0 + \sum_{n=1}^{N} a_n \cos(n\pi x/\ell) \tag{6.2}$$

The symbol ℓ denotes a reference length. The reference length should be chosen such that

$$\beta = \ell[Eh/(4Dr^2)]^{1/4} > 5 \tag{6.3}$$

in order that the location at $x=\ell$ can be regarded as infinitely far away from the ring, and bending has no effect on the shell beyond this location[35]. The symbol D was defined in equation (4.7). The strain energy due to bending of the shell is expressed as

$$U_1 = \int_0^{\ell} \frac{D}{2} \left(\frac{d^2v}{dx^2}\right)^2 dx = \frac{D\pi^4}{4\ell^3} \sum_{n=1}^{N} a_n^2 n^4 \tag{6.4}$$

and the "hoop strain energy," which is defined as the strain energy stored in the shell due to the effect of the "elastic foundation," is

$$U_2 = \int_0^{\ell} \frac{K_h v^2}{2} dx$$

$$= \frac{Eh\ell}{2r^2} \left(\frac{a_0^2}{2} + \sum_{n=1}^{N} a_n^2 \right) \tag{6.5}$$

If the pressure inside the cylindrical shell is p_0, then the work done by this pressure in radially expanding the shell is

$$W = \int_0^{\ell} p_0 v(x)\, dx = p_0 a_0 \ell \tag{6.6}$$

As before, the potential energy is

$$\Pi = U_1 + U_2 - W \tag{6.7}$$

Since the only boundary condition is that the radial defection at x=0 is zero, the only constraint equation is

$$G_1(a_n) = a_0 + \sum_{n=1}^{N} a_n = 0 \tag{6.8}$$

By following the same procedure as described in the previous chapters, the Lagrangian function is formed as follows:

$$L = U_1 + U_2 - W + \lambda_1 G_1 \tag{6.9}$$

and the following relationships exist:

$$a_0 = (p_0 \ell - \lambda_1) / (K_h \ell) \tag{6.10.1}$$

$$a_n = -\lambda_1 / \alpha_n \quad n=1,2,\ldots,N \tag{6.10.2}$$

where

$$\alpha_n = [(D\pi^4 n^4)/(2\ell^3) + K_h \ell/2] \tag{6.11}$$

By substituting these equations back into the constraint equation (6.8), the undetermined multiplier λ_1 can be calculated. By substituting the multiplier into equations (6.10.1) and (6.10.2), the displacement parameters a_0 and a_n (n=1,2,...,N) can be obtained.

The results are shown in figures 6.3 and 6.4. Figure 6.3 shows the deflection curve of three approximations with N=7, 12, and 17 respectively, along with the theoretical deflection curve[35]. In this example, h=0.01, ℓ=1.0, p_0=1.0, r=1.0, E=3x10^7, and ν=0.3. Any appropriate unit system can be chosen for the above information. From the plot, one can see that only ten terms are needed for good accuracy. The value of β is about ten in this case and thus, when x > $\ell/2$, the radial deflection of the reinforced shell becomes the same as the increase in the radius of a cylindrical shell which is free to expand without any constraint. This can be readily seen from the figure. It can then be understood that the bending

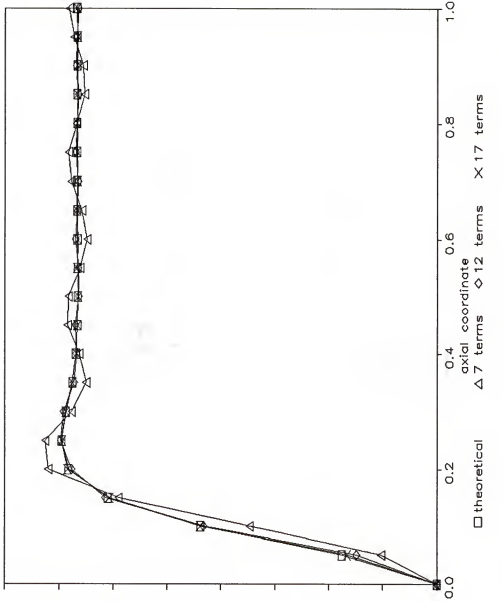

Figure 6.3 Deflection curves of a rigidly supported shell

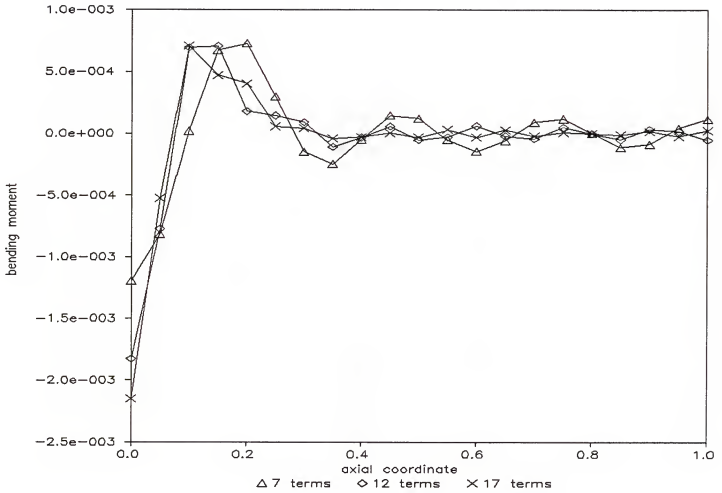

Figure 6.4 Bending moment curves of a rigidly supported shell

effect has a localized character and is only important in the region close to the boundary or reinforcements. As a matter of fact, the deflection due to bending is a rapidly damped oscillatory curve with a wave length $\ell_w = 2\pi\ell / \beta$[35]. This can be seen from the figure.

Figure 6.4 shows the moment diagrams for the three different approximations. As can be seen from the diagrams, the bending moment dies out very rapidly after $x > \ell/2$. Since the bending moment is a quantity resulting from the second derivative of the deflection curve, the fluctuation is much more pronounced than that of the deflection curve. It is, however, possible to smooth out the fluctuation by increasing the number of terms, as will be illustrated in a later case.

Cylindrical Shells of Infinite Length Reinforced by a Narrow Ring

The problem of a shell reinforced with a narrow circular ring will be considered. The solution can be obtained by using the same strategy described above. Consider an infinitely long cylindrical shell reinforced with a ring, as shown in figure 6.5. The coordinate system will be taken as that shown in figure 6.2 with the origin located on the ring. Since the shell is infinitely long, it may be taken to be symmetrical about the ring, and thus only half of the arrangement will be taken into account in the following discussion.

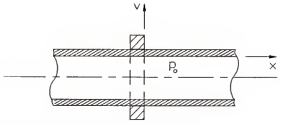

Figure 6.5 A shell reinforced by a narrow ring

Using the approximation series in equation (6.2), the same formulations for strain energy as equations (6.4) and (6.5), and the same expression for work as equation (6.6) are obtained. Since the narrow ring will expand when the shell expands due to the action of the pressure p_0 inside the cylindrical shell, strain energy will be stored. This strain energy must be accounted for in the formulation. The relationship between the increase of the radius of a narrow ring and the pressure p_r applied inside the ring is linear[35][41]:

$$v_r = p_r / K_r \tag{6.12}$$

where v_r is the increase in the inside radius of the ring and K_r is defined as

$$K_r = EA_r / r_r^2 \tag{6.13}$$

In the above equation, E denotes Young's modulus of the ring (which will be taken as the same as that of the shell in this study), A_r is the cross section area of the ring, and r_r is the inside radius of the ring. Since the thickness of the shell is supposed to be very thin in comparison to the other

dimensions, the radius of the ring r_r is considered approximately the same as that of the shell.

Equations (6.12) and (6.13) are only valid when the thickness of the ring in the radial direction is small in comparison with the radius of the ring, and the change in radius is also small in comparison to the original radius. Therefore, in equation (6.13), r_r may be taken as the original radius of the ring and assumed constant over the process of the expansion of the ring. K_r can thus be assumed constant too. The strain energy stored in the ring is

$$U_r = K_r v_r^2 / 2 \tag{6.14}$$

With the same assumed deflection function as in the previous section, the total potential energy of the system, including both the shell and the ring, is

$$\Pi = U_1 + U_2 + U_r - W \tag{6.15}$$

The only difference between this case and the previous one is that now the deflection is nonzero at x=0. Thus, the constraint is that the defection of the shell should be compatible with the increase of the radius of the ring, i.e.,

$$G_1(a_n) = \left(a_0 + \sum_{n=1}^{N} a_n \right) - v_r = 0 \tag{6.16}$$

Then the Lagrangian function takes the form

$$L = U_1 + U_2 + U_r - W + \lambda_1 G_1 \tag{6.17}$$

Following the same procedure as before, the same relationships as equations (6.10.1) and (6.10.2) are obtained.

By taking the partial derivative of L with respect to v_r, an additional equation is found:

$$K_r v_r - \lambda_1 = 0 \qquad (6.18)$$

By comparing equation (6.18) with equation (6.12), it can be seen that λ_1 is the pressure that acts upon the ring when the inside pressure of the cylindrical shell is p_0. Thus, λ_1 controls the deflection of the shell at x=0.

Combining equation (6.18) with the constraint equation (6.16) and equations (6.10), the displacement parameters a_0 and a_n (n=1,2,...,N), and the increase of the radius of the ring, v_r, can be calculated. Figures 6.6 and 6.7 show the results of three different approximations with the same geometry and material used in the previous case, and A_r=0.002. Figure 6.6 shows a comparison of deflections between the approximations and the theoretical solution[35]. For the region far away from the reinforcement, the deflection approaches a constant value, which is the increase of the radius of a similar, nonreinforced cylinder acted upon by the same internal pressure. This is the same for both the present and the previous cases, as would be expected. Figure 6.7 shows the moment diagrams for the three different approximations. It can be seen that the moment decays when x is large enough. This phenomena has been explained in the previous section.

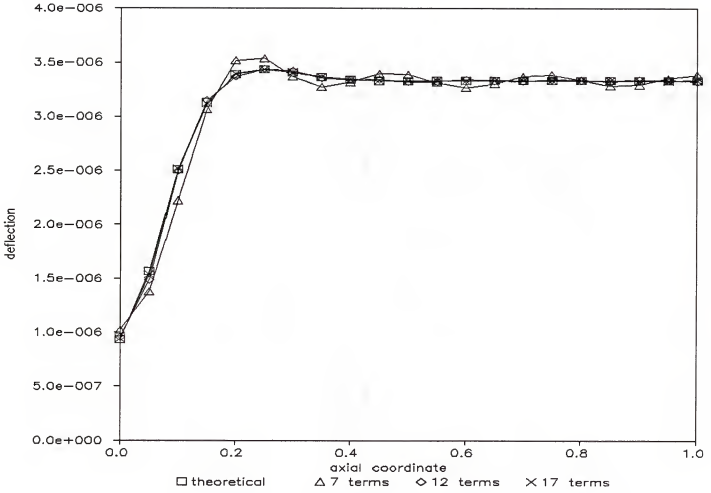

Figure 6.6 Deflection curves of a shell reinforced by a narrow ring

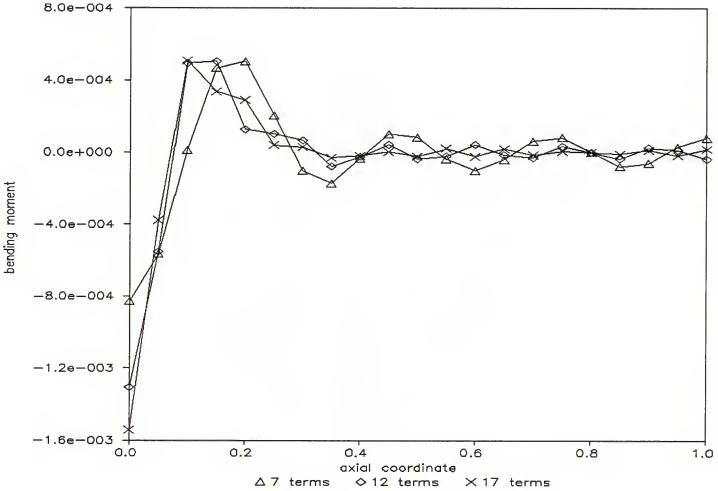

Figure 6.7 Bending moment curves of a shell reinforced by a narrow ring

Cylindrical Shells of Finite Length with Both Ends Clamped

Figure 6.8 shows a cylindrical shell of finite length fixed at both longitudinal ends. The coordinate system of this problem will be taken as the same system shown in figure 6.2, with the origin located at the left boundary of the cylinder and the positive x axis running towards the right.

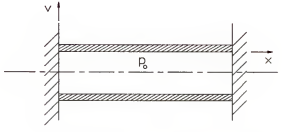

Figure 6.8 A shell fixed at both ends

The only difference between the present case and the previous cases is that the deflection of the shell is zero at the both x=0 and x=ℓ. Here ℓ is no longer a reference length, it is the longitudinal dimension of the shell.

If the same deflection function as equation (6.2) is assumed, then the formulation is the same as before, except that there is one additional constraint:

$$G_2(a_n) = a_0 + \sum_{n=1}^{N} a_n \cos(n\pi) = 0 \qquad (6.19)$$

Under this condition, the Lagrangian function is

$$L = U_1 + U_2 - W + \lambda_1 G_1 + \lambda_2 G_2 \qquad (6.20)$$

The displacement parameters are as follows, using the same procedure illustrated in the previous sections:

$$a_0 = (p_0\ell - \lambda_1 - \lambda_2) / (K_h\ell) \qquad (6.21.1)$$

$$a_n = -[\lambda_1 + \lambda_2\cos(n\pi)] / \alpha_n \qquad (6.21.2)$$

Substituting these relationships (6.21.1) and (6.21.2) into the constraint equations (6.8) and (6.19) will result in two linear equations with the undetermined multipliers λ_1 and λ_2 as unknowns. It then follows that the displacement parameters can be obtained by using equation (6.21).

Using the same geometry and material as in the previous cases, the results shown in figures 6.9 and 6.10 are obtained. In figure 6.9, the deflections of the shell with three different approximations, N=7, 12, and 17 respectively, are shown. The theoretical deflection derived from the basic theory of shells is also shown for comparison. Since the difference between the 12-term approximation and the theoretical curve is almost neligible, the 12-term series may be taken as a very good approximation of the deflection. Again, since β (referring to equation 6.3) is about twice five, the deflection of the shell at the region around $x=\ell/2$ is approximately the same as a similar cylindrical shell without reinforcements. Figure 6.10 shows the moment diagrams corresponding to the approximate deflection curves shown in figure 6.9. The moment is approximately zero around $x=\ell/2$ for the same reason.

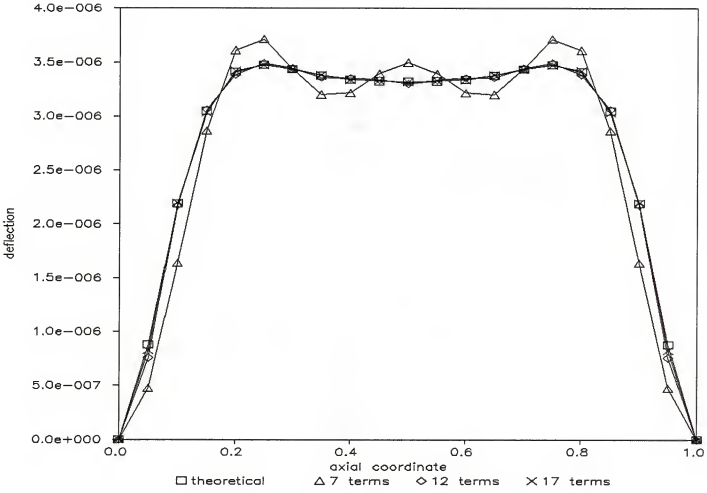

Figure 6.9 Deflection curves of a shell with both ends clamped

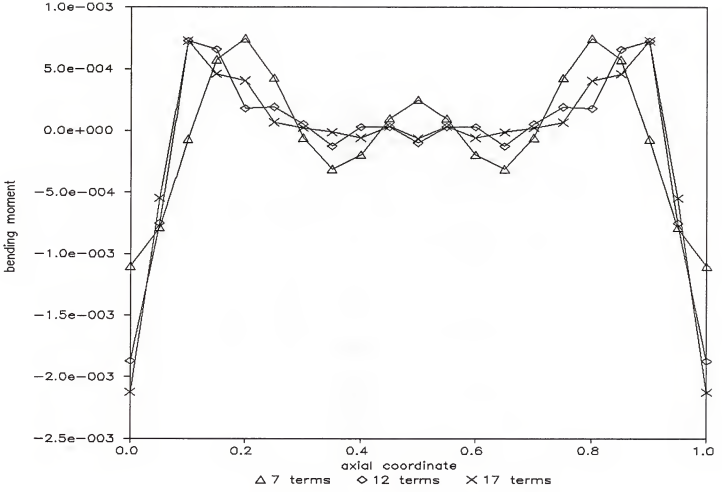

Figure 6.10 Bending moment curves of a shell with both ends clamped

Clamped Cylindrical Shells with Circumferential Ring Reinforcements

The cases discussed so far can be further extended to a cylindrical shell clamped at both ends and reinforced with rings as shown in figure 6.11. The coordinate system will remain the same.

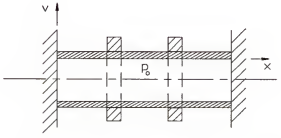

Figure 6.11 A clamped shell reinforced by rings

The strain energy stored in each ring should be added to the total potential energy, i.e.,

$$\Pi = U_1 + U_2 + \Sigma U_{ri} - W \qquad (6.22)$$

where U_{ri} is defined the same as in equation (6.14), with the subscript i denoting the ith ring. The summation in the above equation should be taken over all rings.

The compatibility constraint states that the deflection of the shell should be compatible with the radial expansion of the rings. Besides equations (6.8) and (6.19), the following equations, which define this compatibility, should also be part of the constraint equations:

$$G_{3i}(a_n) = \left(a_0 + \sum_{n=1}^{N} a_n \cos(n\pi x_i/\ell) \right) - v_{ri} = 0$$
$$i=1,2,\ldots,I_r \qquad (6.23)$$

where v_{ri} is the radial expansion of the ith ring and x_i is its location in the x axis. I_r is the number of rings. By following the same procedure outlined in the previous sections, the following equations for the displacement parameters can be obtained:

$$a_0 = \left(p_0\ell - \lambda_1 - \lambda_2 - \sum_{i=1}^{I_r} \mu_i \right) / \left(K_h\ell \right) \qquad (6.24.1)$$

$$a_n = -\left[\lambda_1 + \lambda_2\cos(n\pi) + \sum_{i=1}^{I_r} \mu_i \right] / \alpha_n$$
$$i=1,2,\ldots,I_r \qquad (6.24.2)$$

In equations (6.24.1) and (6.24.2), λ_1 and λ_2 are the undetermined multipliers associated with the clamped boundary conditions (6.8) and (6.19), and μ_i (i=1,2,...,I_r) are associated with the deflection compatibility required by equation (6.23). Also, the following equations for the radial expansion of the rings are found:

$$v_{ri} = \mu_i / K_{ri} \qquad i=1,2,\ldots,I_r \qquad (6.24.3)$$

Substituting these equations into the constraint equations (6.8), (6.19), and (6.23) results in a set of (I_r+2) simultaneous linear equations with the undetermined multipliers λ_1, λ_2, and μ_i (i=1,2,...,I_r) as unknowns. Solving these simultaneous equations and substituting the solution back into equation (6.24) gives the displacement parameters. The radial deflection of the shell can then be calculated.

With I_r equal to two and the rings equally spaced on the shell (figure 6.11), the result is shown in figure 6.12. The geometry and material of the shell are the same as in the previous cases. For the deflection curve shown in figure 6.12, a 17-term approximation was sufficient to obtain convergence. Since it is extremely difficult to formulate the theoretical deflection for this case, it is not available and thus not shown in the figure for comparison. Figure 6.13 shows the moment diagram which is obtained from a 100-term approximation. The diagram is much smoother than the moment diagrams for the previous cases. This is because more terms are taken to approximate the actual deflection, and thus the deflection curve is in excellent agreement with the actual deflection curve. It should be noted that 100 terms is much more than necessary. Thirty terms will give smooth curves, even for the moment diagram.

Shells Reinforced by Rings and Longitudinal Stiffeners

As a general application to shell problem, the method of treating a cylindrical shell reinforced by both circumferential rings and longitudinal stiffeners will be presented in this section. Figure 6.14 shows a general arrangement of how shells can be reinforced by both rings and longitudinal stiffeners. In this situation, the deflection

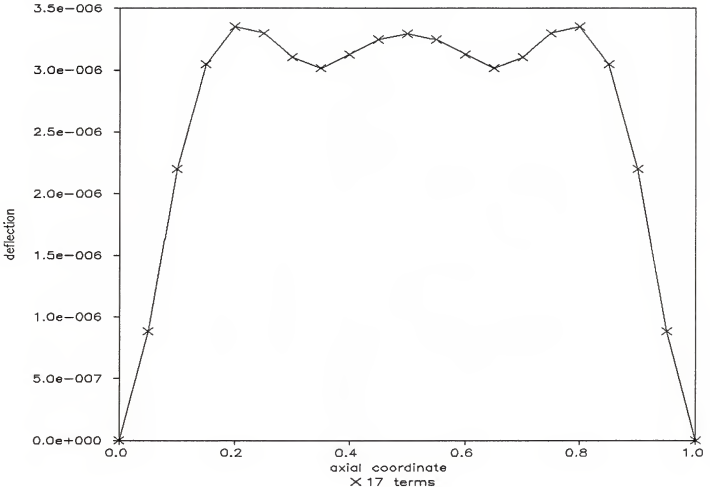

Figure 6.12 Deflection curve of a clamped shell reinforced by rings

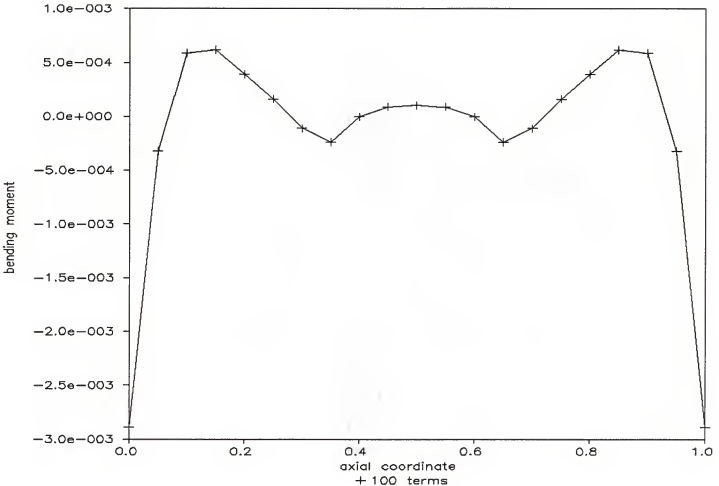

Figure 6.13 Bending moment curve of a clamped shell reinforced by rings

of the shell is no longer a one-dimensional problem, and thus no theoretical solution is available.

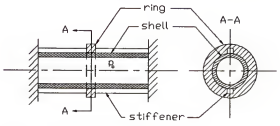

Figure 6.14 A shell reinforced by rings and longitudinal stiffeners

Using the same coordinate system as before, the deflection function of the shell can be taken as

$$v(x,y) = \sum_{m=0}^{Nm} \sum_{n=0}^{Nn} a_{mn} \cos(2m\pi x/\ell) \cos(ny) \tag{6.25}$$

The deflection functions of the longitudinal stiffeners are given by

$$v_{bi}(x) = \sum_{m=0}^{Nm} c_{mi} (1-\cos(2m\pi x/\ell)) \qquad i=1,2,\ldots,I_b \tag{6.26}$$

where I_b is the number of the longitudinal stiffeners. The deflection functions of the rings (expansions of the rings) are

$$v_{rj}(x) = \sum_{n=0}^{Nn} d_{nj} \cos(ny) \qquad j=1,2,\ldots,I_r \tag{6.27}$$

where I_r is the number of rings. If the placement of the reinforcements is symmetric about the center of the cylinder,

then only a quarter of the shell needs to be considered. In this case the bending strain energy of the shell is given by

$$U_1 = (Dr/2) \int_0^{\ell/2} \int_0^{\pi} (\partial^2 v/\partial x^2 + \partial^2 v/\partial y^2)^2 \, dx \, dy \tag{6.28}$$

And the hoop strain energy of the shell is

$$U_2 = (K_h r/2) \int_0^{\ell/2} \int_0^{\pi} v^2 \, dx \, dy \tag{6.29}$$

The total potential energy stored in the shell is

$$U = U_1 + U_2$$

$$= \sum_{m=0}^{Nm} \sum_{n=0}^{Nn} a_{mn}^2 \alpha_{mn} \tag{6.30}$$

where

$$\begin{aligned} \alpha_{mn} &= K_h \pi r \ell/4 && \text{if } m=n=0 \\ &= (K_h \pi r \ell/8) + (D \pi r \ell/8)(2m\pi/\ell)^4 && \text{if } m\neq 0 \text{ and } n=0 \\ &= (K_h \pi r \ell/8) + (D \pi r \ell n^4/8) && \text{if } m=0 \text{ and } n\neq 0 \\ &= (K_h \pi r \ell/16) + (D \pi r \ell/16)[(2m\pi/\ell)^2+n^2]^2 && \text{if } m\neq 0 \text{ and } n\neq 0 \end{aligned} \tag{6.31}$$

The bending energy stored in each longitudinal stiffener is

$$U_{bi} = (EI/2) \int_0^{\ell/2} (\partial^2 v_{bi}/\partial x^2)^2 \, dx$$

$$= \sum_{m=0}^{Nm} c_{mi}^2 \gamma_m \qquad i=1,2,\ldots,I_b \tag{6.32}$$

where

$$\gamma_m = (EI\ell/8)(2m\pi/\ell)^4 \tag{6.33}$$

The strain energy stored in each ring is

$$U_{rj} = (K_r r/2) \int_0^{\pi} v_{rj}^2 \, dy$$

$$= \sum_{n=0}^{Nn} d_{nj}^2 \delta_n \qquad i=1,2,\ldots,I_r \tag{6.34}$$

where

$$\delta_n = K_r r\pi/2 \qquad \text{if } n=0$$
$$= K_r r\pi/4 \qquad \text{otherwise} \tag{6.35}$$

The work done by the pressure p_0 is

$$W = r \int_0^{\ell/2} \int_0^{\pi} p_0 v(x,y) \, dx \, dy$$

$$= \sum_{m=0}^{Nm} \sum_{n=0}^{Nn} a_{mn}\Omega_{mn} \tag{6.36}$$

where

$$\Omega_{mn} = \pi r\ell p_0/2 \qquad \text{if } m=n=0$$
$$= 0 \qquad \text{otherwise} \tag{6.37}$$

The constraints are the zero deflection at the end x=0 and the deflection compatibility between the shell, the stiffeners, and the rings. These are

$$v(0, y_k) = 0 \qquad k=1,2,\ldots,K_{b1} \tag{6.38.1}$$

$$v(x_k, y_i) - v_{bi}(x_k) = 0$$
$$i=1,2,\ldots,I_b, \; k=1,2,\ldots,K_{ii} \tag{6.38.2}$$

where K_{b1} denotes the number of constraint points along the boundary x=0, and K_{ii} denotes the number of constraint points chosen from the ith longitudinal stiffener. Also,

$$v(x_j, y_k) - v_{rj}(y_k) = 0$$

$$j=1,2,\ldots,I_r,\ k=1,2,\ldots,K_{jj} \qquad (6.38.3)$$

where K_{jj} denotes the number of constraint points chosen from the jth ring. In order to simplify the formulation, assume that the number of constraint points on the boundary x=0 and all reinforcements, including the rings and the stiffeners, are the same (K_c), i.e., $K_{b1}=K_{ii}=K_{jj}=K_c$. The constraint equations can then be expressed in the following compact form:

$$\sum_{m=0}^{N}\sum_{n=0}^{N} a_{mn}\, Q_{mnij} - \sum_{m=0}^{N} f_{mi} R_{mj} = 0 \qquad j=1,2,\ldots,K_c \quad (6.39)$$

If the constraint points are regarded as points taken from "constraint lines" which are on the surface of the cylindrical shell, then the subscript i denotes the ith constraint line. These constraint lines include the boundary x=0, the longitudinal stiffeners, and the rings. The subscript j denotes the jth constraint point on the ith constraint line. The definition of Q_{mnij}, R_{mj}, and f_{mi} are listed as follows:

1. When the constraint point is on the boundary x=0

$$Q_{mnij} = \cos(ny_j)$$

$$R_{mj} = 0$$

$$f_{mi} = 0$$

2. When the constraint point is on a longitudinal stiffener

$$Q_{mnij} = \cos(2m\pi x_j/\ell)\cos(ny_i)$$

$$R_{mj} = 1 - \cos(2m\pi x_j/\ell)$$

$$f_{mi} = c_{mi}$$

3. When the constraint point is on a ring

$$Q_{mnij} = \cos(2m\pi x_i/\ell)\cos(ny_j)$$

$$R_{mj} = \cos(ny_j)$$

$$f_{mi} = d_{mi}$$

The following equations relating the displacement parameters a_{mn} and f_{mi} to the undetermined multipliers λ_{ij} can then be derived:

$$a_{mn} = \left(\Omega_{mn} - \sum_{i=1}^{I_c} \sum_{j=1}^{K_c} \lambda_{ij} Q_{mnij} \right) / (2\alpha_{mn}) \qquad (6.40)$$

and

$$f_{mi} = \left(\sum_{j=1}^{K_c} \lambda_{ij} R_{mj} \right) / (2\varsigma_m) \qquad (6.41)$$

where $\varsigma_m = \gamma_m$ when $f_{mi} = c_{mi}$ (6.42.1)

$\varsigma_m = \delta_m$ when $f_{mi} = d_{mi}$ (6.42.2)

and $I_c = I_b + I_r + 1$ (6.43)

In the above equation, I_c denotes the total number of constraint lines. By substituting equations (6.40) and (6.41) into equation (6.39), a set of I_cK_c linear equations can be obtained. Solving these equations gives the undetermined multipliers λ_{ij}. Then, by substituting the undetermined multipliers into equations (6.40) and (6.41), the parameters a_{mn} can be calculated, and the deflection surface can be found.

Figure 6.15 shows the circumferential deflection surface of a shell with length 0.7 units, radius 1.0 unit, and thickness 0.01 units. The cylindrical vessel is reinforced by four rings, and four longitudinal stiffeners, with thickness 0.02 units and cross section height equal to 0.04

units. The result is obtained by assuming a 25-term approximation function (N_m=N_n=25) as given in equation (6.25). This number of terms is large enough to provide a convergent result. The trace of the reinforcements can be identified in the drawing. The deflection of the circumferential surface drawing has been magnified 27,000 times relative to the dimensions of the shell in order to provide detail.

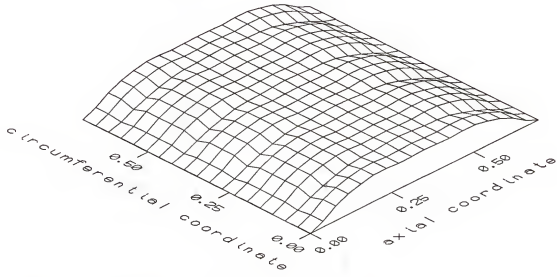

Figure 6.15 The circumferential deflection surface of a shell reinforced by rings and longitudinal stiffeners

CHAPTER 7
APPLICATIONS TO STRUCTURAL DESIGN

The previous chapters illustrate the use of the Rayleigh-Ritz method incorporating undetermined multipliers to the analysis of structural elements such as beams, plates, and shells. As was seen, the proposed method provides an elegant, efficient, and effective way for the analysis of elastic structural elements.

The proposed method can also be used as a valuable design tool, especially for complicated structures, such as the honeycomb discussed in Chapter 4. Designers so far almost exclusively rely on the finite element method to help in the design of this type of complicated structure. In view of the great effort of preprocessing and postprocessing that the finite element method requires, however, the method can be very expensive considering the iterative nature of optimum design. On the other hand, by taking advantage of the modified Rayleigh-Ritz method, the optimum design of complex structural elements can be carried out with relative ease. The proposed method can save a great amount of time and labor used in the iterations required in the optimum design process. In the following sections, some optimum design cases are

illustrated using the modified Rayleigh-Ritz method for the analytical formulation.

Beam Design

Since the proposed method provides a convenient way to analyze the problem of multi-span beams, it is can be used as a design tool for this type of structure. Consider the case that was shown in figure 3.12, with the span length, or the location of the interior support x_s, assumed to be variable. Since x_s is variable, it is possible to make the deflection curve of the beam as close as possible to some prespecified form by adjusting x_s. An "error" function, which indicates the "closeness" of the approximate deflection curve obtained from the modified Rayleigh-Ritz method to the prespecified points can therefore be defined in the following form:

$$R = \sum_{j=1}^{J} \left(v_N(x_j) - v_j \right)^2 \tag{7.1}$$

where R denotes the "error," v_j denotes the prespecified deflections at the particular locations $x=x_j$ $(j=1,2,\ldots,J)$, and J is the number of prespecified points. The approximation deflection function v_N is taken to be the same as equation (3.22).

The next step is to find the particular x_s^* which minimizes R. (Remember, for this case, R is a function of the location of the interior support only.) Since there is only one independent variable x_s, the Newton-Raphson method[42] is

an effective method to find the minimum point x_s^*. It should be noted that for any specific x_s, the displacement parameters a_0, a_n, and b_n (n=1,2,...,N) of the assumed deflection function $v_N(x)$ can be calculated with the modified Rayleigh-Ritz method, and then the error R for that specific x_s can be computed. The first and the second derivatives of R with respect to x_s are approximately calculated as follows:

$$dR/dx_s = (R(x_s+\Delta x_s) - R(x_s)) / \Delta x_s \qquad (7.2)$$

and

$$d^2R/dx_s^2 = (R(x_s+2\Delta x_s) - 2R(x_s+\Delta x_s) + R(x_s)) / (\Delta x_s)^2 \qquad (7.3)$$

where Δx_s is a small increment in x_s. Once again, the displacement parameters for the locations $x_s+\Delta x_s$ and $x_s+2\Delta x_s$ are obtained with the modified Rayleigh-Ritz method. With these parameters, the errors $R(x_s+\Delta x_s)$ and $R(x_s+2\Delta x_s)$ can then be computed.

Using the prespecified deflections outlined in table 7.1, the Newton-Raphson method, incorporating the modified Rayleigh-Ritz method, gives the result shown in figure 7.1 in five iterations.

Table 7.1 Specification of deflection

x_j	v_j
0.1	-0.00035
0.3	0.00055
0.5	0.00330

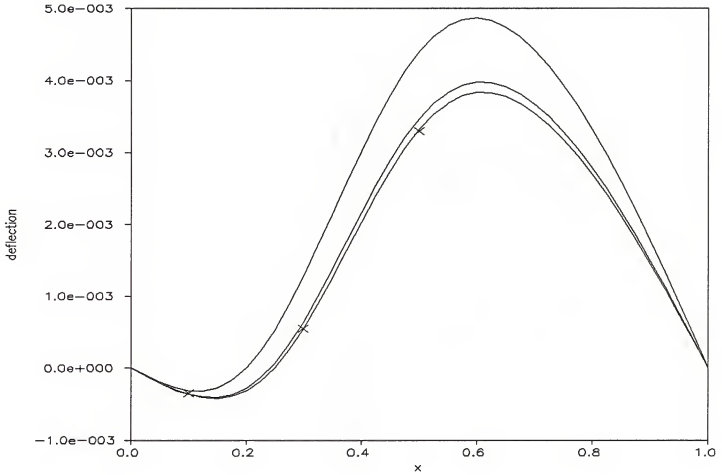

Figure 7.1 Deflection curves at different iteration steps of the case where the location of an interior support is to be determined

In the figure, the symbol X represents the desired deflection. The highest curve corresponds to the result of the first iteration and the other two represent the third and fifth iterations using the Newton-Raphson scheme, respectively. The curve of the fifth iteration (the final configuration) is almost coincident with all the X's. Note that, in general, the final configuration is not always close to the specified curve, and how close the approximate deflection curve will be to the prespecified deflection is dependent upon the shape of the specified curve.

Similarly, an optimum location for an external concentrated force can be found such that the deflection curve will be as close as possible to some prespecified points. Taking a simply-supported beam as an example (figure 3.1) with the distributed load p(x) replaced by a concentrated load, and specifying the required deflection condition (v_j) as outlined in table 7.2, the result obtained from seven iterations of the Newton-Raphson method, using the modified Rayleigh-Ritz procedure in each iteration to calculate the displacement parameters, is shown in figure 7.2. Symbol X denotes the desired deflections at the locations x_j (j=1,2,...,J). It should be understood that the general procedure is similar to the previous one, except that the independent variable is now the location of the load, not that of the interior support.

Since, in this study, the deformation of a body is confined to be within the linearly elastic range, the

deformations that a body undergoes due to several loads can be superimposed. If a simply-supported beam is acted upon by more than one concentrated load, such as the one shown in figure 7.3 where two concentrated loads are applied to the beam, the final configuration that the beam takes is simply the sum of the configurations due to each individual load, i.e.,

$$v(x) = \sum_{i=1}^{I_f} P_i u_i(x) \tag{7.4}$$

where I_f denotes the number of concentrated loads, P_i denotes the magnitude of the ith load, and $u_i(x)$ is the deflection curve due to a unit concentrated load applied at the same location as the ith load. These deflection curves due to unit loads can be obtained by the modified Rayleigh-Ritz method.

Table 7.2 Specification of defection

x_j	v_j
0.2	0.01200
0.4	0.01920
0.6	0.01813
0.8	0.01067

In this case, the error function is defined as

$$R = \sum_{j=1}^{J} \left(\sum_{i=1}^{I_f} P_i u_i(x_j) - v_j \right)^2 \tag{7.5}$$

In the least square sense, equation (7.5) represents the criterion for fitting the discrete data point v_j (j=1,2,...,J)

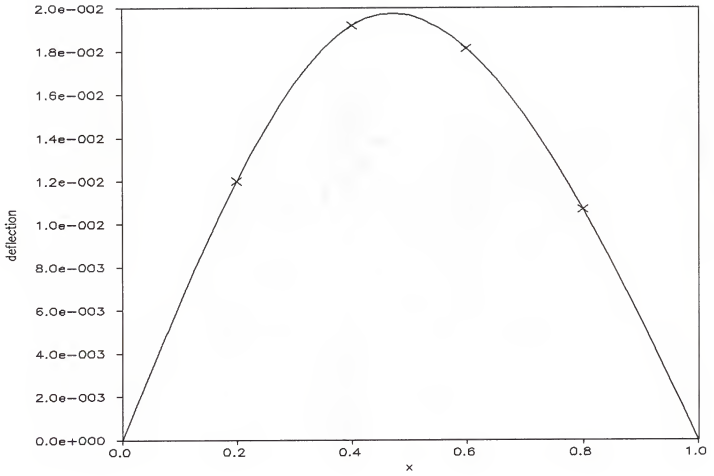

Figure 7.2 Deflection curve of the case where the location of the external load is to be determined

with the functions u_i (i=1,2,...,I_f). It is relatively easy to obtain the magnitude P_i for each load (assuming that the location of P_i is known) so that the error is minimum. This can be done by taking partial derivatives of R with respect to each P_i, setting each derivative equal to zero, and simultaneously solving the equations. The equations take the following form:

$$\sum_{j=1}^{J} \left(\sum_{i=1}^{If} P_i u_i(x_j) u_k(x_j) \right) = \sum_{j=1}^{J} v_j u_k(x_j)$$

$$k=1,2,\ldots,I_f \qquad (7.6)$$

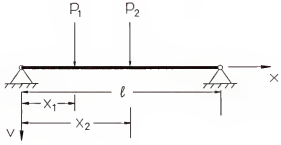

Figure 7.3 A simply-supported beam acted upon by two concentrated loads

By applying these techniques, it is possible to simulate the deflection curve of a beam due to an arbitrarily distributed load. The deflection curve due to the arbitrary load can be regarded as the prespecified curve. A sinusoidal load distribution is taken as an example, and five concentrated loads are used to simulate the distributed load. The locations of the concentrated loads are x=ℓ/10, 3ℓ/10, 5ℓ/10, 7ℓ/10, and 9ℓ/10. The deflection curves due to unit

concentrated loads in these locations can be obtained using the modified Rayleigh-Ritz method. As stated in equation (7.4), these curves, when respectively multiplied by the magnitudes P_i and added together, give the final configuration. The resulting deflection $v(x_j)$, along with the prespecified deflection v_j, is shown in table 7.3. Due to the symmetry about the center of the beam, only half of the data is shown in the table. Note that if the number of prespecified points is the same as that of the concentrated loads, then the deflection curve can be forced to pass through all the specified points.

Table 7.3 Result and comparison of the case where the magnitudes of external loads are unknown

x_j	v_j	$v(x_j)$	error(%)
0.05	1.606×10^{-3}	1.607×10^{-3}	0.062
0.10	3.172×10^{-3}	3.173×10^{-3}	0.032
0.15	4.661×10^{-3}	4.660×10^{-3}	0.021
0.20	6.034×10^{-3}	6.033×10^{-3}	0.017
0.25	7.259×10^{-3}	7.260×10^{-3}	0.014
0.30	8.305×10^{-3}	8.307×10^{-3}	0.024
0.35	9.147×10^{-3}	9.147×10^{-3}	0.000
0.40	9.763×10^{-3}	9.761×10^{-3}	0.020
0.45	1.014×10^{-2}	1.014×10^{-2}	0.000
0.50	1.027×10^{-2}	1.027×10^{-2}	0.000

By combining the approaches used above to determine the optimum location and the optimum magnitude of a concentrated load, it is possible to obtain an optimum load whose location and magnitude are not known. Since the equation (7.6) used to solve for the magnitude is linear, it is always possible

to obtain the best magnitude corresponding to a given location directly, without applying Newton-Raphson method which requires iterations. This suggests that it may be advantageous to treat the problem in an alternate fashion. In other words, to find the magnitude from the location and then find the location from the magnitude. A conceptual algorithm for accomplishing this can be stated as follows:

1. Start with an initial guess of the location of the load.
2. Calculate the best magnitude corresponding to the current location with equation (7.6).
3. Calculate the "error" with the current location and magnitude.
4. With the magnitude held constant temporarily, improve the location with the Newton-Raphson scheme.
5. Check if it is convergent--if not, repeat the procedure.

In table 7.4, the result of an example is shown with the iteration process outlined in table 7.5. Each of the intermediate results was obtained by the modified Rayleigh-Ritz method. The prespecified deflections v_j are calculated from the case of a simply-supported beam acted upon by a concentrated load with P=-0.5 and $x_p=0.8\ell$. It can be seen from table 7.5 that the error gradually decreases as the iteration proceeds. As shown in table 7.4, the final result $v(x_j)$ is almost exactly the same as the prespecified deflection. Nevertheless, how small the minimum error will be, or how close the final configuration will be to the prespecified points, is dependent upon the shape of the specified curve.

Table 7.4 Result of the case where magnitudes of external loads are unknown

x_j	v_j	$v(x_j)$
0.05	-7.979×10^{-4}	-7.979×10^{-4}
0.10	-1.583×10^{-3}	-1.583×10^{-3}
0.15	-2.344×10^{-3}	-2.344×10^{-3}
0.20	-3.067×10^{-3}	-3.067×10^{-3}
0.25	-3.740×10^{-3}	-3.740×10^{-3}
0.30	-4.350×10^{-3}	-4.350×10^{-3}
0.35	-4.885×10^{-3}	-4.885×10^{-3}
0.40	-5.333×10^{-3}	-5.333×10^{-3}
0.45	-5.681×10^{-3}	-5.681×10^{-3}
0.50	-5.917×10^{-3}	-5.917×10^{-3}
0.55	-6.027×10^{-3}	-6.027×10^{-3}
0.60	-6.000×10^{-3}	-6.000×10^{-3}
0.65	-5.823×10^{-3}	-5.823×10^{-3}
0.70	-5.483×10^{-3}	-5.483×10^{-3}
0.75	-4.969×10^{-3}	-4.969×10^{-3}
0.80	-4.267×10^{-3}	-4.267×10^{-3}
0.85	-3.375×10^{-3}	-3.375×10^{-3}
0.90	-2.333×10^{-3}	-2.333×10^{-3}
0.95	-1.192×10^{-3}	-1.192×10^{-3}

Table 7.5 Intermediate results of iteration

iteration	location	magnitude	R
1	0.500000	-0.293777	2.2×10^{-7}
2	0.822525	-0.555668	7.6×10^{-10}
3	0.797026	-0.494130	1.4×10^{-11}
4	0.799914	-0.500245	1.2×10^{-14}
5	0.799950	-0.500322	4.0×10^{-15}

The same approach can be applied to solve the optimum design problem of a beam acted upon by several loads with either the locations, the magnitudes, or both not specified. Furthermore, by using the Rayleigh-Ritz method together with the Lagrangian rule (the modified Rayleigh-Ritz method), the

design of a beam with any boundary conditions acted upon by several loads, for which the magnitudes and locations are not known, can be accomplished.

Consider the case shown in figure 7.3 where two concentrated loads are applied to a simply-supported beam. If the magnitudes of the loads are known, then there are two decision variables, namely the two locations x_1 and x_2 where the loads are applied. Taking the specifications outlined in table 7.6 as an example, the optimum locations of $x_1=0.5\ell$ and $x_2=0.8\ell$, which result in an error of the order of 10^{-21}, are obtained within an average of 35 iterations from different starting points.

Table 7.6 Specification of the case where the locations of loads are unknown

x_j	v_j	x_j	v_j
0.05	2.530×10^{-3}	0.55	1.821×10^{-2}
0.10	5.017×10^{-3}	0.60	1.790×10^{-2}
0.15	7.415×10^{-3}	0.65	1.714×10^{-2}
0.20	9.683×10^{-3}	0.70	1.592×10^{-2}
0.25	1.178×10^{-2}	0.75	1.432×10^{-2}
0.30	1.365×10^{-2}	0.80	1.208×10^{-2}
0.35	1.526×10^{-2}	0.85	9.478×10^{-3}
0.40	1.657×10^{-2}	0.90	6.517×10^{-3}
0.45	1.752×10^{-2}	0.95	3.318×10^{-3}

The solution method is briefly stated as follows: One of the locations, say the second one (x_2) is first assumed to be given and fixed. Then the Newton-Raphson method is used to obtain a better location for the first one, with the

intermediate result obtained by the modified Rayleigh-Ritz method. Next, the location of the first one is assumed fixed, and the Newton-Raphson method, incorporating the modified Rayleigh-Ritz method, is applied to find a better location for the second one. The process is repeated until the optimum locations are found.

In comparison with the procedure stated above, the classical optimization schemes have the disadvantages of either taking more iterations to obtain the solution or needing a good guess of the starting point in order to avoid divergence. An example of the former is the steepest descent method[32], and that of the later is the Hooke and Jeeves method[32].

Plate Design

In this section, the application of the modified Rayleigh-Ritz method to the analytical aspect of the optimum design of plate structures will be illustrated. As an example, consider the structure shown in figure 4.20, which is a honeycomb sandwich structure. This type of structure can hardly be solved by conventional methods. It is also difficult for the finite element method, which is one of the most flexible numerical schemes, although expensive in the sense of computer time. The practicability and efficiency of the modified Rayleigh-Ritz method makes it a very good choice for the optimum design of structures of this kind.

The strength and weight (or equivalently, the volume) of a structure are two important factors which a designer must take into account. For designing the considered structure, the decision variables may include the geometrical dimensions of the overall structure or those of the individual plate elements (the top and the bottom) and the stiffeners. To simplify the problem, assume first that both the top and bottom plates are identical, and the stiffeners, although they may have different lengths, have identical vertical cross sections. Further, assume that the dimensions of the structure are given. The only decision variables left are the thicknesses of the plate elements and the stiffeners, provided the number and the locations of the stiffeners are also given.

Since the stiffeners are usually slender, it is reasonable to determine the thickness of the stiffeners in such a way that buckling in the vertical direction can be avoided. The critical buckling load for a beam can be approximately determined from the following equation[43][44]:

$$P_{cr} = \pi^2 E I_b / h_s^2 \tag{7.7}$$

where h_s is the height of the stiffeners, which is equal to the overall height of the structure (H) minus the thickness of both of the top and bottom plates (h), i.e., $h_s = H - 2h$. I_b is the area moment of inertia per unit length of the stiffeners, taken horizontally:

$$I_b = t_s^3 / 12 \tag{7.8}$$

where t_s is the thickness of the stiffeners.

Assuming that the yield stress of the structure is σ_a, then the maximum uniform load that a "solid plate" can take without exceeding its yield point is[3]

$$p_m = \sigma_a H^2 \; / \; (0.7134 \ell_y^2) \tag{7.9}$$

and the average load per unit length of the stiffeners is

$$p_{as} = p_m \ell_x \ell_y \; / \; \ell_s \tag{7.10}$$

where ℓ_s denotes the total length of all the stiffeners. A reference "solid plate" is defined in this investigation as a regular plate with the same dimensions (length, width and height) and same material as that of the honeycomb structure. If K_{safety} denotes the safety factor for buckling, then the following equation can be obtained:

$$P_{cr} = K_{safety} p_{as} \tag{7.11}$$

The forces p_m and p_{as} can be determined from equations (7.9) and (7.10) with the geometry information of the structure and the strength of the material given. By substituting equations (7.7), (7.8), (7.9), and (7.10) into equation (7.11), a relationship between t_s and h_s can be obtained. When H is given, h_s can be determined by h. The thickness of the stiffeners for any particular h can then be found to insure that buckling is avoided.

Figure 7.4 shows the relationship between the thicknesses of the plate elements and the stiffeners, with the same geometry and material of the honeycomb structure as was shown in Chapter 4. It is seen from the figure that as the thickness of the plate elements increases and approaches 0.05,

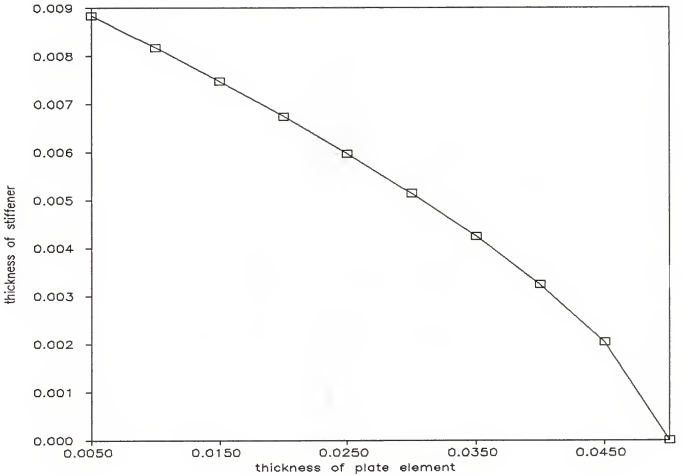

Figure 7.4 Relationship between the thicknesses of the plate elements and the stiffeners

which is half of the overall height of the honeycomb structure, the thickness of the stiffeners decreases and approaches zero. Since the overall height of the structure is assumed to be given, it can be seen that as the thickness of the plate elements increases, the height of the stiffeners is decreased and, consequently, the stiffeners can still support the same buckling load with the smaller thickness. For any given thickness of the plate elements, the thickness of the stiffeners can be determined from equations (7.7 - 7.11) and the total volume of the structure can be determined by adding the volume of the stiffeners and the plate elements together. Figure 7.5 shows the change in total volume as the thickness of the plate elements increases.

Having determined the thickness of the stiffeners in the manner described above, the remaining decision variable is the thickness of the plate elements of the honeycomb structure. Usually, in designing a structure, two quantities, strength and rigidity, can be chosen as reference. If strength is more important than rigidity, the issue becomes what is the best thickness of the plate elements that gives the most gain in strength. On the other hand, putting emphasis on the rigidity means finding the best thickness of the plate elements that gives the most gain in rigidity.

To have a comparison standard for strength, the overall deflection of the structure is taken as the reference to construct a plate with uniform thickness for comparison, which

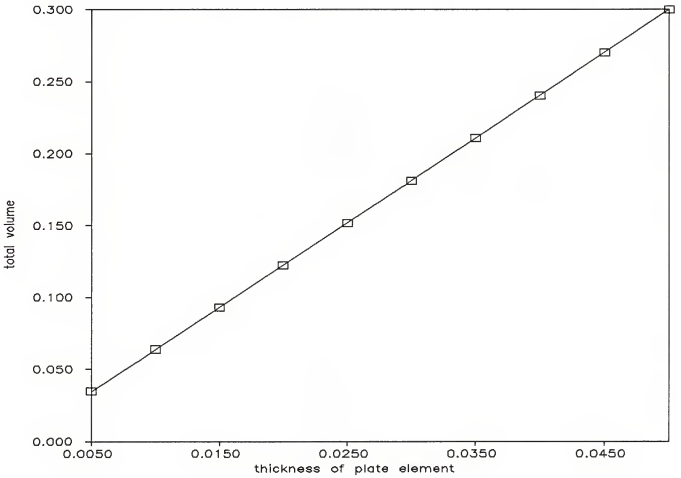

Figure 7.5 Volume of the honeycomb structure

will be called the equivalent plate (whose length and width are the same as those of the honeycomb structure). The thickness of the equivalent plate is so determined that the maximum deflection of the plate is the same as the maximum overall deflection of the honeycomb structure, when they are acted upon by the same load. The ratio of the maximum stress of the honeycomb to that of the equivalent plate will therefore be an indication of the gain in strength.

By using the formulation outlined in Chapter 4, in conjunction with the above equations, the local and global deflections of the structure can be determined and, thus, the corresponding stresses can be readily calculated by applying basic plate theory (a detailed discussion of the relationship between the deflection and the stress has been given by Timoshenko[3]). Certainly, the resulting stresses of both the top plate element and the bottom plate element are the sum of the stresses corresponding to the local and global deflections (the principle of superposition). A plot of the ratio of the maximum normal stress of the top plate of the structure to the maximum normal stress of the equivalent plate is shown in figure 7.6. It can be seen from the plot that there is a minimum for the curve of the stress ratio, indicating that with a specific thickness of the plate elements of the honeycomb structure, there is a maximum gain in strength. In this case, the optimum stress ratio is approximately 0.5159 and the optimum thickness of the plate

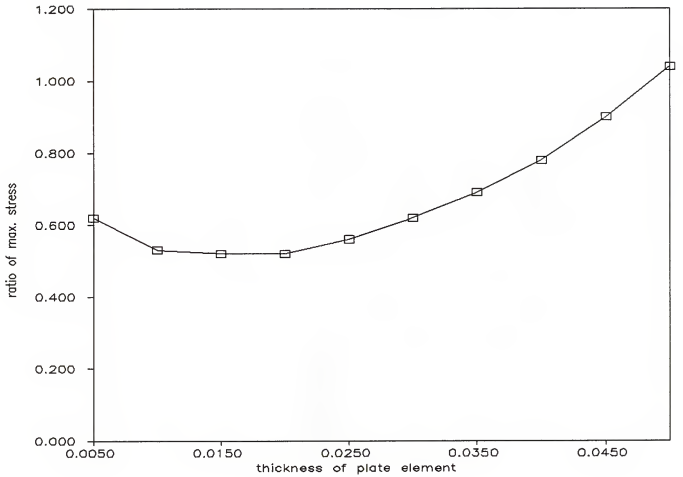

Figure 7.6 Ratio of the maximum stresses

elements is approximately 0.018. For the considered structure, when h=0.018, the maximum normal stress of the honeycomb structure is about 52% of that of the equivalent plate.

If, instead of considering strength, the rigidity is more important, then the main concern is the ratio of the maximum overall deflection of the honeycomb structure to that of a regular plate with uniform thickness and having the same size. The thickness of the regular plate is so determined that its volume is the same as the honeycomb. By using the modified Rayleigh-Ritz method in calculating the maximum deflections of the honeycomb structure and the regular plate, the result shown in figure 7.7 is obtained. The figure shows a plot of the ratio of the maximum deflections of the structure and the plate. In this case, an optimum point can also be obtained. This point corresponds approximately to h=0.016, and the ratio of maximum deflection at the optimum point is approximately 0.192. Accordingly, the maximum deflection of the optimum honeycomb structure is 19.2% of the regular plate when acted upon by the same load. This is a significant gain in rigidity.

It seems that the optimum points for both strength and rigidity are located close to each other, and it may be roughly concluded that for the particular structure considered in this section, the thickness of the plate elements should

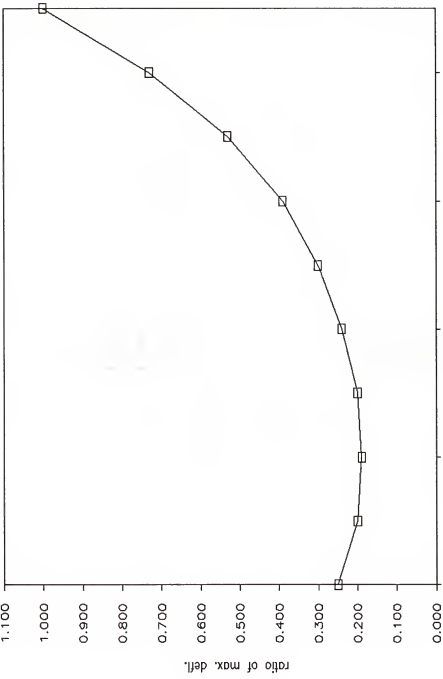

Figure 7.7 Ratio of the maximum deflections

be chosen from between 0.015 and 0.02 to gain the most in both strength and rigidity.

Since it is impossible to have a structure which is ideally light and strong at the same time, another way to apply the concept of optimum design is to construct an objective function to determine the optimum thickness of the plate elements so that a compromise between the rigidity and the weight can be accomplished. The objective function is constructed as follows:

$$F = (\delta_s / \delta_{max}) - Z (V / V_s) \qquad (7.12)$$

where δ_{max} denotes the maximum overall deflection of the honeycomb structure (obtained using the modified Rayleigh-Ritz method), δ_s denotes the maximum deflection of the corresponding solid plate, which can also be obtained by the proposed method, V is the total volume of the honeycomb structure, V_s is the volume of the corresponding solid plate, and Z is a weighting factor defining the compromise between the volume and the rigidity.

By using the modified Rayleigh-Ritz method in the calculation process, the following results are obtained. Figure 7.8 shows three curves of F, corresponding to Z=0.5, 1, and 2, plotted versus the thickness of the plate elements of the honeycomb. It shows that there is always an optimum point for the objective function F. This optimum point represents the best compromise between the requirements of less volume and more rigidity for each particular Z. In

figure 7.9, the optimum thickness of the plate elements of the honeycomb is shown with respect to different weighting factors. As expected, when Z increases, the optimum value of h decreases. It can be seen that when volume is important, the thickness of the plate elements of the honeycomb is decreased to satisfy the requirement of less volume. This is done, however, at the expense of the rigidity of the structure. The maximum overall deflection of the structure increases as Z increases (figure 7.10). Figure 7.11 shows two curves of the volume ratio. The symbol V_s denotes the volume of the corresponding solid plate. The symbol V_e is the volume of the equivalent plate for which the length and width are the same as the honeycomb, and the maximum deflection is the same as the maximum overall deflection of the honeycomb. It can be seen that it is advantageous to use a honeycomb structure to support transverse loads, since the volume of the honeycomb structure is much smaller than that of a solid plate of the same size. It is also smaller than that of an equivalent plate which will deflect the same amount when acted upon by the same load.

There are many possibilities for constructing an objective function in accordance with various design requirements. The objective function described above only serves as an example to demonstrate the applicability of the proposed method to the analytical aspect of the optimum design of elastic structures. The advantage of the modified

Rayleigh-Ritz method over the finite element method in the sense of efficiency can be seen from the fact that for each of the optimizations described above, approximately 10 objective function evaluations were required, and the computing time required for the proposed method to calculate the deflection of an element was observed to be up to 5 times faster than the finite element method. Furthermore, the formulation of the proposed method is less complicated than the finite element method, and the computer coding for the proposed method is easier to achieve than for the finite element method. The proposed method offers designers a more efficient and effective alternative to handle complex elastic structures with various design requirements and, thus, various objective functions.

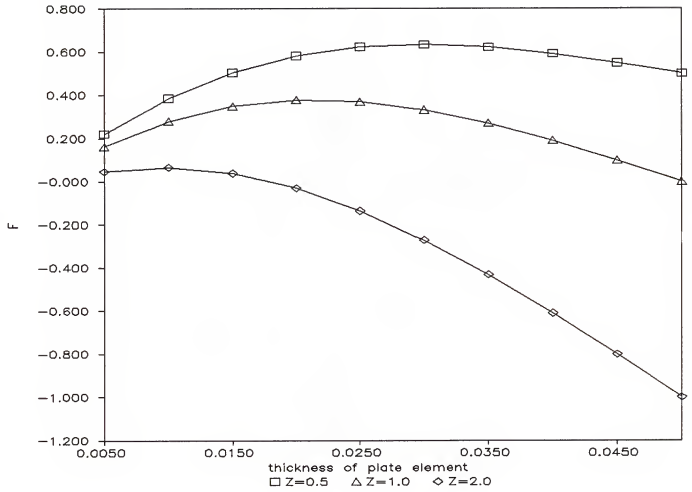

Figure 7.8 Plot of the objective function with respect to the thickness of the plate elements

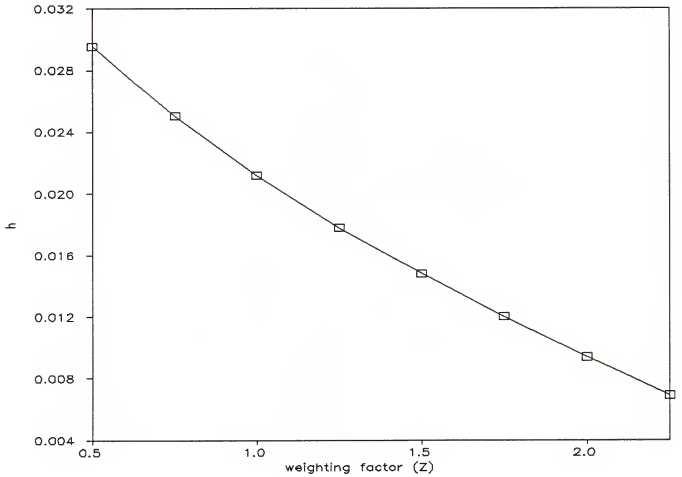

Figure 7.9 Optimum thickness of the plate elements with respect to different weighting factors

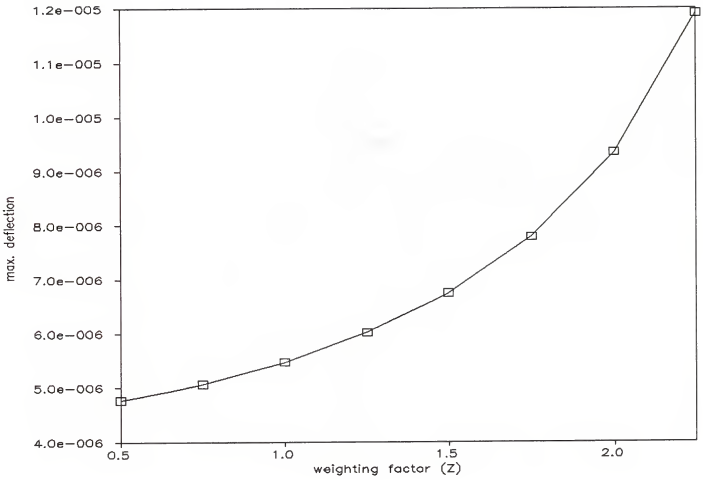

Figure 7.10 Maximum deflection of the honeycomb structure with respect to different weighting factors

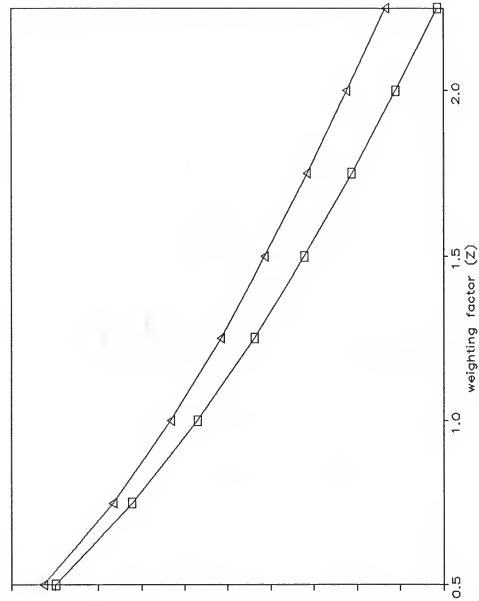

Figure 7.11 Volume ratio with respect to weighting factors

CHAPTER 8
CONCLUSIONS AND RECOMMENDATIONS

Conclusions

It can be concluded from this study that the Rayleigh-Ritz method implemented with undetermined multipliers provides an excellent tool for the analysis and optimum design of a wide variety of elastic structures. The following is a summary of some of the findings.

(1) The proposed method can be used to treat almost all types of beam problems provided that the bending rigidity is constant. This includes beams with different boundary conditions, beams with geometric constraints, as well as beams acted upon by different types of loads. The main advantage is that the boundary conditions can be changed without major modification of the formulation. Interior constraints can be incorporated, and, again, the formulation remains similar.

(2) The proposed method can be applied to many plate problems with different boundary conditions, including mixed boundary conditions. Plates of irregular shape, stiffened plates and honeycomb type structures can be dealt with using the same formulation as that used to handle simple problems.

(3) The proposed method can be applied to shell problems for analyzing the bending effect on deflection. Such problems include infinitely long shells held rigidly, infinitely long shells reinforced by rings, shells with fixed ends and shells reinforced with both rings and longitudinal stiffeners.

(4) It may be concluded that a unified formulation is possible for treating a wide variety of elastic structures.

Beside the concise and elegant nature of the formulation procedure, the solution is also very efficient compared to the finite element method. The computer time required to solve problems of this kind by the finite element method can be up to several times that needed for solution by the developed approach. For the case of a plate with an edge clamped and the other three edges simply supported (as shown in Chapter 4), the CPU time for the proposed method is 96 seconds on an 80286 microcomputer, and that for the finite element method with 400 elements is 510 seconds. The gain in efficiency of the proposed method over the finite element method is obvious.

Another advantage of the modified Rayleigh-Ritz method is that in contrast to the discrete data provided by the finite element method, the proposed method generates a continuous solution.

An important conclusion of this study is that the deflection of a plate with a hole can be obtained from a plate without any hole using the proposed method and an iteration procedure. This configuration occurs in a variety of

constructions, and designers have so far relied almost entirely on the finite element method for solutions. In view of the great effort needed for the preprocessing and postprocessing of the finite element method, the above approach can serve as a valuable tool in the analysis of plates with holes.

In view of the advantages of the proposed method in the analysis of elastic structural elements, the method can also be an excellent tool for optimum design. As shown in the previous chapter, by choosing a suitable objective function and using the Newton-Raphson iteration method, the optimum solution can be obtained in few iterations.

Selection of the Coordinate Functions

The solution generated by the proposed method is assumed to be a linear combination of a set of predetermined coordinate functions. The quality of the result is highly dependent upon an appropriate selection for the coordinate functions. Some guidance for selecting the coordinate functions is discussed below.

Since the essence of the proposed method is to force unsatisfied boundary conditions to be satisfied by choosing the displacement parameters, it can be seen that while it is possible to have the summation of the coordinate functions vanish at a boundary by adjusting the parameters, it is not possible to make the summation of the coordinate functions

equal to a nonzero value at a boundary if all the coordinate functions vanish at the boundary. This is the first guide in selecting appropriate coordinate functions.

Beside the above consideration, care should be exercised in the choice of the coordinate functions in order to improve the efficiency of the modified Rayleigh-Ritz method. For example, when sine functions are chosen as the coordinate functions, if the geometry of the object is symmetrical about the centroid, then choosing odd sine functions and discarding even functions will considerably reduce the computing time.

Although only sine and cosine functions are used in this study, it should be noted that other functions, such as Chebyshev polynomials and Jacobi polynomials, can also be taken as the coordinate functions.

Limitations of the Method

The modified Rayleigh-Ritz method, although possessing valuable advantages in analyzing and designing elastic structural elements, has the following disadvantages:

(1) It is difficult for the proposed method to handle beams with variable bending rigidity or plates with variable thickness. The difficulty arises from the integration of the potential energy. It is difficult to have a closed form solution of the integration if the bending or flexure rigidity is a function of the independent variable(s).

(2) Care must be taken in selecting the approximation series and checking convergency. The selection of the type of solution function can be critical in complex situations.

(3) Applications to nonlinear problems can be difficult.

(4) The proposed method is not readily applicable to optimum designs where the thickness of a plate or the cross section of a beam is the design variable.

Recommendations

The following studies are recommended for future work so that the method presented here can be fully developed:

(1) It is suggested that a procedure to apply the proposed method to nonlinear problems, such as thick plates or plates with large deflections, be developed.

(2) It is also suggested that a procedure to handle plates with variable thickness or beams with variable bending rigidity be developed.

(3) It is further suggested that a procedure to analyze and design a structure which is an integration of different types of structural elements be developed.

(4) Finally, as the original Ritz method was primarily developed for the analysis of the vibrations of plates[45], it is suggested that a procedure for the dynamic analysis of a complex structure with complex boundary conditions could be investigated, and a study on applying the dynamic analysis to the design of elastic structures be conducted.

APPENDIX

PROGRAM FOR THE CASE OF HONEYCOMB SANDWICH PLATES

```
#include <stdio.h>
#include <math.h>
#include <stdlib.h>
#include <alloc.h>

#define  PI             3.14159265358979324
#define  XSTF           1
#define  YSTF           3
#define  NSTF           3

extern unsigned _stklen = 40000;

short    TENF, CENF, BENF, PENF, NENF, NINS=2;
short    XSEC=9;
short    YSEC=5;
short    NODE;
short    TERM=15;
short    TERM2;
short    *npes;
short    *inst;
double   epss=1.0e-12;
double   volume, toln;
double   qt=1.0, qb=0.00;
double   lx=3.0, ly=1.0, tp;
double   ts=0.010000, h=0.100000, h1;
double   Ep=3.0e07, Gp=11.54e06, mup=0.3, density=0.283;
double   yield_stress=6.0e04, ultimate_stress=1.0e05;
double   dpr, dpc, EI, GJ;
double   lnst[NSTF];
double   EIv[NSTF];
double   ornt[NSTF];
double   xstr[NSTF];
double   ystr[NSTF];
double   *u, *v;
double   *eta;
double   *lgmr;
double   *dm;

main()
  {
  short  loop1, loop2;
  short  index1;
```

```
double *cdpm, *tdpm, *bdpm;

void   ini_sf();
void   ini_uv();
void   ini_eta();
void   ini_dm();
void   ini_EIv();
void   solve_LM();
void   cmpt_dfpm();
void   cmpt_defl();
void   memo_free();
short  *s_mem_alc();
double *memo_allc();

scanf("%le", &tp );
TERM2 = TERM * TERM;

printf( " Basic information.\n" );
printf( " 1. MATERIAL:\n" );
printf( "    Poison's ratio: %.3f\n", mup );
printf( "    Yang's modulus: %.3e\n", Ep );
printf( "\n 2. LOAD:\n" );
printf( "    load on top: %.2f, load on bottom: %.2f\n",
                                                qt, qb );

npes = s_mem_alc( NSTF, "npes" );
inst = s_mem_alc( 2*NINS, "inst" );
ini_sf( ornt, lnst, xstr, ystr, npes );

TENF = 0;
for( loop1=0; loop1<NSTF; ++loop1 )
  TENF += ( ( *(npes+loop1) + 1 ) / 2 );
BENF = TENF;
CENF = TENF;
PENF = TENF + CENF + BENF;
NENF = PENF + NINS;

eta = memo_allc( NENF, "eta" );
ini_eta( eta );

u = memo_allc( NENF, "u" );
v = memo_allc( NENF, "v" );
lgmr = memo_allc( NENF, "lgmr" );

toln = (double)XSTF * lx + (double)YSTF * ly;
h1 = h - (double)2.0 * tp;
volume = (double)2.0 * tp * lx * ly;
volume += toln * h1 * ts;
EI = Ep * ts * pow( h1, (double)3 ) / (double)12.0;
ini_EIv( EIv );
dpr = Ep * pow( tp, (double)3 )
                    / ( (double)1.0 - mup * mup );
```

```
dpr /= (double)12.0;
dpc = ( h1 + tp ) / (double)2.0;
dpc = Ep * tp * pow( dpc, (double)2 );
dpc /= ( (double)1.0 - mup * mup );
dpc += dpr;

printf( "\n 3. PLATE:\n" );
printf( "    length: %.2f, width: %.2f, thickness %f\n",
                                          lx, ly, tp );
printf( "    distance between plates %.2f\n", h1 );
printf( "    flextural rigidity (reference) %e\n", dpr );
printf( "    flextural rigidity (nutral pl) %e\n", dpc );
printf( "\n 4. STIFFENER" );
printf( "(based on a quarter of the plate)\n" );
printf( "    no of stiffener: %d\n", NSTF );
printf( "    reference bending rigidity; %e\n", EI );
printf( "    thickness of stiffener: %f\n", ts );
printf( "    Tp / Ts = %e\n", tp / ts );
printf( "       ln    on    xs    ys    rd    cp\n" );
for( loop1=0; loop1<NSTF; ++loop1 )
printf( "  #%2d  %.2f  %.2f  %.2f  %.2f  %.2f   %2d\n" ,
    loop1, *(lnst+loop1), *(ornt+loop1), *(xstr+loop1),
           *(ystr+loop1), *(EIv+loop1), *(npes+loop1) );

ini_uv( u, v, inst, ornt, xstr, ystr, lnst, eta );

printf( "\n     locations of reinforced points\n" );
printf( "     no     x       y      eta\n" );
for( loop1=0; loop1<NENF; ++loop1 )
  printf( "     %d  %f %f %f\n",
          loop1, *(u+loop1), *(v+loop1), *(eta+loop1) );

printf( "\n 5. INTERSECTION:\n" );
for( loop1=0; loop1<NINS; ++loop1 )
  printf( "    #%d: stf #%d and stf #%d\n",
          loop1, *(inst+loop1*2), *(inst+loop1*2+1) );

dm = memo_allc( TERM2, "dm" );
ini_dm( dm, TERM );
cdpm = memo_allc( TERM2, "cdpm" );
tdpm = memo_allc( TERM2, "tdpm" );
bdpm = memo_allc( TERM2, "bdpm" );

solve_LM( lgmr, TERM );
cmpt_dfpm( cdpm, tdpm, bdpm, TERM );
cmpt_defl( cdpm, tdpm, bdpm, TERM );

memo_free( bdpm, "bdpm" );
memo_free( tdpm, "tdpm" );
memo_free( cdpm, "cdpm" );

}
```

```
void ini_sf( ornt, lnst, xstr, ystr, npes )
double   *ornt, *lnst;
double   *xstr, *ystr;
short    *npes;
  {
  short  loop1;

  ornt[0] = (double)0.0;
  ornt[1] = PI / (double)2.0;
  ornt[2] = PI / (double)2.0;
  lnst[0] = lx;
  lnst[1] = ly;
  lnst[2] = ly;
  xstr[0] = (double)0.0;
  ystr[0] = ly / (double)2.0;
  xstr[1] = lx / (double)4.0;
  ystr[1] = (double)0.0;
  xstr[2] = lx / (double)2.0;
  ystr[2] = (double)0.0;
  for( loop1=0; loop1<(XSTF+1)/2; ++loop1 )
    npes[loop1] = 15;
  for( loop1=(XSTF+1)/2; loop1<(XSTF+YSTF+2)/2; ++loop1 )
    npes[loop1] = 10;

  }


void ini_xy( x, y )
double   *x, *y;
  {
  short  loop;
  double ds;

  ds = lx / lx / (double)2.0 / (double)( XSEC - 1 );
  loop = 0;
  do  *(x+loop) = (double)loop * ds;
  while( ++loop < XSEC );

  ds = ly / ly / (double)2.0 / (double)( YSEC - 1 );
  loop = 0;
  do  *(y+loop) = (double)loop * ds;
  while( ++loop < YSEC );

  }


void ini_eta( eta )
double   *eta;
  {
  short  loop1, loop2;
```

```
  short  index1=0, index2=0;
  double deta;

  for( loop1=0; loop1<TENF; ++loop1 )
    *(eta+loop1) = (double)0.0;

  for( loop1=0; loop1<NSTF; ++loop1 )
    {
    *(npes+loop1) += 1;
    deta = *(lnst+loop1) / (double)( *(npes+loop1) );
    *(npes+loop1) /= 2;
    index2 += *(npes+loop1);
    for( loop2=index1; loop2<index2; ++loop2 )
      *(eta+loop2) = (double)( loop2 - index1 + 1 ) * deta;

    index1 = index2;
    }

  }


void ini_uv( u, v, inst, ornt, xstr, ystr, lnst, eta )
short    *inst;
double   *u, *v;
double   *ornt, *xstr, *ystr, *lnst;
double   *eta;
  {
  short  loop1, loop2;
  short  index1=0, index2=0;
  double dcos, dsin, dtan;
  double cos(), sin(), tan(), sqrt();

  for( loop1=0; loop1<NSTF; ++loop1 )
    {
    dcos = cos( *(ornt+loop1) );
    dsin = sin( *(ornt+loop1) );
    if ( fabs( dcos ) < epss ) dcos = (double)0.0;
    if ( fabs( dsin ) < epss ) dsin = (double)0.0;
    index2 += *(npes+loop1);
    for( loop2=index1; loop2<index2; ++loop2 )
      {
      *(u+loop2) = *(xstr+loop1) + *(eta+loop2) * dcos;
      *(u+loop2) /= lx;
      *(u+loop2+CENF) = *(u+loop2);
      *(u+loop2+CENF+TENF) = *(u+loop2);
      *(v+loop2) = *(ystr+loop1) + *(eta+loop2) * dsin;
      *(v+loop2) /= ly;
      *(v+loop2+CENF) = *(v+loop2);
      *(v+loop2+CENF+TENF) = *(v+loop2);
      *(eta+loop2) /= *(lnst+loop1);
      *(eta+loop2+CENF) = *(eta+loop2);
```

```
    *(eta+loop2+CENF+TENF) = *(eta+loop2);
    }
  index1 = index2;
  }

index1 = PENF;
index2 = 0;
for( loop1=0; loop1<NSTF; ++loop1 )
  {
  for( loop2=loop1+1; loop2<NSTF; ++ loop2 )
    {
    if ( fabs( *(ornt+loop1) - *(ornt+loop2) ) > 1.0e-6 )
      {
      if ( fabs( fabs( *(ornt+loop1) )
                        - PI / (double)2.0 ) <= 1.0e-07 )
        dcos = *(xstr+loop1);
      else
        {
        if ( fabs( fabs( *(ornt+loop2) )
                        - PI / (double)2.0 ) <= 1.0e-07 )
          dcos = *(xstr+loop2);
        else
          {
          dcos = *(ystr+loop2) - *(ystr+loop1);
          dcos += ( tan( *(ornt+loop1) ) * *(xstr+loop1) );
          dcos -= ( *(xstr+loop2) * tan( *(ornt+loop2) ) );
          dcos /= ( tan( *(ornt+loop1) )
                                    - tan( *(ornt+loop2) ) );
          }
        }
      if ( dcos <= lx / (double)2.0  &&   dcos >= 0.0 )
        {
        dsin = tan( *(ornt+loop1) )
                                  * ( dcos - *(xstr+loop1) );
        dsin += *(ystr+loop1);
        if ( dsin <= ly / (double)2.0  &&  dsin >= 0.0 )
          {
          *(u+index1) = dcos - *(xstr+loop1);
          *(v+index1) = dsin - *(ystr+loop1);
          *(u+index1) *= *(u+index1);
          *(v+index1) *= *(v+index1);
          *(eta+index1) =
                        sqrt( *(u+index1) + *(v+index1) );
          *(u+index1) = dcos - *(xstr+loop2);
          *(v+index1) = dsin - *(ystr+loop2);
          *(u+index1) *= *(u+index1);
          *(v+index1) *= *(v+index1);
          *(v+index1) = sqrt( *(u+index1) + *(v+index1) );
          *(v+index1) /= *(lnst+loop2);
          *(u+index1) = *(eta+index1) / *(lnst+loop1);
          index1++;
          *(inst+index2) = loop1;
```

```
            index2++;
            *(inst+index2) = loop2;
            index2++;
            }
          }
        }
      }
    }

  }


void ini_EIv( EIv )
double   *EIv;
  {
  short  loop1;
  double epss=1.0e-08;

  for( loop1=0; loop1<NSTF; ++loop1 )
    if ( fabs( *(ornt+loop1) ) < epss
      &&  fabs( *(ystr+loop1) - ly / (double)2.0 ) <= epss )
      *(EIv+loop1) = EI / (double)2.0;
    else
      if ( fabs( *(ornt+loop1) - PI / (double)2.0 ) < epss
       && fabs( *(xstr+loop1) - lx / (double)2.0 ) <= epss )
        *(EIv+loop1) = EI / (double)2.0;
      else
        *(EIv+loop1) = EI;

  }


void ini_dm( dm, term1 )
double   *dm;
short    term1;
  {
  double tmp;
  short  loop1, loop2;
  short  index1, index2;

  for( loop1=0; loop1<term1; ++loop1 )
    {
    tmp = ( (double)( 2 * loop1 + 1 ) / lx );
    tmp *= tmp;
    index1 = loop1 * term1;
    for( loop2=0; loop2<term1; ++loop2 )
      {
      index2 = index1 + loop2;
      *(dm+index2) = ( (double)( 2 * loop2 + 1 ) / ly );
      *(dm+index2) *= *(dm+index2);
```

```
      *(dm+index2) += tmp;
      *(dm+index2) *= *(dm+index2);
      }
    }

  }


double qmn( m, n, i )
short    m, n, i;
  {
  double tmp1, tmp2;
  double sin();

  tmp1 = (double)( 2 * m + 1 ) * PI;
  tmp2 = (double)( 2 * n + 1 ) * PI;
  tmp1 = sin( tmp1 * *(u+i) );
  if ( fabs( tmp1 ) < epss )  tmp1 = (double)0.0;
  tmp2 = sin( tmp2 * *(v+i) );
  if ( fabs( tmp2 ) < epss )  tmp2 = (double)0.0;

  return( tmp1 * tmp2 );

  }


double rmn( k, i )
short    k, i;
  {
  double tmp1;
  double sin();

  tmp1 = (double)( 2 * k + 1 ) * PI;
  tmp1 = sin( tmp1 * *(eta+i) );
  if ( fabs( tmp1 ) < epss )  tmp1 = (double)0.0;

  return( tmp1 );

  }


void solve_LM( lgmr, TERM )
double   *lgmr;
short    TERM;
  {
  double *a;
  short  ele_a;

  double *memo_allc();
```

```
  void   memo_free();
  void   cmpt_a();
  void   cmpt_lgmr();
  short  Choleski();

  ele_a = NENF * NENF + NENF;
  ele_a /= 2;

  a = memo_allc( ele_a, "a" );

  cmpt_a( a, ele_a, TERM );

  cmpt_lgmr( lgmr, TERM );

  if ( !Choleski( a, lgmr, NENF ) )
    {
    printf("Fail to perform Choleski's decomposition (1).\n");
    printf( "Program terminates.\n" );
    exit(0);
    }
  memo_free( a, "a" );

  }


void cmpt_a( a, ele_a, TERM )
double   *a;
short    ele_a, TERM;
  {
  double cons, cont, tmp0, tmp1, tmp2, tmp3;
  short  idn1, idn2;
  short  loop0, loop1, loop2, loop3, loop4;
  short  index1, index2, index3, index4, index5;
  short  indexs, indexe;
  double qmn(), rmn();

  for( loop1=0; loop1<ele_a; ++loop1 )
    *(a+loop1) = (double)0.0;
  index3 = 0;
  for( loop1=1; loop1<=CENF; ++loop1 )
    index3 += loop1;
  index4 = 0;
  for( loop1=1; loop1<=CENF+TENF; ++loop1 )
    index4 += loop1;

  cont = (double)1.0 / lx / ly;
  cons = cont / ( dpc - dpr );
  cont *= ( (double)2.0 / dpr );
  index1 = 0;
  for( loop1=0; loop1<CENF; ++loop1 )
    {
```

```
  index3 += CENF;
  index4 += ( CENF + TENF );
  index1 += loop1;
  for( loop2=0; loop2<=loop1; ++loop2 )
    {
    if ( ( index2=index1+loop2 ) > ele_a )
      {
      printf
    ("Intend to use memory outside the allocated area.\n");
      printf( "Program terminates.\n" );
      exit(0);
      }
    *(a+index2) = (double)0.0;
    tmp0 = (double)0.0;
    loop3 = 0;
    do
      {
      index5 = loop3 * TERM;
      loop4 = 0;
      do
        {
        tmp1 = qmn( loop3, loop4, loop1 );
        tmp1 *= qmn( loop3, loop4, loop2 );
        tmp1 /= *(dm+index5+loop4);
        tmp0 += tmp1;
        }
      while( ++loop4 < TERM );
      }
    while( ++loop3 < TERM );
    *(a+index2) += ( tmp0 * cons );
    tmp1 = tmp0 * cont;
    *(a+index3+index2) = *(a+index2) + tmp1;
    *(a+index3+index2-CENF) = *(a+index2);
    *(a+index4+index2) = *(a+index2) + tmp1;
    }
  }

index2 = 0;
for( loop1=CENF; loop1<CENF+TENF; ++loop1 )
  {
  index1 += loop1;
  index3 = index1 + index2;
  for( loop2=loop1-CENF+1; loop2<CENF; ++loop2 )
    {
    index3 += ( CENF + loop2 );
    *(a+index1+loop2) = *(a+index3);
    }
  ++index2;
  }

index3 = 0;
for( loop1=CENF+1; loop1<=CENF+TENF; ++loop1 )
```

```
  index3 += loop1;

for( loop1=CENF+TENF; loop1<PENF; ++loop1 )
  {
  index1 += loop1;
  for( loop2=0; loop2<CENF; ++loop2 )
    {
    index2 = index1 + loop2;
    *(a+index2) = *(a+index2-index3);
    *(a+index2+CENF) = *(a+index2);
    }
  index3 += CENF;
  }

index1 = 0;
index3 = 0;
index4 = 0;
for( loop4=0; loop4<NSTF; ++loop4 )
  {
  cons = pow( *(lnst+loop4), (double)3 ) / *(EIv+loop4);
  cons /= (double)2.0;
  index4 += *(npes+loop4);
  for( loop1=index3; loop1<index4; ++loop1 )
    {
    index1 += loop1;
    for( loop2=index3; loop2<=loop1; ++loop2 )
      {
      if ( ( index2=index1+loop2 ) > ele_a )
        {
        printf
     ("Intend to use memory outside the allocated area.\n");
        printf( "Program terminates.\n" );
        exit(0);
        }
      tmp0 = (double)0.0;
      loop3 = 0;
      do
        {
        tmp1 = rmn( loop3, loop1 );
        tmp1 *= rmn( loop3, loop2 );
        tmp1 /=
          pow( (double)( 2 * loop3 + 1 ), (double)4 );
        tmp0 += tmp1;
        }
      while( ++loop3 < TERM );
      *(a+index2) += ( tmp0 * cons );
      }
    }
  index3 = index4;
  }

index1 = 0;
```

```
for( loop1=0; loop1<PENF; ++loop1 )
  index1 += loop1;

for( loop1=PENF; loop1<PENF+NINS; ++loop1 )
  {
  index1 += loop1;
  loop3 = loop1 - PENF;
  idn1 = *(inst+2*loop3);
  idn2 = *(inst+2*loop3+1);
  indexs = 0;
  for( loop3=0; loop3<idn1; ++loop3 )
    indexs += *(npes+loop3);
  indexe = indexs + *(npes+idn1);
  cons = pow( *(lnst+idn1) ,(double)3 ) / *(EIv+idn1);
  cons /= (double)2.0;
  for( loop2=indexs; loop2<=loop1 && loop2<indexe;
                                              ++loop2 )
    {
    if ( ( index2=index1+loop2 ) > ele_a )
      {
      printf
   ("Intend to use memory outside the allocated area.\n" );
      printf( "Program terminates.\n" );
      exit(0);
      }
    tmp0 = (double)0.0;
    loop4 = 0;
    do
      {
      tmp3 = (double)( 2 * loop4 + 1 ) * PI;
      tmp1 = sin( tmp3 * *(u+loop1) );
      if ( fabs( tmp1 ) < epss )  tmp1 = (double)0.0;
      tmp1 *= rmn( loop4, loop2 );
      tmp2 = pow( (double)( 2 * loop4 + 1 ), (double)4 );

      tmp0 += ( tmp1 / tmp2 );
      }
    while( ++loop4 < TERM );
    tmp0 *= cons;
    *(a+index2) += tmp0;
    }

  for( loop3=idn1; loop3<idn2; ++loop3 )
    indexs += *(npes+loop3);
  indexe = indexs + *(npes+idn2);
  cons = pow( *(lnst+idn2) ,(double)3 ) / *(EIv+idn2);
  cons /= (double)2.0;
  cons = -cons;
  for( loop2=indexs; loop2<=loop1 && loop2<indexe;
                                              ++loop2 )
    {
    if ( ( index2=index1+loop2 ) > ele_a )
```

```
    {
    printf
 ("Intend to use memory outside the allocated area.\n" );
    printf( "Program terminates.\n" );
    exit(0);
    }
  tmp0 = (double)0.0;
  loop4 = 0;
  do
    {
    tmp3 = (double)( 2 * loop4 + 1 ) * PI;
    tmp1 = sin( tmp3 * *(v+loop1) );
    if ( fabs( tmp1 ) < epss )  tmp1 = (double)0.0;
    tmp1 *= rmn( loop4, loop2 );
    tmp2 = pow( (double)( 2* loop4 + 1 ), (double)4 );
    tmp0 += ( tmp1 / tmp2 );
    }
  while( ++loop4 < TERM );
  tmp0 *= cons;
  *(a+index2) += tmp0;
  }

for( loop2=PENF; loop2<=loop1; ++loop2 )
  {
  loop3 = loop2 - PENF;
  if ( ( index2=index1+loop2 ) > ele_a )
    {
    printf
  ("Intend to use memory outside the allocated area.\n");
    printf( "Program terminates.\n" );
    exit(0);
    }
  if ( *(inst+loop3*2) == idn1 )
    {
    cons = pow( *(lnst+idn1), (double)3 ) / *(EIv+idn1);
    cons /= (double)2.0;
    tmp0 = (double)0.0;
    loop4 = 0;
    do
      {
      tmp3 = (double)( 2 * loop4 + 1 ) * PI;
      tmp1 = sin( tmp3 * *(u+loop1) );
      if ( fabs( tmp1 ) < epss )  tmp1 = (double)0.0;
      tmp2 = sin( tmp3 * *(u+loop2) );
      if ( fabs( tmp2 ) < epss )  tmp2 = (double)0.0;
      tmp1 *= tmp2;
      tmp2 = pow( (double)( 2 * loop4 + 1 ), (double)4 );
      tmp0 += ( tmp1 / tmp2 );
      }
    while( ++loop4 < TERM );
    *(a+index2) += tmp0 * cons;
    }
```

```
      if ( *(inst+loop3*2+1) == idn2 )
        {
        cons = pow( *(lnst+idn2), (double)3 ) / *(EIv+idn2);
        cons /= (double)2.0;
        tmp0 = (double)0.0;
        loop4 = 0;
        do
          {
          tmp3 = (double)( 2 * loop4 + 1 ) * PI;
          tmp1 = sin( tmp3 * *(v+loop1) );
          if ( fabs( tmp1 ) < epss )  tmp1 = (double)0.0;
          tmp2 = sin( tmp3 * *(v+loop2) );
          if ( fabs( tmp2 ) < epss )  tmp2 = (double)0.0;
          tmp1 *= tmp2;
          tmp2 = pow( (double)( 2 * loop4 + 1 ), (double)4 );
          tmp0 += ( tmp1 / tmp2 );
          }
        while( ++loop4 < TERM );
        *(a+index2) += tmp0 * cons;
        }
      }
    }
  }


void cmpt_lgmr( lgmr, TERM )
double   *lgmr;
short    TERM;
  {
  short  loop1, loop2, loop3, loop4;
  short  index1, index2, index3;
  double tmp1, tmp2, tmp3, tmp4;
  double qmn();

  loop1 = 0;
  while( loop1 < NENF )  *(lgmr+(loop1++)) = (double)0.0;

  index2 = CENF;
  index3 = CENF;
  for( loop4=0; loop4<NSTF; ++loop4 )
    {
    index3 += *(npes+loop4);
    for( loop3=index2; loop3<index3; ++loop3 )
      {
      for( loop1=0; loop1<TERM; loop1++ )
        {
        tmp1 = (double)( 2 * loop1 + 1 ) * PI;
        index1 = loop1 * TERM;
        for( loop2=0; loop2<TERM; loop2++ )
          {
          tmp2 = (double)( 2 * loop2 + 1 ) * PI;
```

```
            tmp2 *= tmp1;
            tmp4 = gmn( loop1, loop2, loop3 );
            *(lgmr+loop3) +=
                 ( tmp4 / tmp2 / *(dm+index1+loop2) );
            }
          }
        *(lgmr+loop3+TENF) = *(lgmr+loop3);
        }
      index2 = index3;
      }

    tmp1 = (double)2.0 * qt / dpr;
    tmp2 = (double)2.0 * qb / dpr;
    loop3 = 0;
    do
      {
      tmp3 = (double)0.0;
      if ( loop3 >= CENF ) tmp3 = tmp1;
      if ( loop3 >= (TENF+CENF) ) tmp3 = tmp2;
      if ( loop3 >= PENF ) tmp3 = (double)0.0;
      *(lgmr+loop3) *= tmp3;
      }
    while( ++loop3 < NENF );

    }


short Choleski( A, lambda, max_lambda )
double  *A, *lambda;
short   max_lambda;
    {
    void    forward_substitute();
    void    backward_substitute();

    short   i=0, j=0, k, l, m, n;


    do
      {
      l = ( j += i, j+i );
      for ( k=0; k<i; ++k )
        *(A+l) -= pow( *(A+j+k), (double)2 );
      if ( *(A+l) <= 0.0 )
        {
        printf("Stop %d %le\n", l, *(A+l) );
        return(0);
        }
      *(A+l) = sqrt( *(A+l) );

      n = l;
      for ( k=i+1; k<max_lambda; ++k )
```

```
      {
      n += k;
      for ( m=0; m<i; ++m )
        *(A+n) -= *(A+n-m-1) * *(A+l-m-1);
      *(A+n) /= *(A+l);
      }
    } while ( ++i < max_lambda );

  forward_substitute( A, lambda, max_lambda );
  backward_substitute( A, lambda, max_lambda );

  return( 1 );
  }


void forward_substitute( A, lambda, max_lambda )
double  *A, *lambda;
short   max_lambda;
  {
  short   i, j, k;

  k = 0;
  for ( i=0; i<max_lambda; ++i )
    {
    k += i;
    for ( j=0; j<i; ++j )
      *(lambda+i) -= *(lambda+j) * *(A+k+j);
    *(lambda+i) /= *(A+k+i);
    }

  }


void backward_substitute( A, lambda, max_lambda )
double  *A, *lambda;
short   max_lambda;
  {
  short   i=0, j=0, k, l, m, n;


  --max_lambda;
  for ( i=max_lambda; i>=0; --i )
    {
    k = 0;
    for ( l=1; l<=i; ++l )  k += l;
    m = 0;
    for ( j=i+1; j<=max_lambda; ++j )
      {
      m += j;
      *(lambda+i) -= *(lambda+j) * *(A+k+i+m);
      }
```

```
    *(lambda+i) /= *(A+k+i);
    }

  }


double *memo_allc( size, string )
char     *string;
short    size;
  {
  double *p;
  void   err_memo();

  size *= sizeof(double);
  p = (double *)malloc( (unsigned)size );
  if ( p == NULL )  err_memo( string );

  return( p );
  }


short *s_mem_alc( size, string )
char     *string;
short    size;
  {
  short  *p;
  void   err_memo();

  size *= sizeof(short);
  p = (short *)malloc( (unsigned)size );
  if ( p == NULL )  err_memo( string );

  return( p );
  }


void  memo_free( array_pointer, string )
char     *string;
double   *array_pointer;
  {

  free( array_pointer );
  printf( "Array %s is released\n", string );

  }
```

```
void err_memo( string )
char     *string;
  {

  printf("Warning!!\n");
  printf("Fail to allocate memory for array ");
  printf( "%s", string );
  printf("\nProgram terminates.\n");
  exit(0);

  }



void cmpt_dfpm( cdpm, tdpm, bdpm, TERM )
double   *cdpm, *tdpm, *bdpm;
short    TERM;
  {
  double tmp1, tmp2, tmp3, tmp4;
  short  loop1, loop2, loop3;
  short  index1, index2;
  double qmn();

  tmp3 = lx * ly / PI / PI;
  tmp1 = tmp3 * qt;
  tmp3 *= qb;
  for( loop1=0; loop1<TERM; loop1++ )
    {
    index1 = loop1 * TERM;
    tmp2 = tmp1 / (double)( 2 * loop1 + 1 );
    tmp4 = tmp3 / (double)( 2 * loop1 + 1 );
    for( loop2=0; loop2<TERM; loop2++ )
      {
      index2 = index1 + loop2;
      *(cdpm+index2) = (double)0.0;
      *(tdpm+index2) = tmp2 / (double)( 2 * loop2 + 1 );
      *(bdpm+index2) = tmp4 / (double)( 2 * loop2 + 1 );
      }
    }

  for( loop1=0; loop1<TERM; ++loop1 )
    {
    index1 = loop1 * TERM;
    for( loop2=0; loop2<TERM; ++loop2 )
      {
      index2 = index1 + loop2;
      tmp1 = (double)0.0;
      loop3 = 0;
      do
        {
        tmp2 = qmn( loop1, loop2, loop3 );
        tmp1 += ( *(lgmr+loop3) * tmp2 );
```

```
      }
    while( ++loop3 < CENF );
    *(cdpm+index2) += tmp1;

    tmp1 = (double)0.0;
    loop3 = CENF;
    do
      {
      tmp2 = qmn( loop1, loop2, loop3 );
      tmp1 += ( *(lgmr+loop3) * tmp2 );
      }
    while( ++loop3 < TENF+CENF );
    *(tdpm+index2) -= tmp1;
    *(cdpm+index2) += tmp1;

    tmp1 = (double)0.0;
    loop3 = CENF+TENF;
    do
      {
      tmp2 = qmn( loop1, loop2, loop3 );
      tmp1 += ( *(lgmr+loop3) * tmp2 );
      }
    while( ++loop3 < PENF );
    *(bdpm+index2) -= tmp1;
    *(cdpm+index2) += tmp1;
    }
  }

tmp1 = (double)8.0 / lx / ly / ( PI * PI * PI * PI );
tmp2 = tmp1 / ( dpc - dpr );
tmp1 *= ( (double)2.0 / dpr );
for( loop1=0; loop1<TERM; ++loop1 )
  {
  index1 = loop1 * TERM;
  for( loop2=0; loop2<TERM; ++loop2 )
    {
    index2 = index1 + loop2;
    tmp3 = tmp1 / *(dm+index2);
    *(cdpm+index2) *= ( tmp2 / *(dm+index2) );
    *(tdpm+index2) *= tmp3;
    *(bdpm+index2) *= tmp3;
    }
  }

}


void cmpt_defl( cdpm, tdpm, bdpm, TERM )
double   *cdpm, *tdpm, *bdpm;
short    TERM;
  {
```

```
FILE   *fpgt, *fpot, *fpgb, *fpob, *fpgc, *fpoc;
double *cdef, *tdef, *bdef;
double *x, *y;
double tmp1, tmp2, tmp3, tmp4;
short  loop1, loop2, loop3, loop4;
short  index1, index2, index3;
void   ini_xy();
void   outp_grd();
void   memo_free();
double *memo_allc();
double sin();

NODE = XSEC * YSEC;
x = memo_allc( XSEC, "x" );
y = memo_allc( YSEC, "y" );
ini_xy( x, y );

cdef = memo_allc( NODE, "cdef" );
tdef = memo_allc( NODE, "tdef" );
bdef = memo_allc( NODE, "bdef" );

for( loop1=0; loop1<NODE; ++loop1 )
  {
  *(cdef+loop1) = (double)0.0;
  *(tdef+loop1) = (double)0.0;
  *(bdef+loop1) = (double)0.0;
  }

for( loop1=1; loop1<XSEC; ++loop1 )
  {
  index1 = loop1 * YSEC;
  for( loop2=1; loop2<YSEC; ++loop2 )
    {
    loop3 = 0;
    do
      {
      index2 = loop3 * TERM;
      tmp4 = (double)( 2 * loop3 + 1 ) * PI;
      tmp1 = sin( tmp4 * *(x+loop1) );
      if ( fabs( tmp1 ) < epss )  tmp1 = (double)0.0;
      loop4 = 0;
      do
        {
        tmp4 = (double)( 2 * loop4 + 1 ) * PI;
        tmp4 = sin( tmp4 * *(y+loop2) );
        if ( fabs( tmp4 ) < epss )  tmp4 = (double)0.0;
        tmp4 *= tmp1;
        index3 = index2 + loop4;
        tmp2 = *(cdpm+index3) * tmp4;
        tmp3 = *(tdpm+index3) * tmp4;
        tmp4 *= *(bdpm+index3);
        index3 = index1 + loop2;
```

```
            *(cdef+index3) += tmp2;
            *(tdef+index3) += tmp3;
            *(bdef+index3) += tmp4;
            }
          while( ++loop4 < TERM );
          }
        while( ++loop3 < TERM );
        }
      }

    fpot = fopen( "eye2t.out", "w" );
    fpgt = fopen( "eye2t.grd", "w" );
    fpob = fopen( "eye2b.out", "w" );
    fpgb = fopen( "eye2b.grd", "w" );
    fpoc = fopen( "eye2c.out", "w" );
    fpgc = fopen( "eye2c.grd", "w" );
    outp_grd( fpgt, fpot, tdef );
    outp_grd( fpgb, fpob, bdef );
    outp_grd( fpgc, fpoc, cdef );
    fclose( fpgc );
    fclose( fpoc );
    fclose( fpgb );
    fclose( fpob );
    fclose( fpgt );
    fclose( fpot );

    memo_free( cdef, "cdef" );
    memo_free( bdef, "bdef" );
    memo_free( tdef, "tdef" );
    memo_free( y, "y" );
    memo_free( x, "x" );

    }


void outp_grd( fpg, fpo, df )
FILE     *fpg, *fpo;
double   *df;
    {
    short  loop1, loop2;
    short  index1, index2;

    for( loop1=0; loop1<XSEC; ++loop1 )
      {
      index1 = loop1 * YSEC;
      for( loop2=0; loop2<YSEC; ++loop2 )
        {
        index2 = index1 + loop2;
        fprintf( fpo, " w[%2d][%2d]=%le\n",
                      loop1, loop2, *(df+index2) );
        }
      }
```

```
loop1 = 2 * XSEC - 1;
loop2 = 2 * YSEC - 1;

fprintf( fpg, "DSAA\n" );
fprintf( fpg, "%d %d\n", loop1, loop2 );
fprintf( fpg, "0.0 %.2f\n", lx );
fprintf( fpg, "0.0 %.2f\n", ly );
fprintf( fpg, "0.0 1.0\n" );

index1 = YSEC - 1;
index2 = NODE - YSEC;
for( loop1=0; loop1<index1; ++loop1 )
  {
  for( loop2=loop1; loop2<index2; loop2+=YSEC )
    fprintf( fpg, "%le\n", *(df+loop2) );
  for( ; loop2>=loop1; loop2-=YSEC )
    fprintf( fpg, "%le\n", *(df+loop2) );
  }
for( ; loop1>=0; --loop1 )
  {
  for( loop2=loop1; loop2<index2; loop2+=YSEC )
    fprintf( fpg, "%le\n", *(df+loop2) );
  for( ; loop2>=loop1; loop2-=YSEC )
    fprintf( fpg, "%le\n", *(df+loop2) );
  }

}
```

REFERENCES

1. Richards, T. H., "Energy Methods in Stress Analysis," New York: John Wiley and Sons, 1977.

2. Hartmann, F., "The Mathematical Foundation of Structural Mechanics," New York: Springer-Verlag, 1985.

3. Timoshenko, S. and Woinowsky-Kriger, S., "Theory of Plates and Shells," New York: McGraw-Hill Book Company, 1954.

4. Weinstock, R., "Calculus of Variations with Applications to Physics and Engineering," New York: Dover Publications, 1974.

5. Forry, M., "Variational Calculus in Science and Engineering," New York: McGraw-Hill Book Company, 1968.

6. Washizu, K., "Variational Methods in Elasticity and Plasticity," Oxford: Pergamon Press, 1968.

7. Rektorys, K., "Variational Methods in Mathematics, Science and Engineering," Dordercht, Holland: D. Reidel Publishing Company, 1975.

8. Destuynder, P. and Nevers, T., "A New Finite Element Scheme for Bending Plates," Computer Methods in Applied Mechanics and Engineering, vol. 68, 1988, pp. 127-139.

9. Hughes, T. J. R. and Franca, L. P., "A Mixed Finite Element Formulation for Reissen-Mindlin Plate Theory: Uniform Convergence of All Higher-Order Spaces," Computer Methods in Applied Mechanics and Engineering, vol. 67, 1988, pp. 223-240.

10. Cooke, R., "Concept and Application of Finite Elements Analysis," New York: John Wiley and Sons, 1974.

11. Spilker, R. L. and Engelmann, B. E., "Hybrid-Stress Isoparametric Elements for Moderately Thick and Thin Multilayer Plates," Computer Method in Applied Mechanics and Engineering, vol. 56, 1986, pp. 339-361.

12. Venkatesh, A. and Roa, K. P., "Analysis of Laminated Shells with Laminated Stiffeners Using Rectangular Shell

Finite Elements," Computer Methods in Applied Mechanics and Engineering, vol. 38, 1983, pp. 255-272.

13. Owen, D. R. J. and Hinton, E., "Finite Elements in Plasticity: Theory and Practice," Swansea, United Kingdom: Pineridge Press, 1980.

14. Kanagasundaram, S. and Harihaloo, G. L., "Limitations of Galerkin's Method in Optimal Design of Beam Columns," Computer Methods in Applied Mechanics and Engineering, vol. 58, 1986, pp. 121-134.

15. Timoshenko, S. P. and Gere, J. M., "Mechanics of Materials," New York: Van Nostrand Company, 1972.

16. Saada, A. S., "Elasticity: Theory and Application," New York: Pergaman Press, 1974.

17. Boot, J. C. and Moore, D. B., "An Efficient Analysis for Thin Plates of General Quadrilateral Shape Subject to Bending Stresses," Computer Methods in Applied Mechanics and Engineering, vol. 43, 1984, pp. 57-79.

18. Al-Shareedah, E. M. and Seireg, A. A., "Use of Undetermined Multipliers in the Solution of Plate Problems," Computers in Mechanical Engineering, vol. 4, No. 3, 1985, pp. 59-68.

19. Al-Shareedah, E. M. and Seireg, A. A., "The Design of Slabs with Constraining Columns Using the Undetermined Multipliers Method," Computers in Mechanical Engineering, vol. 4, No. 4, 1986, pp. 59-68.

20. Al-Shareedah, E. M. and Seireg, A. A., "Use of Undetermined Multipliers in the Design of Stiffened Plates," Computers in Mechanical Engineering, vol. 4, No. 5, 1986, pp. 57-64.

21. Sizilard, R., "Theory and Analysis of Plates, Classical and Numerical Methods," Englewood Cliffs, New Jersey: Prentice-Hall, 1974.

22. Bares, R., "Tables for the Analysis of Plates, Slabs and Diagrams Based on the Elastic Theory," 2nd ed., Wiesbaden, West Germany: Bauverlay, Grabh, 1971.

23. Clifton, R. J., Change, J. C. L., and Au, T., "Analysis of Orthotropic Plate Bridges," Proc. of ASCE, Journal of Structure Div., vol. 39, 1963, pp. 133-171.

24. Srinivasan, R. S. and Thiruvenkatachari, V., "Static Analysis of Stiffened Plates," AAIA Journal, vol. 22, no. 9, 1984, pp. 1342-1344.

25. Srinivasanm R. S. and Ramachandran, S. V., "Linear and Nonlinear Analysis of Stiffened Plates," International Journal of Solid and Structure, vol. 13, 1977, pp. 897-912.

26. Dohrmann, D. J., Wu, J. N., and Beckett, R. E., "A Parametric Approach for the Stress Analysis of Orthogonally Stiffened Rectangular Plates," Journal of Pressure Vessel Technology, vol. 105, 1983, pp. 363-368.

27. Huffington, H. J., "Theoretical Determination of Rigidity Properties of Orthogonally Stiffened Plates," Journal of Applied Mechanics, vol. 23, 1956, pp. 15-20.

28. Levy, R. and Levy, O. E., "Recent Development in Structural Optimization," Journal of Structural Engineering, vol. 113, no. 9, 1987, pp. 1939-1962.

29. Seong, H., "A Numerical Method for Shape Design Sensitivity Analysis and Optimization of Built-Up Structures," Proceeding of the First Ajou University / University of Forida Joint Workship, 1988.

30. Haftka, R. T., "Structural Shape Optimization--A Survey," Computer Methods in Applied Mechanics and Engineering, vol. 57, 1986, pp. 91-106.

31. Hoff, N. J., "The Analysis of Structures," New York: John Wiley and Sons, 1956.

32. Vanderplaats, G. N., "Numerical Optimization Techniques for Engineering Design with Application," New York: McGraw-Hill Book Company, 1984.

33. Tabarrok, B. and Assamoi, L., "A New Variational Principle in Elastodynamics," Computer Methods in Applied Mechanics and Engineering, vol. 61, 1987, pp. 303-321.

34. Tolstov, G. P., "Fourier Series," New York: Dover Publications, 1976.

35. Timoshenko, S., "Strength of Materials: Part II," New York: Van Norstrand Company, 1941.

36. Love, A. E. H., "A Treatise on the Mathematical Theory of Elasticity," 4th ed., New York: Dover Publications, 1944.

37. Rayleigh, J. W. S., "The Theory of Sound," New York: Dover Publications, 1986.

38. Burden, R. L., Faires, J. D., and Reynolds, A. C., "Numerical Analysis," Massachusetts: Prindle, Weber and Schmidt, 1978.

39. Boot, J. C. and Moore, D. B., "Stiffened Plates Subject to Transverse Loading," International Journal of Solids Structures, vol. 24, No. 1, 1988, pp. 89-104.

40. Burgess, G. and Mahajerin, E., "A Numerical Method for Laterally Loaded Thin Plates," Computer Methods in Applied Mechanics and Engineering, vol. 49, 1985, pp. 1-15.

41. Shigley, J. E. and Mitchell, L. D., "Mechanical Engineering Design," 4th ed., New York: McGraw-Hill Book Company, 1983.

42. Conte, S. D. and Carl de Boor, "Elementary Numerical Analysis: An Algorithmic Approach," New York: McGraw-Hill Book Company, 1980.

43. Timoshenko, S., "Theory of Elasticity Stability," New York: McGraw-Hill Book Company, 1936.

44. Seireg, A. A., "Mechanical System Analysis," Pennsylvania: International Textbook Company, 1969.

45. Young, D., "Vibration of Rectangular Plates by the Ritz Method," Journal of Applied Mechanics, vol. 17, 1950, pp. 448-453.

BIOGRAPHICAL SKETCH

Tzu-Yang Chen was born on December 6, 1959, in Tainan, Taiwan, Republic of China.

He received his B.S. and M.S. degrees in mechanical engineering from National Chiao-Tung University, Taiwan, R. O. C. in June 1981 and June 1983, respectively. He then served in the Marines as a second lieutenant to fulfill mandatory military service from July 1983 to May 1985. After finishing the military service, he worked for Tai E International Patent and Law Office as a patent engineer in the Foreign Department for a short period.

In August 1986, he joined the Department of Mechanical Engineering, University of Florida, Gainesville, where he studied optimum design with emphasis in elastic structures under the direction of Dr. Ali A. Seireg.

I certify that I have read this study and that in my opinion it conforms to acceptable standards of scholarly presentation and is fully adequate, in scope and quality, as a dissertation for the degree of Doctor of Philosophy.

Ali A. Seireg, Chairman
Ebaugh Professor of Mechanical Engineering

I certify that I have read this study and that in my opinion it conforms to acceptable standards of scholarly presentation and is fully adequate, in scope and quality, as a dissertation for the degree of Doctor of Philosophy.

George N. Sandor
Research Professor of Mechanical Engineering

I certify that I have read this study and that in my opinion it conforms to acceptable standards of scholarly presentation and is fully adequate, in scope and quality, as a dissertation for the degree of Doctor of Philosophy.

Joseph Duffy
Graduate Research Professor of Mechanical Engineering

I certify that I have read this study and that in my opinion it conforms to acceptable standards of scholarly presentation and is fully adequate, in scope and quality, as a dissertation for the degree of Doctor of Philosophy.

Gary K. Matthew
Associate Professor of Mechanical Engineering

I certify that I have read this study and that in my opinion it conforms to acceptable standards of scholarly presentation and is fully adequate, in scope and quality, as a dissertation for the degree of Doctor of Philosophy.

Ulrich H. Kurzweg
Professor of Aerospace Engineering, Mechanics, and Engineering Science

This dissertation was submitted to the Graduate Faculty of the College of Engineering and to the Graduate School and was accepted as partial fulfillment of the requirements for the degree of Doctor of Philosophy.

August 1989

Dean, College of Engineering

Dean, Graduate School